INFORMATION TO USERS

This manuscript has been reproduced from the microfilm master. UMI films the text directly from the original or copy submitted. Thus, some thesis and dissertation copies are in typewriter face, while others may be from any type of computer printer.

The quality of this reproduction is dependent upon the quality of the copy submitted. Broken or indistinct print, colored or poor quality illustrations and photographs, print bleedthrough, substandard margins, and improper alignment can adversely affect reproduction..

In the unlikely event that the author did not send UMI a complete manuscript and there are missing pages, these will be noted. Also, if unauthorized copyright material had to be removed, a note will indicate the deletion.

Oversize materials (e.g., maps, drawings, charts) are reproduced by sectioning the original, beginning at the upper left-hand corner and continuing from left to right in equal sections with small overlaps.

Photographs included in the original manuscript have been reproduced xerographically in this copy. Higher quality 6" x 9" black and white photographic prints are available for any photographs or illustrations appearing in this copy for an additional charge. Contact UMI directly to order.

ProQuest Information and Learning
300 North Zeeb Road, Ann Arbor, MI 48106-1346 USA
800-521-0600

Growth and Function of Transgenic Endocrine Cells on Silanized Surfaces

by

James Raymond Bain

A dissertation submitted in partial fulfillment of the
requirements for the degree of

Doctor of Philosophy

University of Washington
2001

Program authorized to offer degree: Department of Bioengineering

UMI Number: 3013927

Bell & Howell Information and Learning Company
300 North Zeeb Road
P.O. Box 1346
Ann Arbor, MI 48106-1346

In presenting this dissertation in partial fulfillment of the requirements for the Doctoral degree at the University of Washington, I agree that the Library shall make its copies freely available for inspection. I further agree that extensive copying of the dissertation is allowable only for scholarly purposes, consistent with "fair use" as prescribed in the U.S. Copyright Law. Requests for copying or reproduction of this dissertation may be referred to Bell and Howell Information and Learning, 300 North Zeeb Road, P.O. Box 1346, Ann Arbor, MI 48106-1346, to whom the author has granted "the right to reproduce and sell (a) copies of the manuscript in microform and/or (b) printed copies of the manuscript made from microform."

Signature James R. Bain

Date 5 JUNE 2001

University of Washington
Graduate School

This is to certify that I have examined this copy of a doctoral dissertation by

James Raymond Bain

and have found that it is complete and satisfactory in all respects,
and that any and all revisions required by the final
examining committee have been made.

Chair of Supervisory Committee:

Allan S. Hoffman, Sc.D.

Reading Committee:

Thomas A. Horbett, Ph.D.

Patrick S. Stayton, Ph.D.

Wayne R. Gombotz, Ph.D.

Mark S. Cooper, Ph.D.

Date: 6/08/01

University of Washington

Abstract

Growth and Function of Transgenic Endocrine Cells on Silanized Surfaces

by James Raymond Bain

Chairperson of the Supervisory Committee: Professor Allan S. Hoffman
Department of Bioengineering

Interactions of transplantable cells with synthetic polymers might influence the function of biohybrid artificial organs. This study explored growth and secretion of human insulin by transgenic βG I/17 insulinoma cells cultured on surfaces bearing diamine groups (N2), trifluoropropyl groups (F3), and mixtures of the two. Glass and untreated polystyrene served as controls. Composition of N2-F3 surfaces was controlled by the ratio of monomers in the silanization bath, as confirmed by electron spectroscopy for chemical analysis and by conjugation of surface amines with fluorescein-5-isothiocyanate. Atomic-force microscopy revealed that silanized surfaces were patchy, though their root-mean-square roughnesses did not differ significantly from that of smooth glass (0.3 nm). Surfaces richest in trifluoropropyl residues were the most hydrophobic, with advancing water-contact angles $\geq 90°$. Cells cultured on pure F3 and pure N2 surfaces spread well, grew rapidly, and produced > 1.8 moles lactate per mole glucose consumed, closely resembling cells grown on the permissive control, glass. On one mixed surface, 33 N2: 67 F3, cells had a lower lactate/glucose ratio, adopted a rounded form, grew slowly, and were quick to form emergent aggregates, similar to cultures on the inhibitory control, untreated polystyrene. Cultures on F3-rich surfaces secreted the most insulin, and, in the case of the pure F3 surface, showed improved responsiveness to secretagogues. F3 surfaces conditioned by βG I/17 cells stimulated insulin secretion by subsequent cultures. Incubation of conditioned surfaces with high concentrations of a polyclonal anti-laminin serum prior to re-plating partially abolished this improvement in secretory function. Together, these observations suggest that polymers bearing trifluoropropyl groups and coated with laminin might be attractive candidates for use in the artificial endocrine pancreas.

Table of Contents

List of Figures

List of Tables

Acknowledgments

Development of silanized surfaces, along with protein-adsorption studies and preliminary cell-culture work, were funded by grants from the National Institutes of Health, U.S. Department of Health and Human Services (NIH # 1-T32-GM-08437-01 and 5-T32-HL-07403-15). Gore Hybrid Technologies, Inc., Flagstaff, AZ, supported cell studies. The cell line, βG I/17, was a gift from BetaGene, Inc., Dallas, TX. Mark E. Blaylock gave substantive, hands-on help with silane chemistry. Deborah Leach-Scampavia, National ESCA and Surface Analysis Center for Biomedical Problems (NESAC/BIO), University of Washington (UW), Seattle (NIH # RR01296), assisted with electron spectroscopy and provided the paragraph of text describing ESCA analysis in Chapter 2. Dr. Sergei N. Magonov, Digital Instruments, Inc., Veeco Metrology Group, Santa Barbara, CA, conducted the exploratory work on atomic-force microscopy. Perry Spevack, W.L. Gore and Associates, Inc., Elkton, MD, performed the definitive atomic-force microscopy. The staff at Glaswarenfabrik Karl Hecht GmbH and Company, Sondheim/Rhön, Germany, gave freely of their knowledge of glass chemistry. Henry A. Zebroski and Dr. Patrick S.H. Chou, Chemical Synthesis Facility, Howard Hughes Medical Institute, UW, synthesized and purified the oligopeptide used in Chapter One. Margot Truini sketched the rodent cartoons shown in Chapter Two. Administrative support from the Department of Bioengineering, UW, was provided by Isabel V.H. Landsberg, Kelli Jayn Nichols, Rita Jensen, and Dr. F.A. "Sandy" Spelman.

Monoclonal antibodies employed in Chapter 3 were donated by Dr. Joshua R. Sanes, Department of Anatomy, Washington University Medical School, Saint Louis, MO (clones C4, D18, D5, and D7), Dr. Eva Engvall, La Jolla Cancer Research Foundation, La Jolla, CA (clone 2E8), and Dr. Thomas M. Jessell and Dr. Jane Dodd, Center for Neurobiology and Behavior, Columbia University, New York, NY (clone 3.1C12). Monoclonals were obtained via Dr. David R. Soll, Developmental Studies Hybridoma Bank, National Institute of Child Health and Human Development, Department of Biological Sciences, University of Iowa, Iowa City, IA.

Bobbie D. Becker, Benita Benigni, Nina Burns, Dr. Mark D. Butler, Dr. William G. Carter, Dr. Sam Clark, Vickey Finger, Katie Gooby, Dr. Keith A. Knisley, Brian H. Kram, Stanley L. Mish, Dr. Michael J. Muehlbauer, Dr. Christopher B. Newgard, S. Craig Newman, Dr. Nancy P. Robertson, Beth Roche, Dr. Ann E. Schmierer, Dr. George Schuppin, and Greg E. Smith helped with cell culture, immunology, metabolic assays, cytology, statistical analysis, software challenges, literature study, and critical reviews of oral presentations and draft manuscripts. All these friends and more were generous with their support and encouragement.

Words cannot fully express my gratitude to my supervisory committee, Dr. Allan S. Hoffman, Dr. Thomas A. Horbett, Dr. Patrick S. Stayton, Dr. Wayne R. Gombotz, and Dr. Mark S. Cooper, for guiding me through my graduate program.

Dedication

This work is dedicated to my son, Edward William Bain.

Chapter 1. Tissue-culture surfaces with mixtures of aminated and fluorinated functional groups: Growth and function of transgenic rat insulinoma cells (βG I/17)

1.0. Summary

Interactions of transplantable cells with synthetic polymers might influence the function of biohybrid artificial organs. This study explored growth and secretion of human insulin by βG I/17 cells cultured on surfaces bearing diamine groups (N2), trifluoropropyl groups (F3), and mixtures of the two. Glass and untreated polystyrene served as controls. Composition of N2-F3 surfaces was controlled by the ratio of monomers in the silanization bath, as confirmed by electron spectroscopy for chemical analysis and by conjugation of surface amines with fluorescein-5-isothiocyanate. Atomic-force microscopy revealed that silanized surfaces were patchy, though their root-mean-square roughnesses did not differ significantly from that of smooth glass (0.3 nm). Surfaces richest in trifluoropropyl residues were the most hydrophobic, with advancing water-contact angles $\geq 90°$. Cells cultured on pure F3 and pure N2 surfaces spread well, grew rapidly, and produced > 1.8 moles lactate per mole glucose consumed, closely resembling cells grown on the permissive control, glass. On one mixed surface, 33 N2: 67 F3, cells had a lower lactate/glucose ratio, adopted a rounded form, grew slowly, and were quick to form emergent aggregates, similar to cultures on the inhibitory control, untreated polystyrene. Cultures on F3-rich surfaces secreted the

most insulin, and, in the case of the pure F3 surface, showed improved responsiveness to secretagogues. Polymers bearing trifluoropropyl groups appear to be attractive candidates for use in the artificial endocrine pancreas.

1.1. Introduction

Surgeons might someday be able to restore function of diseased tissues by implanting composites of living cells and artificial materials. Since chemistry and morphology of biomaterials can influence the phenotype of transplantable cells, knowledge of these interactions is fundamental to the creation of successful biohybrid organs, including the artificial endocrine pancreas. Type I or insulin-dependent diabetes mellitus arises from autoimmune destruction of the β cells of the pancreatic islets of Langerhans. Millions of Americans suffer from Type I diabetes, and incidence of this serious disease is increasing worldwide [1-3].

Despite massive investments in research in recent decades, the etiology of this devastating disease remains obscure. Insulin-replacement therapy by injection has been the standard treatment for decades. Though injection therapies improve the quality and length of life, they are not able to provide the close control of blood glucose necessary to prevent diabetic complications in later life, including damage to the kidneys, nerves, blood vessels, and eyes [3].

Treatment of human patients by transplantation of islets or whole pancreata from humans (allografts) and pigs (xenografts) has had variable success. Challenges include limited donor supply, immune reactions, and the fastidious nature and limited growth potential of human β cells [4-19].

To overcome these challenges, proliferative cells capable of processing and secreting

human insulin are attracting interest as platforms for the creation of transplantable β-cell surrogates by genetic engineering. Popular candidates include insulinoma cell lines, which are derived from rare β-cell tumors (Fig. 1.2a), along with other cell types that share the insulinoma's secretory phenotype [3, 10, 12, 15, 17, 20-67]. Concomitantly, synthetic materials are being developed to serve as anchorage supports or immune-protection barriers to foster growth of β-cell surrogates in the human body. Hybrid artificial organs employing mitotically-expanded islets, insulin-secreting cell lines, or fragments of insulinoma tumors have been grown in vitro, implanted in laboratory animals, and used to treat several cases of human diabetes [11, 13-14, 19, 23, 25, 36-37, 54, 60, 63, 68-87], but little is known about the effects of device composition on the phenotype of transplantable insulinoma cells [84, 88-91].

In the present study, I examined the growth and phenotype of βG I/17, a line of genetically modified rat insulinoma cells (RINs), cultured on borosilicate glass modified with organosilane coupling agents to create surfaces rich in diamine groups, trifluoropropyl groups, and mixtures of the two. I chose silanized borosilicate glass as a model system because I was able to fine-tune the surface chemistry by competitive chemisorption from binary, aqueous solutions of silane monomers. Silanization of glass surfaces results from the hydrolysis and subsequent condensation of chloro- or alkoxysilanes with surface silanols (SiOH, Fig. 1.1). Lateral condensation polymerization of silanes on the surface creates thin deposits of polysiloxanes [92-93]. Numerous investigators have employed silanes and the related silazanes to create chemically defined surfaces for the study of cell-material interactions [94-132]. Swalec

[113] created cell-culture surfaces of mixed character by vapor-phase deposition of methyl- and chloropropyl silanes. I hoped that competitive chemisorption from aqueous solutions of mixed silanes would offer a practical, controllable, and inexpensive alternative to vapor-phase deposition. Competitive chemisorption of organosilanes from water and other solvents has previously been used to create surfaces of mixed character [92-93, 133-139], but to my knowledge such surfaces have not heretofore been evaluated in cell culture.

Portions of this Chapter are reproduced from my preliminary report [140].

1.2. Materials and methods

1.2.1. Selection of silane monomers for competitive chemisorption

A priori, I expected amine-rich surfaces to favor cell growth and perhaps gene expression, and surfaces rich in fluorine atoms to be less suitable for RIN cells, so I selected silane monomers bearing these functional groups. I sought a competitive pair of monomers that are stable for a reasonable time in a common aqueous solvent, and in which the pendant chains of both moieties are grossly similar in length.

1.2.1.1. Diamine monomer "N2:" 3-(2-Aminoethylamino) propyltrimethoxysilane

Many anchorage-dependent vertebrate cells spread and grow well on surfaces rich in amines, amides, and other nitrogen-containing groups, including surfaces rendered nitrogenous by organosilanization [95, 97-98, 103, 106, 115-119, 123, 141-142, 127, 131]. Limited data indicate that some insulin-secreting endocrine cell lines will grow and function on amide- and amine-rich surfaces [88, 143-145]. I chose silane N2, with its primary and secondary amine groups, because it has been used in previous studies to create surfaces acceptable to a wide variety of mammalian cells, including such

fastidious cells as neurons and endothelial cells [98, 100, 102-104, 108, 112, 120, 122, 124-126]. For the promotion of cell attachment, spreading, and growth, N2's diamine structure might be preferable to monoamines and other common aminosilane structures [124]. The residue remaining after aminosilanization with N2 is shown in Fig. 1.1. Several hypotheses have been put forth to account for the "cell-friendly" nature of N2 residues (i.e., 3-(2-aminoethylamino) propyl- pendant groups) and other solid-phase amines, including direct association of cell-surface proteoglycans with synthetic cations by electrostatic or hydrogen-bonding interactions [102, 112, 115, 118, 120, 124, 126, 141, 146-149] and the preferential adsorption of soluble cell-attachment proteins, such as fibronectin and vitronectin, to nitrogen-rich surfaces [103, 125-126, 141-142, 150].

1.2.1.2. Trifluorinated monomer "F3:" (3,3,3-Trifluoropropyl) trimethoxysilane

I chose F3 because I expected surfaces rich in fluorine atoms groups to be relatively poor growth substrata for RIN cells. In general, well-fluorinated materials have large advancing contact angles with water (θ_A > ~85 °), low critical surface tensions (Zisman's γ_c < ~25 dynes/cm), and do not support vigorous cell growth [151-157]. Previous work by several laboratories indicates that the poor cell growth seen on many fluorinated materials might be due to low binding strengths or unfavorable binding conformations adopted by physisorbed cell-adhesion proteins [158]. I was unable to find evidence that surfaces modified with silane F3 have previously been evaluated in cell culture. The C_3 residue resulting from its use is shown in Fig. 1.1.

Silanized surfaces bearing longer, partially fluorinated, aliphatic side chains have been shown to inhibit growth of mammalian cells. Side-chain lengths in past studies have included C_8 [112], C_{10} [131], and C_{18} [107]. Silanes with such long fluoroalkyl side

chains were not considered for use in the present study, because they are insoluble in the aqueous solutions I wished to use for deposition with the diamine co-monomer, N2. Although a perfluoropropyl side chain would give a higher surface density of fluorine upon chemisorption, the side chain in silane F3 is not fully fluorinated, since fluorines on the two carbons nearest the silicon atom would be unstable, due to rearrangements with the reactive methoxy groups around the silicon atom, high susceptibility to nucleophilic attack, and poor thermal stability [159]. As with similar halogenated silanes, stability is imparted by the $-(CH_2)_2-$ bridge between silicon and the $-CF_3$ group [160]. "The trifluoropropyl group is the smallest fluorine-containing nonreactive group on Si that is chemically stable..." [161]. Once chemisorbed to glass and annealed in an air oven, I predicted that siloxane deposits containing F3 would give acceptable stability in the aqueous environment of tissue culture. A monofunctional analog of the trifunctional F3, trifluoropropyldimethylsilyl-N-methylacetamide, has been used to prepare commercial chromatographic supports for biochemical separations in aqueous media [161-162]. Finally, in selecting the hydrophobic member of the monomer pair, I chose the fluoroalkyl silane F3 over nonfluorinated alkylsilanes because it bears an element (F) not present in N2. Extreme electronegativity of fluorine makes it especially easy to detect at low degrees of incorporation; F3's fluorines provided a strongly reporting atomic marker for surface characterization by electron spectroscopy for chemical analysis, or ESCA [162].

1.2.2. Glass selection, cleaning, and etching

Conventional borosilicate cover glasses for microscopy (thickness ~200 μm) were purchased from Carolina Biological Supply (Burlington, NC). Raw glass sheets of the

borosilicate glass D263 were poured by Schott-Deutsche Spezialglas (Mainz, Germany), and cut into the final shape and sold under the trade name "Assistent" by Glaswarenfabrik Karl Hecht GmbH and Company (Sondheim/Rhön, Germany). According to the manufacturer, the bulk formulation, in weight percent, is 65 % SiO_2, 12 % (Na_2O + K_2O), 7.5 % B_2O_3, 6.5 % ZnO, 5.5 % TiO_2, 3 % Al_2O_3, and 0.5 % Sb_2O_3. This formulation is expressed in terms of atomic percentages in Table 1.1. Squares (12 mm) provided a constant circumference for Wilhelmy-plate, contact-angle goniometry (infra). Circles (15 mm diameter) fit snugly in 24-well plates for cell culture. Cleaning, etching, and silanization were conducted on cover glasses mounted in custom racks machined from polytetrafluoroethylene (PTFE). Two such racks (holding 32 slides each) were placed side-by-side in a Wheaton histological staining dish with a matching glass lid (Wheaton 400 USP Type I borosilicate glass; Wheaton Industries, Millville, NJ). Volumes of reagents for glass treatment were 150 mL unless otherwise noted. Aqueous solutions were based on deionized, then distilled water (ddH_2O), resistance ~18 MΩ/cm. Organic solvents were from J.T. Baker, Inc., Phillipsburg, NJ, and were "analyzed-reagent" grade or better. Reaction vessels were etched with 0.5 N NaOH between uses. After two dip rinses in fresh acetone, racked cover glasses were ultrasonically cleaned 10 minutes in 2 % Micro All-Purpose Liquid Cleaner (International Products Corporation, Burlington, NJ) in ddH_2O, pH 9.6, at 335 W, 47 kHz (Bransonic model B3210DTH, Branson Ultrasonics Corporation, Danbury, CT). Micro is an aqueous solution of N,N'-1,2-ethanediylbis(N-(carboxymethyl)) glycine, tetrasodium salt; benzenesulfonic acid, dimethyl-, ammonium salt; benzenesulfonic acid, dodecyl-, compounded with 2, 2', 2"-nitrilotris(ethanol); and poly (oxy-1,2-

ethanediyl), α-(nonylphenyl)-ω-hydroxy, branched. Samples were then rinsed in running ddH_2O, followed by three dip rinses in ddH_2O, an acetone dip, 5 minutes ultrasonication in methylene chloride, then dried at 90 °C in air until just dry, and stored in vacuo at ~0.5 mm Hg in polystyrene Petri dishes. On the day of silanization, glass surfaces were etched in unstirred 0.5 N NaOH for 30 minutes at ~20 °C, followed by three dip rinses in ddH_2O.

1.2.3. Silanes, silanization, and annealing

(3,3,3-Trifluoropropyl) trimethoxysilane, or F3, and 3-(2-aminoethylamino) propyltrimethoxysilane, or N2, were used as received from PCR, Incorporated (Gainesville, FL). In all cases, silanization mixtures had a total silane concentration of 0.1 M in 50: 50 ddH_2O: isopropanol, apparent pH 4.75. Extensive experimentation showed that departures from this solvent condition led to instability of mixtures of N2 and F3, with rapid polymerization or precipitation of the monomers, particularly those richest in the F3 monomer. Solutions were used immediately after adjustment of pH. Silanization proceeded 2 hours at ~20 °C, with stirring, followed by extensive rinsing in 50: 50 ddH_2O: isopropanol, apparent pH 4.75, followed by a final rinse in 70 % v/v ethanol in ddH_2O to disinfect samples in preparation for cell culture.

Annealing by heat is necessary to give stable deposits of siloxanes on glass surfaces, but can destroy amines if carried to excess [93, 163-164]. To assess the effects of annealing regimens on amine reactivity, I conjugated fluorescein-5-isothiocyanate (FITC; Aldrich Chemical Company, Milwaukee, WI) to surfaces, using 1 mg/mL FITC in N,N-dimethylformamide (DMF), with 0.712 μL/mL triethylamine as a base catalyst (Fig. 1.2). Thiourea conjugation proceeded 2 hours at ~20 °C, unstirred. After a 30-

minute rinse in DMF, samples were rinsed thrice in ddH_2O, and dried in vacuo at ~20 °C, ~0.5 mm Hg. Bound FITC residues were then stripped in 0.1 M NaOH, 2 hours, unstirred, at ~20 °C. Fluorescence of the acid-neutralized stripping solution was determined in a Perkin-Elmer LS-5B luminescence spectrometer, using a xenon source (excitation 495 nm, emission 519 nm; Perkin-Elmer Corporation, Norwalk, CT).

1.2.4. Electron spectroscopy for chemical analysis (ESCA)

Analyses were performed with an X-Probe ESCA instrument (Surface Science Instruments or SSI, Mountain View, CA). This instrument permits analysis of the outermost ~50 Å of a sample in an elliptical area whose short axis was ~600 μm [165]. An aluminum Kα1,2 monochromatized X-ray source was used to stimulate photoemission. Energy of the emitted electrons was measured in a hemispherical energy analyzer at pass energies ranging from 25 eV to 150 eV. Spectral data were collected with the analyzer at 55 ° with respect to the surface normal of the sample. SSI data-analysis software was used to calculate the elemental compositions from the peak areas and to peak-fit the high-resolution spectra. An electron flood gun set at 5 eV was used to minimize surface charging. The binding energy (BE) scale was referenced by setting the CH_x peak maximum in the C1s spectrum to 285.0 eV. Typical pressures in the analysis chamber during spectral acquisition were 10^{-9} torr.

1.2.5. Contact-angle goniometry

Advancing (θ_A) and receding contact angles (θ_R) with ddH_2O, pH ~7.4, were determined by the Wilhelmy-plate method [166], using a Cahn DCA 312 Contact Angle Analyzer (Cahn Instruments, Inc., Cerritos, CA). Purity of ddH_2O was monitored by daily measurements of the surface tension of water (γ_{LV} ddH_2O), using freshly-flamed

cover glasses, which were used as soon as they cooled to room temperature. Crosshead velocity was 10 mm/minute. Three independent samples were assayed, and θ_A and θ_R were measured during the first three immersion-emergence cycles. Data presented below are the means of these nine values. Throughout this report, error bars show ± one standard deviation.

1.2.6. Atomic-force microscopy (AFM)

Annealed, silanized surfaces were imaged in air in tapping mode with the NanoScope Dimension 3100 Scanning Probe Microscope (Digital Instruments, Inc., Santa Barbara, CA). Root-mean-square (RMS) roughness, the standard deviation of height measurements (z), was calculated over a square sample area 3 μm on a side (512 × 512 pixels). Heights, widths, and lengths of randomly-selected surface features were measured in the same area. Images were recorded with a false-color scheme showing a 5-nm full z-axis in all cases.

1.2.7. Culture in 24-well plates

Etched and silanized glass discs were mounted for cell culture in the bottom of 24-well, surfaced-oxidized, tissue-culture plates (Falcon Multiwell 3047, Becton Dickinson Labware, Franklin Lakes, NJ), and were held in place by fluoroelastomeric o-rings made of poly (vinylidene fluoride-co-hexafluoropropylene), size 014 (Viton A, Kontes Glass Company, Vineland, NJ). Prior to use, o-rings were ultrasonically cleaned 10 minutes in neat ethanol, rinsed thrice in ddH_2O, ultrasonically cleaned 10 minutes in 2 % Micro, rinsed four times in ddH_2O, dried at 90 °C, and autoclaved. In addition to wells containing glass circles, o-rings were placed in wells of untreated polystyrene (Falcon 1147), the negative control.

1.2.8. Cell line and cell culture

The lineage leading to the engineered insulinoma cell line, βG I/17, began with a rat insulinoma (RIN) that developed in an NEDH rat (New England Deaconess Hospital) after high-dose X-irradiation [167] (Fig. 1.2a). The cell line RINr was established from this insulinoma after nine serial tumor transplants in NEDH rats [12, 168]. RINr secretes both somatostatin and insulin. A RINr clone, RINr1046-38, or RIN-38 for short, secretes insulin, but not somatostatin [169]. RIN-38 has a faster growth rate and a more clustered morphology than the parental RINr [169]. Low-passage RIN-38 cells demonstrate glucose-induced secretion of native rat insulin [170-171]. Genetic engineers at BetaGene, Inc. (Dallas, TX), created βG I/17 from RIN-38 by transfection with a human proinsulin cDNA. βG I/17 contains approximately 410 ng insulin per 6 μg DNA, more than tenfold that of the parental RIN-38 line, and is capable of processing human proinsulin to insulin [29, 172-173]. Its transgenic phenotype has been maintained after a year of continuous culture [173]. βG I/17 has retained its ability to grow as a solid tumor in both nude and NEDH rats. In time, these tumors grow large enough to secrete sufficient insulin to cause hypoglycemia. In the present study, βG I/17 was used at the 53rd passage after introduction of a single copy of the human proinsulin gene, under the influence of the cytomegalovirus promoter/enhancer element, as confirmed by Southern analysis [173]. βG I/17 expresses aminoglycoside phosphotransferase, which confers neomycin resistance [173]. I maintained it under selection with the neomycin analog, G418 sulfate (Geneticin, GibcoBRL, Life Technologies, Grand Island, NY), until the 27th passage. Phenotypic expression was

stable at the 53rd passage, as demonstrated by background production of human insulin. Immediately prior to use in this study, βG I/17 was shown to be free of contamination with mycoplasmata by the Hoechst bisbenzamide 33258 fluorochrome (Sigma Chemical Company, Saint Louis, MO).

For this study, near-confluent cultures of βG I/17 on tissue-culture polystyrene were rinsed twice with Hanks' balanced-salt solution without $CaCl_2$, $MgCl_2$, $MgSO_4$, or Phenol Red (HBSS; Gibco BRL Products, Grand Island, NY), then trypsinized (0.05 % porcine trypsin, 0.53 mM tetrasodium salt of ethylene diamine tetraacetic acid, in HBSS; GibcoBRL). Cells were suspended and centrifuged in the culture fluid, Medium 199 (with Earle's salts, 100 mg/L L-glutamine, 2.2 g/L $NaHCO_3$, and 25 mM N-2-hydroxyethylpiperazine-N'-2-ethane sulfonic acid (HEPES) buffer; Gibco BRL), plus 4.8 % v/v fetal bovine serum (HyClone Laboratories, Inc., Logan, UT), and 7.54 mg/L gentamicin sulfate (Gibco BRL), enriched to a final concentration of 188 mg/dL (10.4 mM) D-glucose using 10 % w/v glucose (Sigma). Supernatant was aspirated; cells were resuspended in culture medium, and counted (Coulter Counter, model ZBI, Coulter Electronics, Inc., Hialeah, FL). A final cell suspension was prepared in culture media such that 1 mL of media was added to each dry sample well, with a plating density of 80,000 cells/cm^2, approximately one fifth of confluence. Cultures proceeded seven days in a humidified incubator set to 95 % air, 5 % CO_2, 37 °C, with daily changes of media. Conditioned media were frozen for later assays of metabolites.

1.2.9. Basal insulin secretion at seven days

After a week of culture, insulinoma cells were washed twice for 15 minutes at 37 °C in RPMI Medium 1640 (300 mg/L L-glutamine, and 0 mM D-glucose; GibcoBRL)

containing 0.1 % w/v radioimmunoassay-grade bovine-serum albumin (RIA-BSA; Sigma), pH adjusted to 7.4. Basal levels of insulin secretion were then established by a one-hour 37 °C incubation in RPMI 1640, with 0.1 % RIA-BSA, 20 mM HEPES, 100 μM 7-chloro-3-methyl-2H-1,2,4-benzothiadiazine 1,1-dioxide or diazoxide (Sigma), pH 7.4. Diazoxide, or DZ, is a strong inhibitor of regulated insulin secretion [174]. Under the influence of DZ, secretion is reduced to basal levels, and occurs only by the constitutive pathway of secretion. DZ is poorly soluble in water at neutral pH, so it was necessary to first create a 1000-× stock solution by suspending 23 mg DZ in 600 μL dimethyl sulfoxide, adding 5 μL 10 N NaOH, agitating until the DZ dissolved, then diluting to 1 mL with ethanol.

1.2.10. Maximal stimulation of insulin secretion

Cultures were then washed for 15 minutes with RPMI 1640 containing 0.1% RIA-BSA, then stimulated for one hour with a "Swiss cocktail" of secretagogues to assess their maximum potential for insulin secretion. Formulation of the cocktail used in the present study was devised by workers at BetaGene, Inc. (Dallas, TX), based on one originally developed by Doctor Philippe Halban, Laboratoires Jeantet, Centre Medical Universitaire, University of Geneva, Switzerland. In the present study, the cocktail comprised 0.1 mM 3-isobutyl-1-methylxanthine or IBMX, 12.1 mM L-arginine, 5 mM (90 mg/dL) D-glucose, 10 mM L-leucine, 10 mM L-glutamine, 0.11 mM carbamylcholine chloride or carbachol (an acetylcholine analogue), 20 mM HEPES buffer, and 1 mg/mL RIA-BSA (all "Swiss cocktail" reagents were from Sigma), dissolved in RPMI 1640, pH adjusted to 7.4. Finally, samples were fixed in 10 % neutral, buffered formalin, stained with Harris's hematoxylin and eosin, inverted, and

mounted on microscope slides.

1.2.11. Assays of glucose consumption and lactate production

Media conditioned by the βG I/17 cultures were frozen in polypropylene microcentrifuge tubes, thawed, and assayed for glucose consumption and lactate production on a Kodak Ektachem DT60 II dry-slide analyzer (Ortho-Clinical Diagnostics, Inc., Johnson and Johnson, Rochester, NY). Unconditioned media were assayed daily to assure consistency in the initial glucose concentration (~188 mg/dL) and the presence of minimal initial lactate introduced by the fetal-calf serum (1.0 mM). Aliquots of 10 μL conditioned media were spotted onto dry slides. Reagents in each slide consisted of 0.7 Units of the oxidases of glucose and lactate, respectively, with a chromogenic system based on 7 Units peroxidase, 150 μg 1,7-dihydroxynaphthalene, and 250 μg 4-aminoantipyridine hydrochloride.

1.2.12. Assay of human insulin

Insulin levels were assessed in the conditioned media from the seventh day of routine culture, the basal incubation under diazoxide, and the Swiss-cocktail stimulation, using the radioimmunoassay (RIA) kit from the Incstar Corporation (Stillwater, MN), calibrated for detection of human insulin. Calibration history is traceable to World Health Organization insulin standard 66/304. Briefly, a sample is incubated with guinea pig anti-insulin serum and a known quantity of competitive ^{125}I-porcine insulin, and then incubated at 4 °C for 16 to 20 hours. A precipitating complex is then added. This complex comprises normal guinea pig serum, pre-precipitated with goat anti-guinea pig serum and poly (ethylene glycol). After 20 minutes incubation at room temperature, the

precipitate is centrifuged 20 minutes at 760 × g at 20-25 °C (Beckman TJ-6, Beckman Instruments, Inc., Palo Alto, CA). Supernatant is decanted, assay tubes are blotted, and activity of the precipitate so obtained is counted in a gamma counter (model 1282 Compugamma CS, Pharmacia-LKB Wallac, Turku, Finland). Porcine-insulin standards are used to create a calibration curve, using a curved spline fit. Data are then converted from μU/mL to ng/mL using a conversion factor of 25 μU/ng. Finally, where necessary, insulin secretion is expressed in molar units using a molecular weight of 5.808 kiloDaltons for fully processed human insulin.

1.2.13. Statistical analysis

Pair-wise comparisons of data from physical and biologic experiments were evaluated post hoc with the Tukey-Kramer "honestly significantly different" (HSD) test [175], using version 3.0 of the JMP software (SAS Institute, Inc., Cary, NC). Differences were considered significant at $p < 0.05$. In some data sets, the Tukey-Kramer HSD test separated results into discrete groups, in which no group member differed from any other member of that group, and there was no overlap among different groups. Such results are presented as simple tables. Where relationships among groups were more complex, data for treatment groups are compared to the glass and polystyrene controls, or data are presented for every possible pair-wise comparison, in tables resembling the mileage charts showing city-to-city distances on highway maps.

1.3. Results

1.3.1. Surface composition by electron spectroscopy for chemical analysis

Silicon and oxygen dominate the surface of borosilicate cover glasses cleaned with acetone (Table 1.1). Theoretical values for composition are based on formulation data

from the glassmaker. Presence of carbon is the most striking departure of the observed composition from theoretical values. This optical glass does not contain carbonates--carbon is probably introduced by physisorption of hydrocarbons and other organic contaminants onto the surface from the atmosphere. This is perhaps inevitable on such high-energy surfaces as clean metals and glasses [135, 176-178]. Though the surface can be cleaned by flaming, as was done with the standards used in the Wilhelmy-plate experiments (infra), it rapidly fouls upon standing in the laboratory air (in ~20 minutes). Carbon is further enriched in the alkaline-detergent-washed sample (Table 1.1), possibly by deposition of surfactants from the Micro cleaning solution. Detergent residue would also account for the appearance of small amounts of sulfur and nitrogen at this stage (Table 1.1). Nitrogen, sulfur, and nearly half the carbon are subsequently removed by etching in 0.5 N NaOH on the day of silanization (Table 1.1). Consistent with published reports that describe etching of glass surfaces at extremes of pH, the two alkaline treatments (Micro detergent, followed by the 0.5 N NaOH etchant) depleted the surface of most minor elements (Na, B, K, Zn, and Ti), and the surface was concomitantly enriched with silicon and oxygen [176-177]. Antimony (Sb) was not detected by ESCA (Table 1.1), probably because it is present at less than 0.1 atomic percent, and because of strong interference from the 2s and 2p lines of silicon.

Silanization with pure, 0.1-M solutions of the diaminosilane, N2, gave 2.5 atomic percent nitrogen, while the pure, 0.1-M trifluoropropyl silane, F3, gave 8.1 atomic percent fluorine (Table 1.1). The trace amount of nitrogen present in the surface silanized with a pure solution of F3 might represent residual soap scum. Normalized data on atomic ratios of nitrogen and fluorine show good agreement between observed

surface compositions and those predicted from stoichiometry of the reactive silane monomers (Fig. 1.3). A slight excess of nitrogen was observed in every case except the pure aminosiloxane deposits.

1.3.2. Reactivity of amine groups with fluorescein-5-isothiocyanate

Organosiloxane deposits condensed on glass are unstable in water, a property that is often overlooked by biologists who culture cells on silanized surfaces. Hydrolysis of organosiloxanes can be greatly slowed if surfaces are heat-annealed prior to use [93, 138, 178]. An interactive series of short studies on annealing, contact-angle goniometry, and reactivity of FITC toward surface amine groups (Fig. 1.2) demonstrated that an air-oven cure of 2 hours at 100 °C offered an acceptable compromise between annealing and loss of amine reactivity, producing silanized surfaces resistant to hydrolysis, while at the same time preserving ~85 % of the reactive amines of the uncured surface (data not shown). Gradual loss of amine reactivity upon heating aminosiloxanes in air might be due to reactions with CO_2, conversion of amines to amides, or the formation of internal zwitterions when amines "bite back" with free silanol anions or other anions on the surface (e.g., borates, metal oxides) [179-180]. Fig. 1.4 shows a monotonic decrease of binding and subsequent alkaline hydrolysis of FITC residues with increasing mole fraction of silane monomer F3 in surfaces of mixed composition. These surfaces were annealed at 100 °C for 2 hours.

1.3.3. Contact angles

All pure and mixed surfaces of N2 and F3 showed advancing contact angles, θ_A, greater than 80 °, and receding contact angles, θ_R, greater than 55 ° (Figs. 1.5 and 1.6). The relatively high contact angles observed on many aminosilanized surfaces have been

ascribed to the aforementioned formation of internal zwitterions and concealment of high-energy head groups among alkane and siloxane groups [181]. Heat-annealed surfaces were stable during repeated wetting, showing only a slight decrease in θ_A and θ_R as the polysiloxanes hydrated during the first three immersion-emergence cycles (Fig. 1.5). Surprisingly, both θ_A and θ_R reach their maxima at a mole fraction of 2/3 F3 (Fig. 1.6), and not at 100 % F3, as expected. Surface roughness, hydrogen bonding (e.g., -F_2CF•••HNH-), or heterogeneity in surface chemistry might account for the peak in θ_A and θ_R at intermediate mixtures of N2 and F3. Nanometer-scale roughness, as studied with the AFM, did not vary significantly among the glass and silanized surfaces ($p > 0.05$, infra). In view of the insular nature of the silanized surfaces (infra), patchiness in surface chemistry seems to be the most likely explanation for the peak in θ_A and θ_R at 2/3 silane F3 [152].

Chemical heterogeneity of surfaces is often invoked to explain contact-angle hysteresis, θ_H, defined as $\theta_A - \theta_R$ [154]. Though I had expected θ_H to reach its maximum in mixed surfaces of N2 and F3, θ_H was in fact greatest in surfaces of pure N2 (26.6 °), and declined gradually with increasing mole fraction of F3, reaching a minimum of 17.9 ° in surfaces of pure F3 (Fig. 1.7). Declining θ_H with increasing fluorine content was significant at $p < 0.05$ (Tukey-Kramer HSD test; Fig. 1.7). This might have been due to greater hydration of the diamino functional groups on surfaces richer in N2 residues. Hydration is manifest as an upward shift in measured load between the first and third immersion-emergence cycles in Fig. 1.5.

1.3.4. Atomic-force microscopy (AFM)

As expected, solvent-cleaned and alkaline-etched borosilicate glass surfaces were extremely smooth. Four randomly selected spots were evaluated on both materials, and every area sampled had a root-mean-square (RMS) roughness less than 0.5 nm (Figs. 1.8 and 1.9). This is consistent with previous reports of roughness values $\leq$ 0.5 nm for the smoothest known surfaces of glass, muscovite mica, silica, and silicon [181-189]. On all seven silanized surfaces studied by AFM, the RMS roughness averaged more than 0.5 nm (Figs. 1.8 and 1.9). Four of the seven silanized surfaces had average RMS roughness values greater than 0.9 nm (viz., the pure diaminosilanized surface, 0/3 F3, along with three mixed surfaces, 1/2 F3, 2/3 F3, and 5/6 F3; Fig. 1.9). These same four surfaces exhibited the most striking decoration with ellipsoid, elevated features in the false-color portraits (Fig. 1.8). Such features, which Brunner et al. [190] called "submonolayer islands," probably represent domains of polymerized silanes on a background of flat, unmodified glass. This is consistent with the strong reporting by minor constituents of the underlying borosilicate glass in all samples evaluated by ESCA (e.g., Na, B, K, Al, Zn, and Ti; Table 1.1). Lateral variability in surface roughness was most pronounced in the 0/3 F3 and 1/2 F3 surfaces (Fig. 1.9). One randomly selected area on the 1/2 F3 surface had an RMS roughness in excess of 7 nm (Fig. 1.9). Roughness and its variability (Figs. 1.8 and 1.9) showed no clear relationship with contact angle and its hysteresis (Figs. 1.6 and 1.7).

Section analysis was performed to profile individual, randomly selected surface asperities on all materials (data not shown). Ellipsoid excrescences on silanized surfaces generally had lengths of 140 to 240 nm, and aspect ratios (greatest length over

narrowest width) of 1.3 to 1.9. Heights generally ranged from 1.5 to 5 nm. Previous investigators have noted asperities of similar size emerging from flat backgrounds of silanized surfaces. Several studies suggest that the size and shape of features on silanized surfaces are influenced by such variables as cleaning, etching, and hydration prior to surface modification, as well as silanization conditions, and any subsequent annealing by heat [139, 181, 183-199].

In the most heavily studied silanized surface, residues of octadecyltrichlorosilane or OTS silanes, with their long (C_{18}), pendant alkyl chains, are known to form orderly structures under some conditions, including densely packed, self-assembled monolayers. Independent observers have measured the height of condensed phases of OTS residues as ~2.2 to 2.5 nm, which corresponds well to the theoretical extended-chain length of the OTS residue [183, 190, 192-193, 198, 200]. In contrast to these orderly OTS systems, I speculate that the short, chemically disparate, trialkoxy silane monomers used in the present study (viz., N2, F3) form more random or dispersed networks, without discernible microstructure [181]. False-color images such as those shown in Fig. 1.8 might give the reader an exaggerated impression of surface roughness. Please note that while each image covers an area of 3 μm × 3 μm, the vertical scale is in nanometers. Though slightly rougher than clean glass, all surfaces in this study were quite smooth on the scale of cells.

1.3.5. Growth form of βG I/17 transgenic rat insulinoma cells

The rat insulinoma (RIN) line, βG I/17, exhibits an unusual morphology when grown on planar substrata in vitro. Unlike many cell lines, which exhibit contact inhibition and cessation of growth when cultures mature to a confluent monolayer, cultures of βG

I/17 sprout emergent foci (supra-confluent structures) in late log phase when grown on such permissive surfaces as glass, as shown by white arrows in Fig. 1.10. Cell-material interactions appear to dominate early development of βG I/17 cultures, while cell-cell interactions dominate late events. In this study, growth of βG I/17 cells to near confluence, followed by formation of emergent foci, was quite similar on alkaline-etched borosilicate glass (Figs. 1.10 and 1.11), the pure aminosiloxane, N2 (Figs. 1.11 and 1.12), surfaces with a mole fraction of 1/3 F3 (not shown), and the pure fluorosiloxane, F3 (Figs. 1.11 and 1.13).

A generic description of the growth of βG I/17 on these permissive surfaces follows. At one day, βG I/17 cells, smaller than most immortal mammalian cells, exhibit an unremarkable attachment and spreading into irregular bipolar, three-pointed, or stellate shapes, with pronounced, neurite-like cytoplasmic processes [12, 47] (Figs. 1.10 to 1.13). Cells are dispersed. Doublets, triplets, and higher aggregates are rare at 24 hours. During days three to five, βG I/17 cells spread further, and grow rapidly by mitosis (Figs. 1.10 to 1.13). The underlying surface is never fully covered. Groups of spread cells have scalloped margins, leaving bare lacunae demarcated by cells. By days five to seven, most cells appear to be joined by cytoplasmic processes, large areas of nearly-confluent cells are seen, and it becomes increasingly difficult to distinguish individual cells (Figs. 1.10 to 1.13). A similar sequence of morphologic events has been observed when disaggregated islet cells from normal rats are grown in plate culture [201].

Emergent, multicellular domes then begin to appear, progressing to oblate, tethered

spheroids, apparently by combined processes of mitosis, aggregation, and local delamination of cell sheets. Incipient supra-confluent structures are visible at seven days along the margins of a delaminating cell sheet on etched borosilicate glass in Fig. 1.11. Multicellular character of these emergent structures is evident after Swiss-cocktail stimulation, formalin fixation, and staining with hematoxylin and eosin (Fig. 1.11). Occasionally, these large aggregates become lobulate, grow to macroscopic dimensions, and develop arms hundreds of microns in length (e.g., Fig. 1.14, day 5, taken at low magnification). In similar studies, I have sectioned such macroscopic aggregates and stained them, using standard histologic techniques. Internal regions of emergent structures deeper than approximately five to at most ten cell diameters from the surface of the cell mass show blebbing and nuclear fragmentation, followed by extensive death and disintegration of cells. Ultimately, these dead areas become hyalinized. DNA "laddering" indicates that this is a process of apoptosis and not necrosis (data not shown).

Similar observations have been made in studies of the rat insulinoma cell line, RINm5F [202], which was derived from the same tumor as the ancestors of βG I/17 (Fig. 1.2a). In such large, three-dimensional colonies, the endocrine βG I/17 and RINm5F cells do not appear to be polarized, and hollows do not develop, as is seen when some other types of secretory cells sprout emergent structures in plate culture [203]. In the present study and similar studies in my laboratory, domes and larger colonies of maturing βG I/17 cells sometimes break free from the surface. Such "floaters" might be lost during daily changes in media. Concomitant with the scattered and apparently stochastic development of domes, spheroids, and larger colonies at the

end of the week of culture, well-to-well variability in metabolic measurements tended to increase (data on glucose and lactate, infra).

I have seen this formation of three-dimensional structures and a loss of strong adherence to the substratum in maturing cultures of βG I/17 cells grown on other permissive materials, including tissue-culture polystyrene (TCPS, data not shown). Fong et al. [204] grew the closely rat insulinoma line, RINr, on TCPS. Morphology of their five-day cultures is strikingly similar to my own (compare their Fig. 2A to Figs. 1.10, 1.12, and 1.13 in the present work). Clark and Chick [205] also noted delamination of maturing RINr clusters. As described in detail above, RINr is ancestral to my βG I/17 [173] (Fig. 1.2a). A similar morphologic progression occurs when diverse lines of insulin-secreting cells from mice are grown on permissive surfaces [25, 206-208]. These findings of adhesion to surfaces by freshly-plated cells, followed by later aggregation and partial delamination, contrast sharply with studies of two related insulinoma lines from rats, RINm5F and BRIN-BD11, in which cultures grow on TCPS as a monolayer of well-spread, stellate cells [12, 88-89, 209]. Many, perhaps most insulin-secreting cell lines are unstable, and change their phenotype with time [10, 12, 15, 20, 68, 210, 211].

In the present study, growth form of βG I/17 correlated with some measures of metabolic performance (infra). But generalizations about form-function relationships in cultured insulinoma cells must be made with caution. Functional significance of the diverse growth morphologies observed when insulin-secreting cells are grown on permissive culture surfaces is uncertain [12, 169]. Confounding the interpretation of published studies is the apparent genetic heterogeneity of many insulin-secreting lines:

βG I/17 is clonal [173], but many other insulinoma lines are not [12, 27, 34]. Similarly, great caution must be exercised when making predictions about in-vivo performance from studies in vitro. Whether implanted into laboratory animals or humans, insulinoma cells encapsulated in an artificial endocrine pancreas exist under conditions substantially different from those experienced by the exponentially-growing plate cultures of the present study [212]. Further study is needed to ascertain whether slow-cycling, space-limited insulinoma cells are sensitive to biomaterials chemistry and morphology in vivo.

To my surprise, some aminofluorosiloxane surfaces of mixed character inhibited growth of βG I/17 cells. Depression of cell growth was most pronounced at a mole fraction of 2/3 F3, where cells never approached confluence (Figs. 1.11 and 1.15). Sparse aggregates of poorly-spread cells were visible at 24 hours (Fig. 1.15). Compared to cells grown on more permissive surfaces, cells on 2/3 F3 displayed an earlier tendency toward the formation of emergent domes and spheroids, often giving isolated small aggregates a "sunny-side-up, fried-egg" appearance (Figs. 1.11 and 1.15). In all these characteristics, βG I/17 cells grown on 2/3 F3 resembled cultures grown on the negative control, untreated polystyrene (Fig. 1.14). Thivolet et al. [213] made similar observations when they cultured the rat insulinoma line, RINm5F, on uncoated "plastic" dishes, which might have been untreated polystyrene. Phenotype of cells grown on mixed surfaces with a mole fraction of 5/6 F3 (not shown) was intermediate in appearance between the inhibitory 2/3 F3 (Fig. 1.15) and the permissive 100 % F3 (Fig. 1.13).

I have grown other types of mammalian cells on silanized surfaces of the N2-F3

series, and I have not yet found another case where the culture surface has such striking effects on cellular morphology. When grown under serum-containing medium, the human melanoma cell line, A-375 (American Type Culture Collection, Manassas, VA), for example, spreads and grows equally well on all surfaces of the N2-F3 series (data not shown).

1.3.6. Glucose consumption and lactate production

Metabolic data from assays of conditioned media correlated well with the qualitative observations of cell growth described above. βG I/17 insulinoma cells have a highly active metabolism, as measured by their consumption of glucose and production of lactate (Figs. 1.16 to 1.18). My plate cultures of βG I/17 cells grew so rapidly that by the end of the first week, they consumed more than half of the available glucose in 24 hours (Fig. 1.16). Related rat insulinoma (RIN) cell lines exhibit a similar voracious appetite for glucose, which is much higher than that of the native β cells from which they were derived [12]. In the later days of the present seven-day study, rapid glucose consumption produced so much lactate in 24 hours that the Phenol Red in the media changed from red to orange-yellow, indicating that the pH had dropped from ~7.4 to ~7.0. A plot of raw data of lactate and glucose concentration in one representative well shows the "saw tooth" profile (Fig. 1.16) characteristic of intermittently fed plate cultures. With appropriate scaling, the lactate profile would nearly mirror the glucose profile. Papas et al. [14, their Fig. 2c] reported a similar stoichiometry in glucose-lactate metabolism in cultures of the mouse insulinoma cell line, βTC3.

Roughly exponential plots of glucose consumption (Fig. 1.17) and lactate production

(Fig. 1.18) during the week of culture confirm observations of morphology (Figs. 1.10 to 1.15). Culture surfaces of glass, pure N2 (0/3 F3), 1/3 mole fraction F3, and pure F3 are permissive. Solid lines in Figs. 1.17 and 1.18 show data for cultures grown on these permissive surfaces. Untreated polystyrene and 2/3 mole fraction F3 are inhibitory, and 5/6 mole fraction F3 is intermediate. Broken lines in Figs.1.17 and 1.18 show metabolic data for the latter three, less-than-permissive surfaces.

Pancreatic β cells, hepatocytes, myocytes of skeletal muscle, K cells of the gut, and white adipocytes are key fuel-sensor cells in the human body. Any attempt to replace them with genetically engineered surrogates must include a consideration of their use of and response to metabolic fuels. Mammalian cells can exploit several biochemical pathways as energy sources in vitro and in vivo [214-216]. Insulinoma cells and normal β cells can switch among energy sources with changing conditions [215, 217-219]. The following account of energy metabolism by βG I/17 cells of the present study addresses several of the major metabolic pathways that yield high-energy molecules, such as adenosine 5'-triphosphate or ATP, when nutrient fuels are consumed.

In cultured vertebrate cells, oxidation of amino and fatty acids is often an important source of energy, especially the conversion of glutamine to glutamate, which in turn enters the citric-acid cycle as α-ketoglutarate [216]. This pathway is said to provide a major energy source in many mammalian-cell-culture systems [216, 220], especially tumoral cells, such as the rat insulinoma line, RINm5F [144, 214]. Catabolism of glutamine by this route generates the toxin, ammonia [216, 221]. When fresh, my cell-culture medium, based on Medium 199, contained approximately 0.6 mM glutamine,

which is relatively sparse in comparison to many other conventional media used for mammalian cell culture. Late in the present study, I determined that βG I/17 cells consumed glutamine and produced ammonia when cultured on the N2-F3 series of surfaces, but I was unable to fully develop assays for these labile metabolites before samples of conditioned media were degraded by repeated freeze-thaw cycles (data not shown).

Complete catabolism of glucose to carbon dioxide via glycolysis, the citric-acid cycle, and the electron-transport chain requires oxygen, but yields a large amount of energy, typically 36 to 38 moles of ATP per mole of glucose [216, 220, 222]. Aerobic mitochondrial respiration is known to occur in native pancreatic β cells [215, 218, 223-225] and in the insulinoma lines derived from them [61, 223-226].

Alternately, glucose can undergo catabolism to pyruvate, and then to lactate. Glycolysis to lactate yields relatively little energy, only two moles of ATP per mole of glucose consumed [216, 220, 222], but this chain of reactions is rapid, and can proceed under anaerobic conditions. "Most of the glucose consumed by mammalian cells cultivated in vitro is converted to lactate" [221]. Normal pancreatic β cells and insulinoma cells are known to express the enabling enzyme, lactate dehydrogenase or LDH [215, 217-218, 223-224, 226]. In a third pathway of glucose catabolism, conversion of glucose to glucose-6-phosphate, then to ribulose-5-phosphate, and subsequent steps in the pentose-phosphate shunt can provide substantial metabolic energy to some specialized mammalian cells [214, 227]. Though I did not assay for the distinctive intermediates of the pentose-phosphate shunt, this shunt is not suspected to be a dominant energetic pathway in natural islet β cells or insulinoma cells [215, 223,

226, 228].

The molar ratio of lactate produced to glucose consumed provides a useful measure of cell metabolism in vitro [220]. In the present study, the roughly two-to-one stoichiometry of production of the triose, lactate, to consumption of the hexose, glucose, remained relatively stable throughout the week of culture (Figs. 1.16 to 1.21). This suggests that catabolism of glucose to pyruvate to lactate was a significant energetic pathway in these rapidly growing cultures of insulinoma cells. To facilitate comparison, data on consumption of glucose and production of lactate during the seventh day of culture are plotted as a function of surface composition in Fig. 1.19. Analysis of lactate and glucose data (Fig. 1.19) with the Tukey-Kramer HSD statistic separated cultures into three exclusive groups, based on identity of their culture surfaces: Group A surfaces are permissive, those in Group B are inhibitory, and surfaces with a mole fraction of 5/6 F3 are intermediate (Group C). Group separations were significant at $p < 0.05$. These correspond to the three classes defined by growth morphology.

βG I/17 cells grown on permissive surfaces converted more glucose to lactate than those grown on inhibitory or intermediate surfaces. The molar ratio of glucose consumed to lactate produced was > 1.90 for cultures grown on the permissive aminofluorosiloxane surfaces (Fig. 1.20), indicative of a highly anaerobic metabolism. Cultures on the other permissive surface, alkaline-etched borosilicate glass, were similar, and produced an average of 1.84 moles lactate per mole glucose (Fig. 1.20). Cultures on the inhibitory and intermediate surfaces averaged less than 1.80 moles lactate per mole glucose. Many paired comparisons were significant (Tukey-Kramer HSD test, $p < 0.05$, Fig. 1.20).

Thus, in the present study, a picture emerges that rapidly growing cultures tended to be more anaerobic in their metabolism than cultures with slower growth. Confirming this, a cross plot of glucose consumption and the lactate/glucose ratio (Fig 21) shows a weak, positive correlation between these two variables (r^2 ~0.6), and a separation of data into groups based on the permissiveness of the growth surface. Constantinidis and coworkers [229] observed a similar relationship between growth morphology and glucose/lactate metabolism when they compared gel-entrapped and plate cultures of the mouse insulinoma cell line, βTC3.

Poorly differentiated rat insulinoma lines, such as RINm5F, are known to express much higher levels of lactate dehydrogenase (LDH) than natural islet β cells or well-differentiated insulinoma lines, such as INS-1 from rats, and MIN6 from mice (Figs. 1.2a and b) [219, 224-225, 230]. Some RIN lines show high conversion of glucose to lactate, with only minor reliance on aerobic oxidation of glucose to CO_2 [224, 231]. Under the conditions of the present study, this appears to be the case with the engineered RIN line, βG I/17. Combined effects of hypoxia and proliferation in vitro might stimulate elevated expression of LDH, which is observed during the initial establishment of a wide variety of mammalian cell lines [227]. When oxygen concentration is decreased, one mouse insulinoma line, βTC3, shows an increasing ratio of lactate production to glucose consumption in vitro [14]. This ratio approaches 2.0 under complete hypoxia [232]. In studies similar to the present investigation, I have observed that the lactate/glucose ratio of βG I/17 cultures falls well below 2.0 when aeration is improved by convection or by increasing the oxygen concentration in the

headspace of the flask (data not shown). Together, these observations suggest that the oxygen supply might have been suboptimal in the present study, possibly due to the depth of the liquid medium. Freshney made a general recommendation that media be no deeper than 2 to 5 mm in stagnant cultures of vertebrate cells [233]. Liquid medium was at least 6 mm deep over my cultures, and this might have posed a diffusional barrier to oxygenation of the highly active βG I/17 cells.

1.3.7. Secretion of human insulin

All cultures in this study secreted 17 or more nanograms of human insulin per well per hour on the seventh and final day of culture (Fig. 1.22). Moreover, all cultures grown on aminofluorosiloxane surfaces showed a higher mean seventh-day and Swiss-cocktail-stimulated insulin secretion than cultures grown on the two reference materials, etched glass and untreated polystyrene. Insulin secretion was highest when the transgenic insulinoma cells were grown on the three surfaces with the highest fluorine content (Fig. 1.22 and Table 1.2).

Fig. 1.22 illustrates an important limitation of extant the insulinoma cell lines that are candidates for therapeutic use in the artificial endocrine pancreas. In the present study, cells in routine culture secreted maximal levels of insulin. That is, secretion stimulated by the Swiss cocktail of secretagogues was no different than secretion during normal culture (Fig. 1.22). Fresh media in the present study had glucose concentrations (10.4 mM) well above the diabetic threshold for human plasma (~7.8 mM), so maximal insulin secretion was appropriate in fresh media. But maximal insulin secretion by βG I/17 apparently persisted when glucose was depleted down into the range of plasma from normal humans (~3.9 to 6.1 mM). Ideally, a cell used in an artificial pancreas

would cease insulin secretion when normoglycemia was attained. In fact, βG I/17 and many other rodent insulinoma cell lines exhibit glucose-stimulated insulin secretion, but the glucose-response curve is shifted far to the left of the curve characteristic of the β cells of healthy pancreatic islets. That is, insulin secretion is hyper-stimulated under normoglycemia, and insulin secretion is not "turned off" until perilously low glucose concentrations are reached, often < 1 mM [10, 11, 68, 83-84, 172, 234]. A human patient with plasma glucose levels this low would be dangerously hypoglycemic and at risk of convulsions, ketoacidotic coma, and death. Engineering appropriate glucose-stimulated insulin secretion into transplantable cells is a central focus of current efforts in this field [10, 12, 21, 27-28, 43-44, 56, 59, 60-62, 172, 225]. Unfortunately, most cellular engineering efforts to date have resulted in β-cell surrogates with maximal insulin secretion at micromolar, not millimolar concentrations of environmental glucose [61].

Cell biologists evaluating responsiveness to secretagogues by primary pancreatic β cells, insulinoma cells, hepatocytes, hepatoma cells, and similar secretory cells often examine the ratio of stimulated to basal secretion [10, 12, 27-28, 31, 51, 61-62, 84, 172, 235]. In the present study, the "fold stimulation" was similar for βG I/17 cells grown the two reference materials, etched glass and untreated polystyrene (2.3- and 2.4-fold, respectively; Fig. 1.23). This surprised me, since the insulinoma cells showed strikingly divergent morphology and glucose-lactate metabolism on the two materials. In all cases, the mean responsiveness of βG I/17 cells grown on N2-F3 surfaces was ~3-fold or greater. The broad similarity in responsiveness between cells with a spread

morphology (e.g., those grown on glass and 0/3 F3) and a rounded morphology (e.g., 2/3 F3 and untreated polystyrene) contrasts with the results of Grampp et al. [234], in which the mouse insulinoma, βTC3, showed better responsiveness when spread, rather than crowded. In the present study, mean responsiveness averaged high as 5.0-fold for cultures propagated on the pure F3 surface, a significant departure from the two control materials ($p < 0.05$; Fig. 1.23).

Once again, these data illustrate limitations of βG I/17 as a potential islet surrogate. When subjected to the same regimen of diazoxide inhibition, followed by Swiss-cocktail stimulation, natural human β cells and the newer rat insulinoma line, βG11/3E9, a descendant of βG I/17, can show a greater-than-19-fold stimulation of insulin secretion [28].

I was intrigued to find high insulin secretion in the 2/3 F3 wells (Fig. 1.22), even though there were seemingly fewer cells in these wells, as estimated by gross observation and photomicrography (Figs. 1.11 and 1.15), and by assays of glucose-lactate metabolism (Figs. 1.17 and 1.18). Note especially that while the untreated-polystyrene control wells showed growth morphology, glucose consumption, and lactate production similar to the 2/3 F3 wells, and apparently had a similar number of cells, mean insulin secretion was much lower in cultures grown on untreated polystyrene. Human insulin secreted per cell was apparently higher in cultures grown on the 2/3 F3 materials than those propagated on the other materials examined in this study, during both routine culture and "Swiss-cocktail" stimulation. While no attempt was made to assay cell numbers per se at the end of this study, it might be instructive to

examine insulin secretion as a function of glucose consumed in the final day of routine culture (Fig. 1.24). In exponentially-growing, regularly-fed plate cultures such as these, I have found that glucose consumption is grossly indicative of cell number (data not shown). Regardless of whether glucose consumption is interpreted as an indicator of cell number [64] or not, the ratio of insulin produced to glucose consumed is of interest to those using insulinoma cells to produce human insulin in bioreactors [27, 44, 64, 234].

Insulin/glucose ratios were highest when βG I/17 cells were cultured on the more-highly-fluorinated members of the N2-F3 series, peaking at 2/3 F3 (Fig. 1.24). Cultures on untreated polystyrene were intermediate in rank between the aminofluorosiloxanes with a high insulin/glucose ratio (i.e., those with a mole fraction > 50 % F3) and those with a lower insulin/glucose ratio (i.e., surfaces relatively rich in N2 residues). Surprisingly, during both routine culture and "Swiss-cocktail" stimulation, the ratio of insulin secreted to glucose consumed was lowest on the classic permissive material, glass (Fig. 1.24).

1.4 Discussion

1.4.1. How might the surface influence growth and function of βG I/17 insulinoma cells?

Table 1.2 summarizes the results of this study. As I had hoped, I was able to control the surface chemistry by adjusting the reaction mixture. ESCA and FITC binding confirmed this (Figs. 1.3 and 1.4). Topography of silanized surfaces was insular and complex, though their root-mean-square roughness did not differ significantly from that of smooth glass (Figs. 1.8 and 1.9). Surfaces richest in trifluoropropyl residues were the

most hydrophobic ($\theta_A \geq 90$ °, Fig. 1.6), and I was surprised that they supported cell growth and function. A priori, I had expected F3-rich surfaces to be poor culture supports (supra). Not only did βG I/17 insulinoma cells grow on F3-rich surfaces, but the pure F3 surface supported cell growth and glucose-lactate metabolism equivalent to the positive control, alkaline-etched borosilicate glass (Figs. 1.10, 1.13, 1.11, 1.17, 1.18, 1.19, and 1.21). Most surprising of all, cultures grown on surfaces richest in -$CH_2CH_2CF_3$ residues showed the highest secretion of human insulin (Figs. 1.22, 1.24), and, in the case of the pure F3 surface, improved responsiveness to secretagogues (Fig. 1.23).

Mammalian cells that can be grown on artificial materials generally do best when the surface has an advancing water contact angle, θ_A, between 20 and 60 ° [115], though exceptions are known [142, 131]. The 20-to-60 ° range includes tissue-culture polystyrene, the dominant commercial culture material in the world today. Why do βG I/17 cells grow and function well on the hydrophobic, F3-rich materials ($\theta_A \geq 90$ °, Fig. 1.6)?

1.4.2. Does cell spreading influence insulin secretion?

While the cell-culture phase of the present study was underway, my attention was first drawn to the observed correlation of a spread phenotype with rapid growth. Cell shape is suspected to be an important determinant of growth and function for many types of vertebrate cells, including such secretory cells as hepatocytes and mammary epithelium [10, 203, 236-238]. Several insulin-secreting cells are known to exhibit such form-function relationships, including the rat insulinoma line, RINm5F [20, 88-89, 145,

213, 234, 239-241]. In this study, βG I/17 insulinoma cells showed striking differences in morphology when cultured on surfaces ranging from the pure diaminosilane (viz., 0/3 F3) to the pure trifluoropropyl silane (3/3 F3), particularly over the narrow range between 2/3 F3 to 3/3 F3 (Figs. 1.11, 1.12, 1.13, and 1.15, and Table 1.2). Webb et al. [127] recently suggested that cell behavior is sometimes "surface chemistry dependent, and [varies] with individual functional groups rather than general surface properties such as wettability."

But while it is true that βG I/17 cells grew more rapidly when spread than when rounded, the three cultures with the highest insulin production (Fig. 1.22) had cell morphologies that were variously rounded (2/3 F3), well spread (3/3 F3), and intermediate (5/6 F3). Moreover, cultures with similar morphologies and similar glucose-lactate metabolism, but grown on other materials, produced less insulin (e.g., spread cells on glass, rounded cells on untreated polystyrene).

Together, these observations prompted me to shift my attention away from cell shape as a proximate cause of increased insulin secretion by βG I/17 cells grown on surfaces rich in trifluoropropyl groups.

Instead, I wonder whether cell function was influenced by:

- soluble siloxane oligomers of monomer F3.
- surface density and mobility of the trifluoromethyl group ($-CF_3$), or
- cell-adhesion ligands adsorbed or secreted onto the surface.

Let us examine these three hypotheses in more detail.

1.4.3. Do eluted F3 oligomers promote insulin secretion?

It is conceivable that F3 monomers or oligomers came off of the glass surface during

the week of culture and that the eluted substances or condensates thereof had drug-like effects on the βG I/17 insulinoma cells (Figs. 1.25 and 1.26). In this scenario, F3 oligomers might have influenced such phenotypic traits as the amount of insulin secreted and responsiveness to the Swiss cocktail of secretagogues.

As noted above in sections 1.2.3. and 1.3.2., all silanized surfaces are inherently unstable in water. The heat-annealing protocol developed in the present study permitted the creation of surfaces that were far more stable in water than surfaces created by silanization alone. Still, in aqueous media, over time, all such polysilane films are inherently susceptible to hydrolysis by water. This applies to all silanized systems exposed to water, including clinical dental varnishes and coupling agents used to bond industrial polymers to glass fillers. Decades of work on industrial coupling agents have failed to overcome this fundamental property of materials whose fabrication relies on chemisorption of silanes to glasses, ceramics, or minerals.

Certain siloxane oligomers, especially small cyclic compounds, are known to exert biologic effects, both in vitro and in vivo [130, 242-245] (Fig. 1.27). This includes small cyclic silicones bearing the trifluoropropyl group employed in monomer F3 of the present study (Figs. 1.1 and 1.27). In particular, some cyclic polysiloxanes are known to have potent estrogen-like effects in mammals [249]. Insulin production by natural β cells and insulinoma cells is responsive to many known polypeptide and steroid hormones [250], and might conceivably be influenced by silane oligomers.

The hypothetical F3 condensation products proposed in Fig. 1.26 would be poorly soluble in aqueous media, but such fluorinated silsesquioxanes might be able to form and persist in solution in the lipid bilayer of cell membranes. Even still, the doses

would be vanishingly small. Of the hypotheses I have proposed to explain enhanced insulin secretion on F3-rich surfaces, drug-like effects of eluted F3 oligomers seem to be the least likely.

1.4.4. Do solid-phase trifluoropropyl residues promote insulin secretion?

Based on previous work, it is tempting to speculate that the pendant functional group on F3-rich surfaces, $-CH_2CH_2CF_3$, might promote tight binding or favorable conformations of physisorbed proteins [251-252]. Steele, Griesser, and their coworkers have demonstrated that relative affinities and binding states of adsorbed cell-adhesion proteins can in turn influence cell function [142, 150]. The ways in which the terminal $-CF_3$ group is tethered to the surface and the chemical nature of the underlying and surrounding groups all appear to be important determinants of protein binding to surfaces bearing the trifluoromethyl group. Horbett, Hoffman, and their coworkers have previously observed that $-CF_3$ groups created by certain radio-frequency, glow-discharge (RFGD) plasmas seem to favor tight binding by a variety of proteins [251-252], while the $-CF_3$ groups on the surface of perfluorinated poly (ethylene-co-propylene) or FEP do not [158].

It is tempting to speculate that mobility of $-CF_3$ groups might affect the tightness with which proteins adsorb to surfaces bearing this group. In the FEP molecule, $-CF_3$ groups are bound directly to the polymer's rigid backbone ($-CF_2CF-$), without tethers. Atomic-scale morphology of fluorine-rich deposits created by RFGD plasmas is indeterminate. In the present study, it seems possible, though unlikely, that the short ethylene tethers ($-CH_2CH_2-$) could provide their $-CF_3$ termini with a mobility that favors strong interaction with the fatty milieu of cell membranes.

Rather than a direct cell-surface interaction, $-CF_3$ groups might modulate cellular response via adsorbed proteins. Proteins adsorbing to hydrophobic surfaces tend to undergo a high degree of conformational change, favoring unfolding, multi-point attachment, and tight binding [252-253]. Mobile $-CF_3$ groups might conceivably enhance these conformational changes and binding events. As discussed above in the section on atomic-force microscopy, the short F3 residues employed in the present study probably form random or dispersed networks, without discernible microstructure [181]. Interestingly, surfaces silanized with longer, fluorine-rich monomers, such as $-(CH_2)_8(CF_2)_9CF_3$ [107] and $-(CH_2)_2(CF_2)_5CF_3$ [112], do not support growth and function of mammalian cells, possibly because these residues have a greater tendency toward self assembly into crystalline structures, reducing the mobility of their $-CF_3$ termini. Alternately, condensed phases of these long, fluorine-rich residues might attract tight binding by albumin, which does not favor cell spreading and growth [198, 254].

Tightness of protein binding might also be affected by the nanometer-scale, insular morphology of the F3-silanized surfaces (Fig. 1.8). Investigators examining protein adsorption to surfaces with silane gradients [114, 191, 255-257] have commented on the patchy nature of silane residues [191]. Anomalously tight protein binding in transition regions led one group to speculate, "such increased adsorption affinity of an amphiphilic molecule can be envisaged if such a molecule can interact with hydrophobic and hydrophilic adsorption sites simultaneously" [255]. Thus, in the present study, boundaries between un-silanized glass and islands rich in $-CF_3$ groups (Fig. 1.8) might have constituted sites that favored strong adsorption of cell-adhesion proteins. Protein ligands bound tightly or in favorable conformations might have in turn

influenced the secretory phenotype of βG I/17 cells.

1.4.5. Do cell-adhesion ligands adsorbed or secreted onto the surface favor promote insulin secretion?

Which cell-adhesion ligands are used by native islet β cells and the insulinomas derived from them? In vivo, the connective tissue supporting pancreatic islets contains collagens, laminins, and fibronectins. Interactions between pancreatic endocrine cells and their extracellular matrix, or ECM, might influence such processes as embryogenesis, proliferation, secretion, inflammation, healing, neoplasia, senescence, apoptosis, and necrosis [17, 258-265].

In vitro, islets of Langerhans, purified beta cells, and insulinoma cells from mammals, as well as the homologous cells from birds, typically grow and function well on surfaces or inside gels comprising collagen, fibronectin, laminin, or ECM [17, 24, 39, 51, 57, 69, 86, 202, 205, 208, 213, 235, 239-240, 259, 265-279]. The present study is one of many to demonstrate that some mammalian insulinoma cell lines will spread and grow on glass when cultured under serum-containing medium, a source of such attachment factors as vitronectin, fibronectin, and laminin [142, 150].

Which cell-surface receptors mediate interactions of the islets and insulinomas with their surrounding ECM? Islets, adenomas (benign tumors), and carcinomas (malignant tumors) of the human pancreas express laminin and laminin receptors in vitro and in vivo (e.g., α6β4, α3β1, α6β1), including some primary insulinomas [264, 275, 280-285]. The present study employed rodent cell lines. Fewer data are available for rodents. Rodent islets and at least some rodent insulinoma lines express laminin and laminin receptors, including various combinations of the α3, β1, and α6 integrin

subunits [42, 241, 266, 285-286, and my unpublished results].

Effects of integrin-ECM interactions on the secretory phenotype of insulin-secreting cells are largely unknown and in need of further investigation. Even in long-term culture, βG I/17 and similar rodent insulinoma lines secrete very little ECM of their own. When designing artificial endocrine organs containing transgenic insulinoma cells, it might be advantageous to provide the cells with an appropriate ECM in the form of fibers, gels, or surface coatings. This hypothesis is examined in Chapter 2.

1.5. Conclusions

In this study, I was surprised to find that βG I/17 insulinoma cells grown on surfaces richest in the trifluoropropyl group, $-CH_2CH_2CF_3$, exhibited the greatest insulin secretion and responsiveness to secretagogue drugs (Table 1.2).

Polymers bearing trifluoropropyl residues might therefore be attractive candidates for use in the artificial endocrine pancreas. Silicone polymers that include this pendant group have been used clinically in contact lenses, voice prostheses, and a variety of soft-tissue implants [244, 247-248, 287-290].

Four hypotheses were generated to explain the improved insulin secretion by βG I/17 insulinoma cells grown on F3-rich surfaces:

1. Cell spreading influences insulin secretion.
2. Eluted F3 oligomers promote insulin secretion.
3. Solid-phase trifluoropropyl residues promote insulin secretion.
4. Cell-adhesion ligands adsorbed or secreted onto the surface promote insulin secretion.

In view of the available data, the fourth hypothesis seems to offer the best

explanation of enhanced insulin secretion by βG I/17 cells grown on F3-rich surfaces.

This hypothesis is explored in Chapter 2.

1.6. Tables

Table 1.1. ESCA characterization of borosilicate glass surfaces after cleaning, etching, and two different organosilanizations (atomic percentages). *Theoretical values. **Approximate values.

	Glassmaker's nominal formulation*	Acetone-rinsed glass	Detergent-washed glass	Alkaline-etched glass	Silanized with 0/3 F3 (100 % N2)	Silanized with 3/3 F3 (100 % F3)
O	61.79	53.2	49.4	57.0	48.8	49.4
Si	22.60	22.8	21.8	24.4	24.3	23.9
Na	4.04**	4.5	3.0	2.6	2.3	1.9
B	4.50	3.0	3.4	2.5	2.8	1.9
K	2.66**	2.4	1.3	1.5	0.6	1.0
Al	1.23	1.5	2.0	1.6	2.1	1.9
Zn	1.67	1.5	0.6	1.0	0.6	0.6
Ti	1.44	0.6	0.6	0.6	0.4	0.6
Sb	0.07	0.0	0.0	0.0	0.0	0.0
S	0.00	0.0	0.8	0.0	0.0	0.0
N	0.00	0.0	1.4	0.0	2.5	0.4
F	0.00	0.0	0.0	0.0	0.0	8.1
C	0.00	10.5	15.8	8.9	15.6	10.4

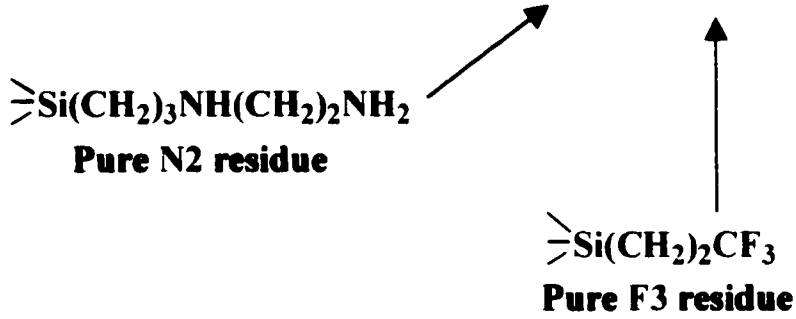

Table 1.2. Summary of physical and biological studies of silanized surfaces and two reference materials. nd = experiment not done. ESCA = electron spectroscopy for chemical analysis. UPS = untreated polystyrene. Contact angles on glass refer to freshly flamed material.

	Etched glass	0/3 F3	2/3 F3	3/3 F3	UPS
Atomic ratio (F/F+N) by ESCA	0 %	0 %	72 %	96 %	nd
Reactive amines by FITC binding	nd	high	low	trace	nd
Advancing water-contact angle, θ_A	< 10 °	83 °	99 °	90 °	nd
Receding water-contact angle, θ_R	< 10 °	57 °	76 °	72 °	nd
Contact-angle hysteresis, θ_H	< ~5 °	26 °	23 °	18 °	nd
Roughness by AFM, root-mean-square	0.32 nm	1.1 nm	1.0 nm	0.58 nm	nd
Morphology at nanometer scale	smooth	islands	islands	islets	nd
Growth rate, βG I/17 insulinoma	rapid	rapid	slower	rapid	slower
Growth form, βG I/17 insulinoma	spread	spread	round	spread	round
Formation of emergent cell aggregates	late	late	early	late	early
Glucose consumed, day 7	high	high	lower	high	lower
Lactate produced, day 7	high	high	lower	high	lower
Moles lactate/mole glucose, day 7	1.85	1.95	1.76	1.91	1.79
Insulin secreted, day 7	modest	higher	highest	highest	modest
Secretagogue sensitivity (Swiss/basal)	< 3.5 ×	< 3.5 ×	< 3.5 ×	> 5.0 ×	< 3.5 ×
Insulin secreted per glucose consumed	modest	modest	highest	highest	modest

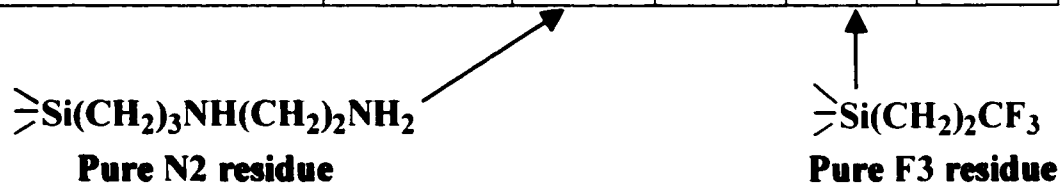

1.7. Figures

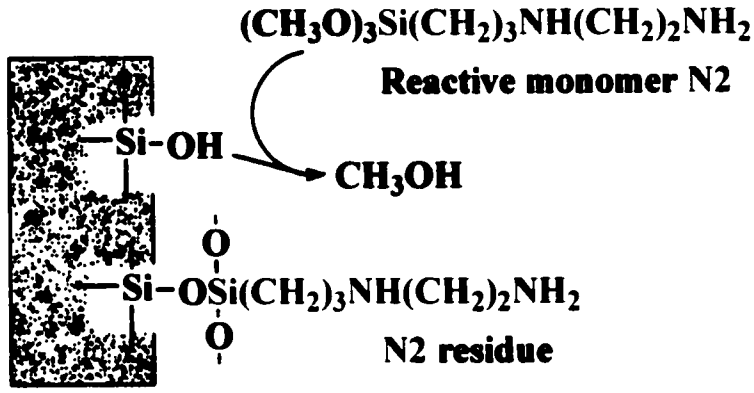

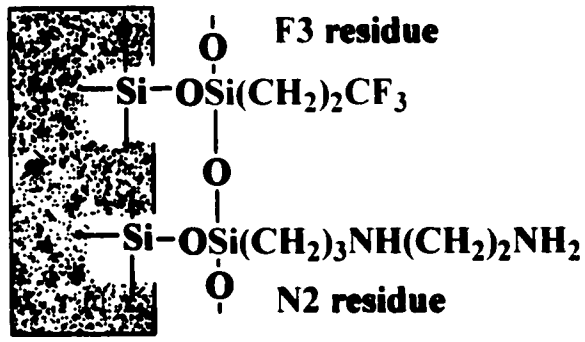

Figure 1.1. Silanization of etched borosilicate glass with monomers N2 and F3. A monolayer is shown for simplicity. Silanized surfaces are in fact patchy (see text).

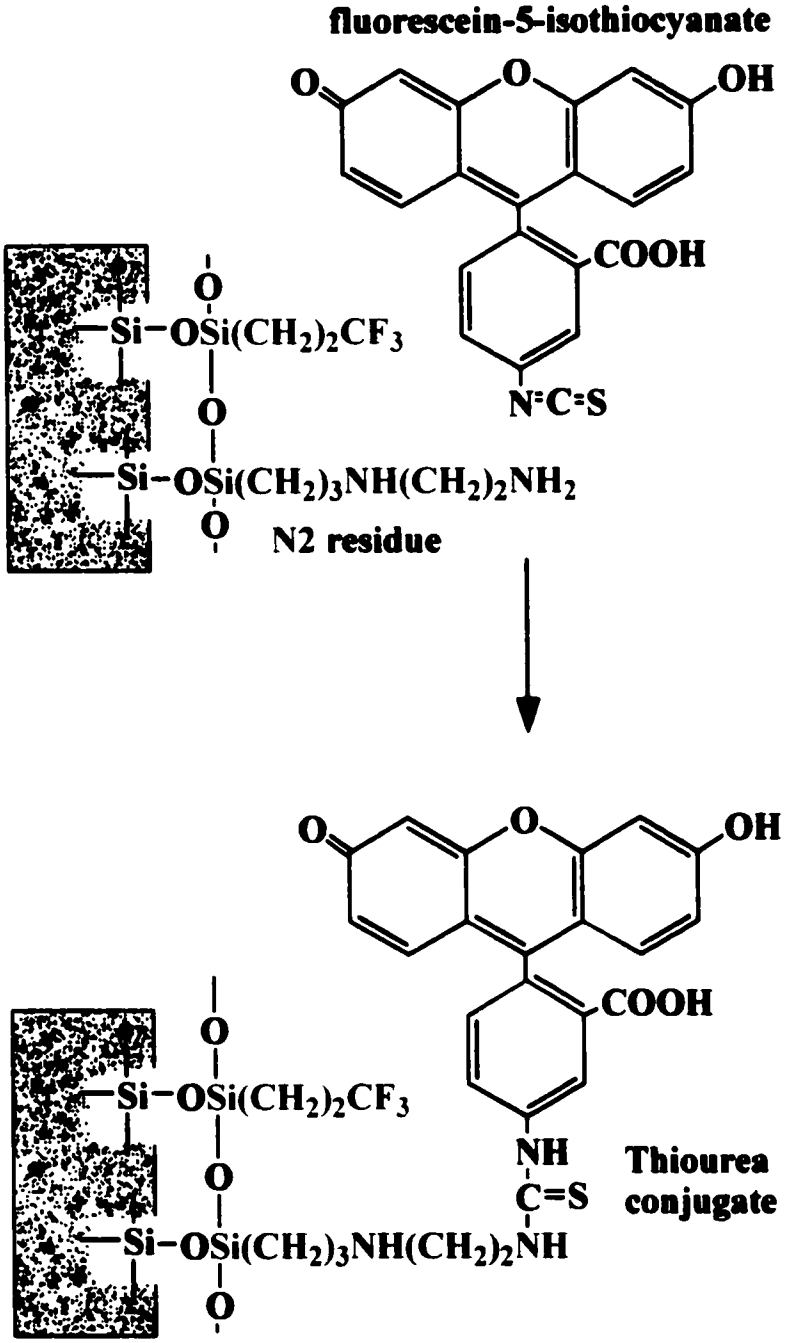

Figure 1.2. Reactivity of aminosiloxane (N2) residues with fluorescein-5-isothiocyanate.

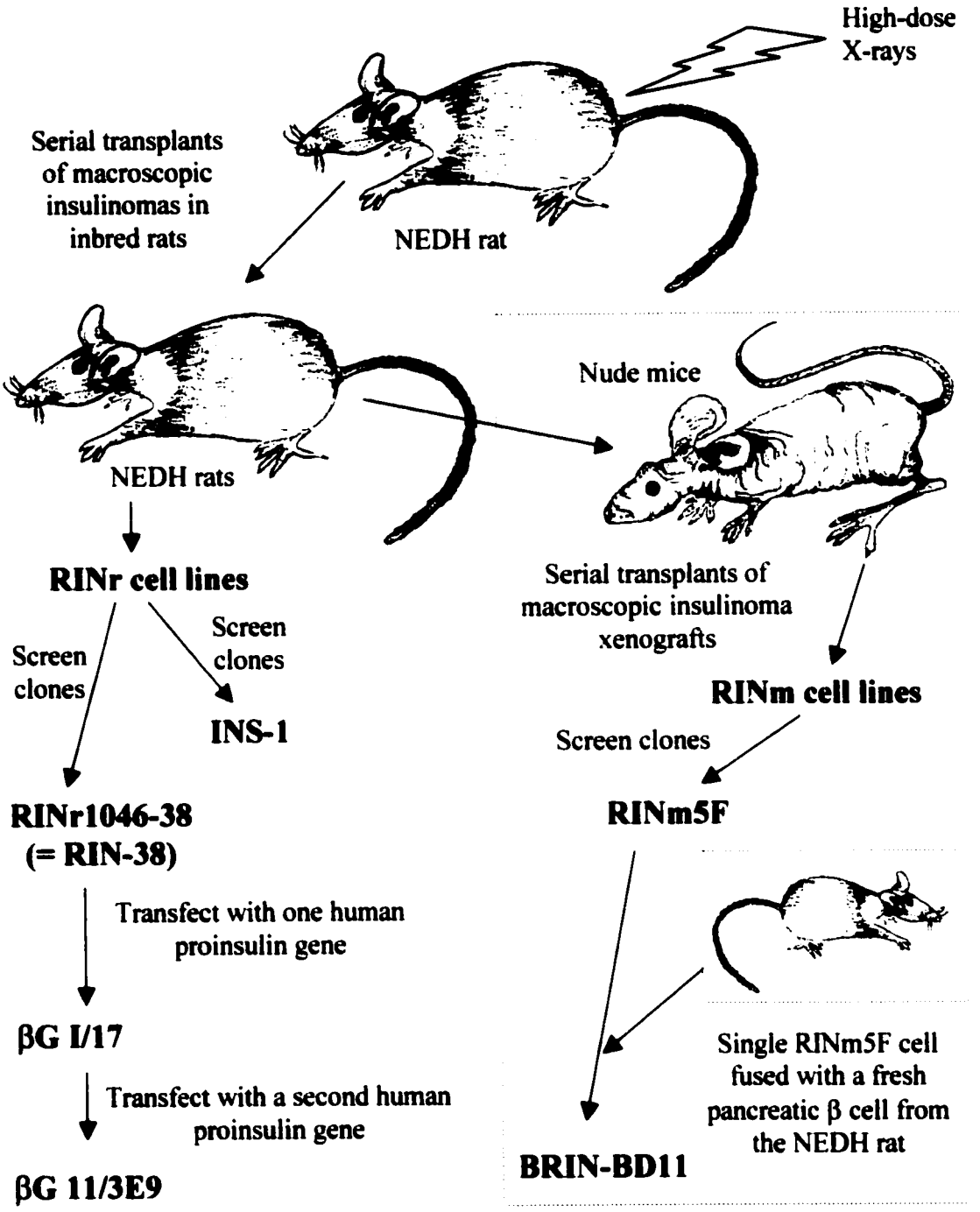

Figure 1.2a. Interrelationships among rat insulinoma (RIN) cell lines discussed in the text. All derive from a single, radiation-induced tumor in the New England Deaconess Hospital (NEDH) rat [167-168, 173, 209]. These and related RIN lines have become mainstays of diabetes research, worldwide. RIN line βG I/17 was used in the present study.

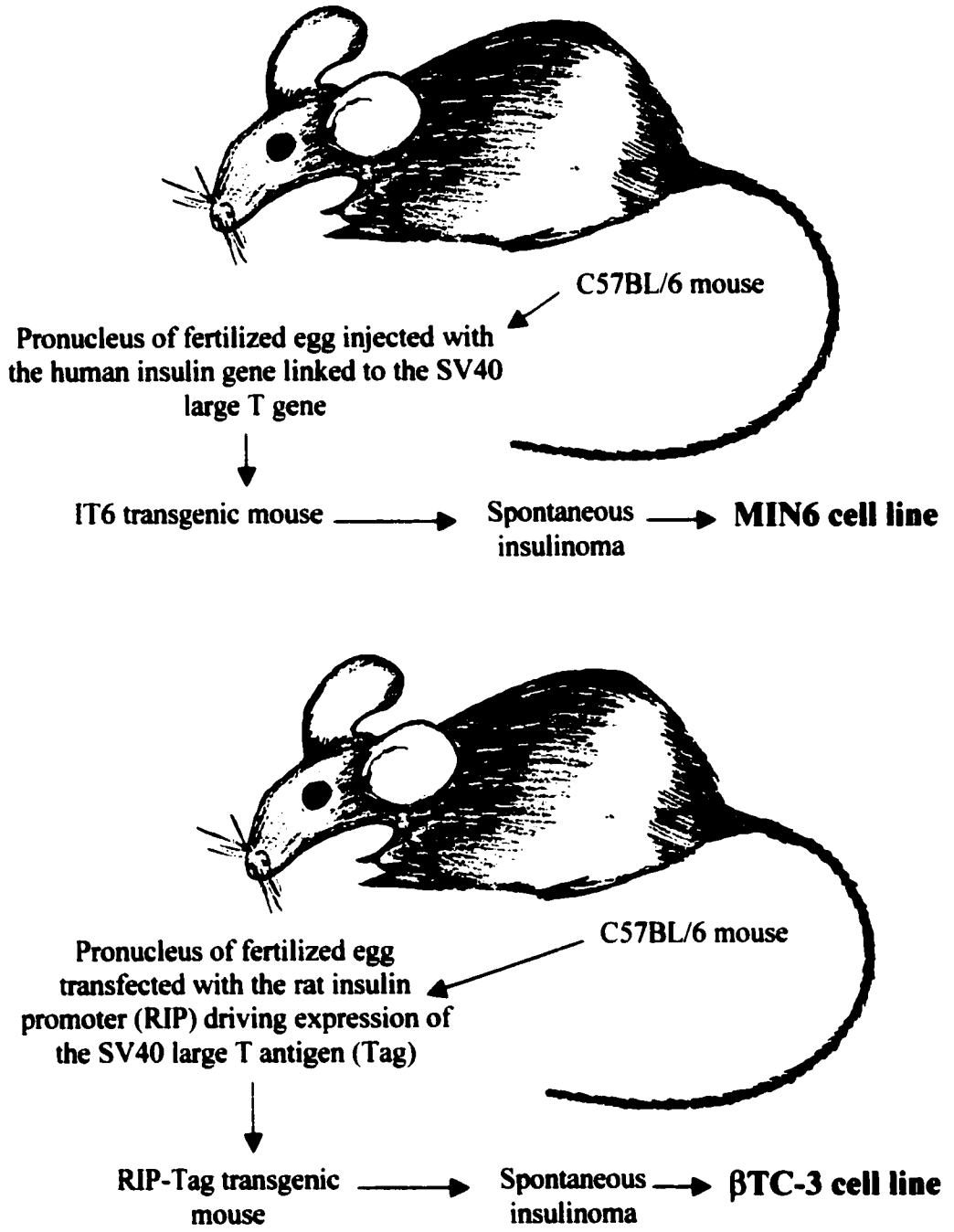

Figure 1.2b. Derivations of mouse insulinoma cell lines discussed in the text [14, 20, 206-207, 229, 232, 234]. Both development efforts relied on the same oncogene, the simian virus 40 large tumor antigen (SV40 T), to effect cellular transformation.

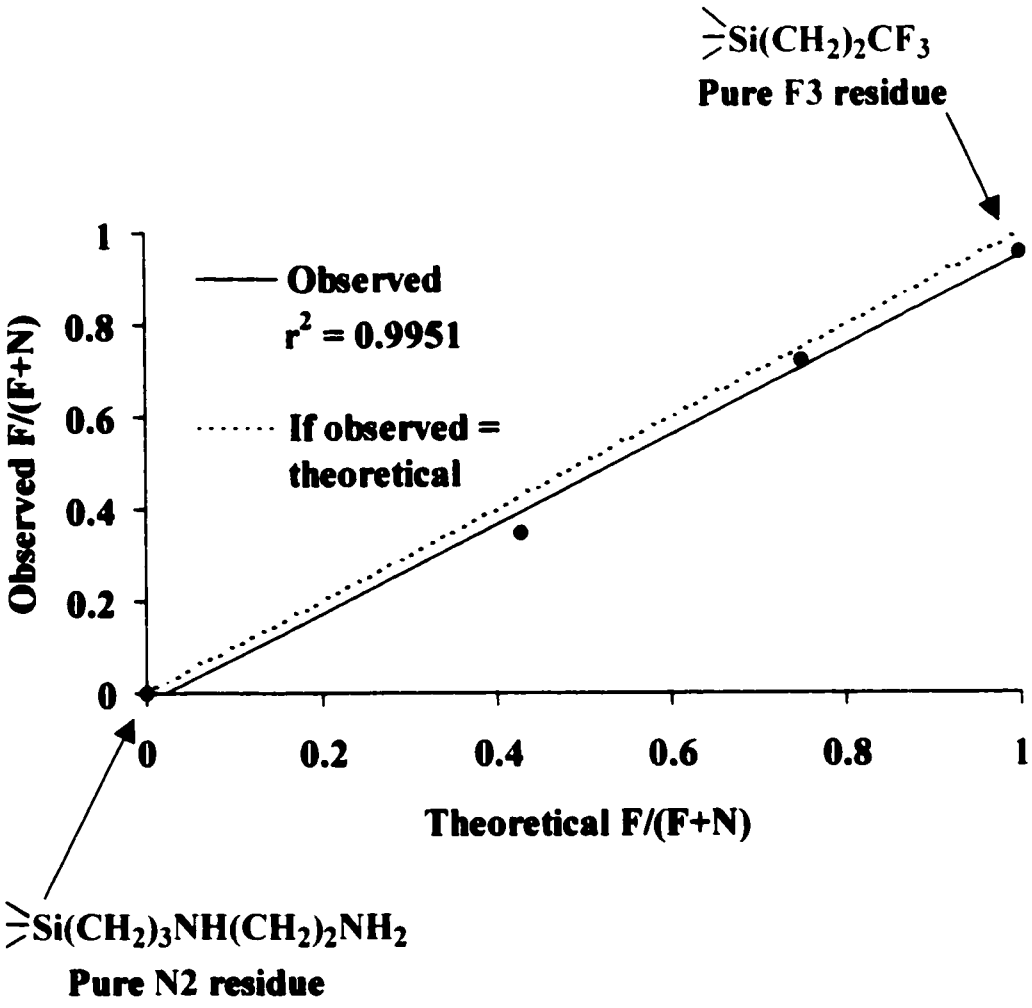

Figure 1.3. Normalized ESCA data on atomic percentages of nitrogen (N) and fluorine (F) in mixed aminofluorosiloxane surfaces, expressed as the ratio F/(F+N).

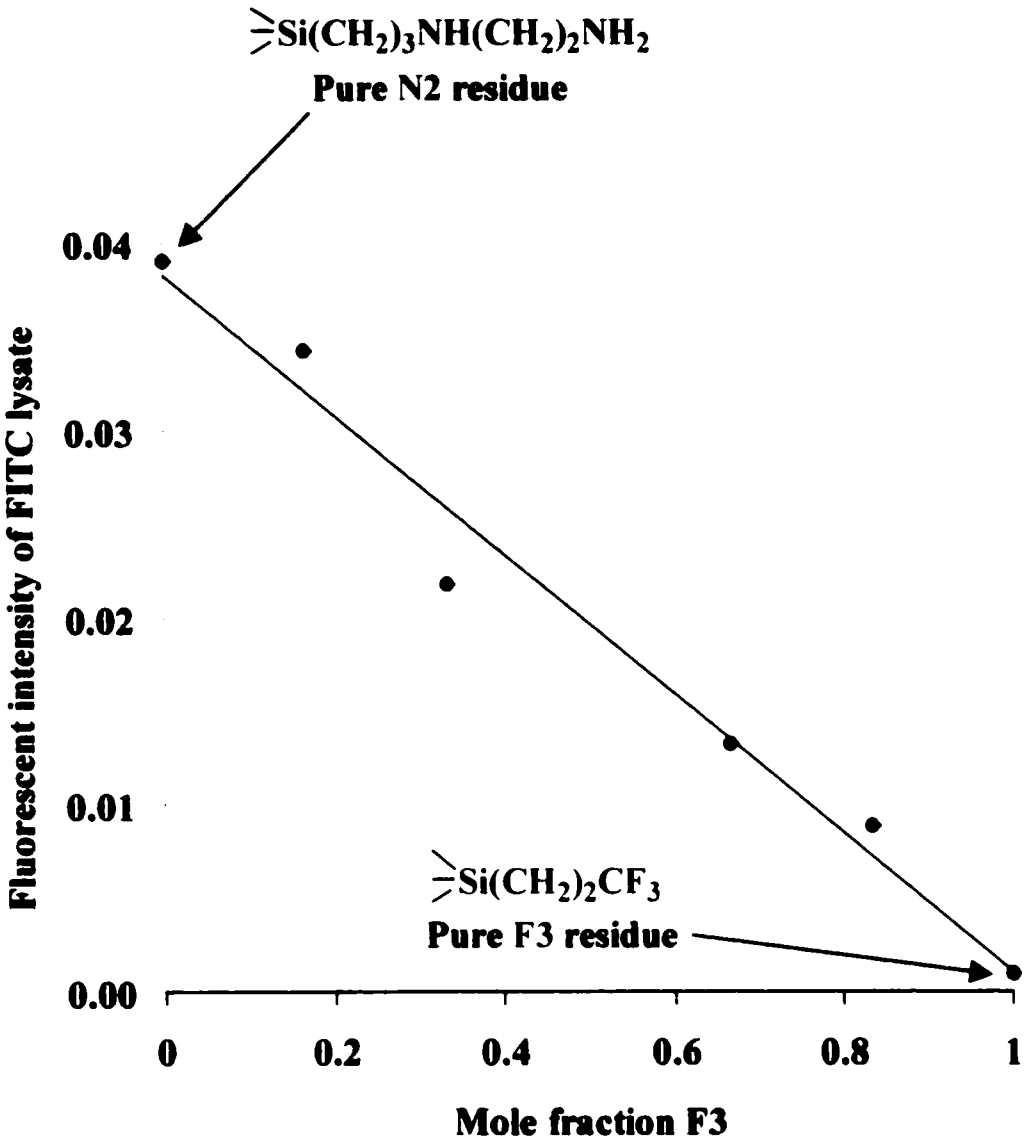

Figure 1.4. Decrease in binding and subsequent lysis of fluorescein-5-isothiocyanate residues in silanized surfaces with increasing mole fractions of the trifluoropropyl residues ($r^2 = 0.977$).

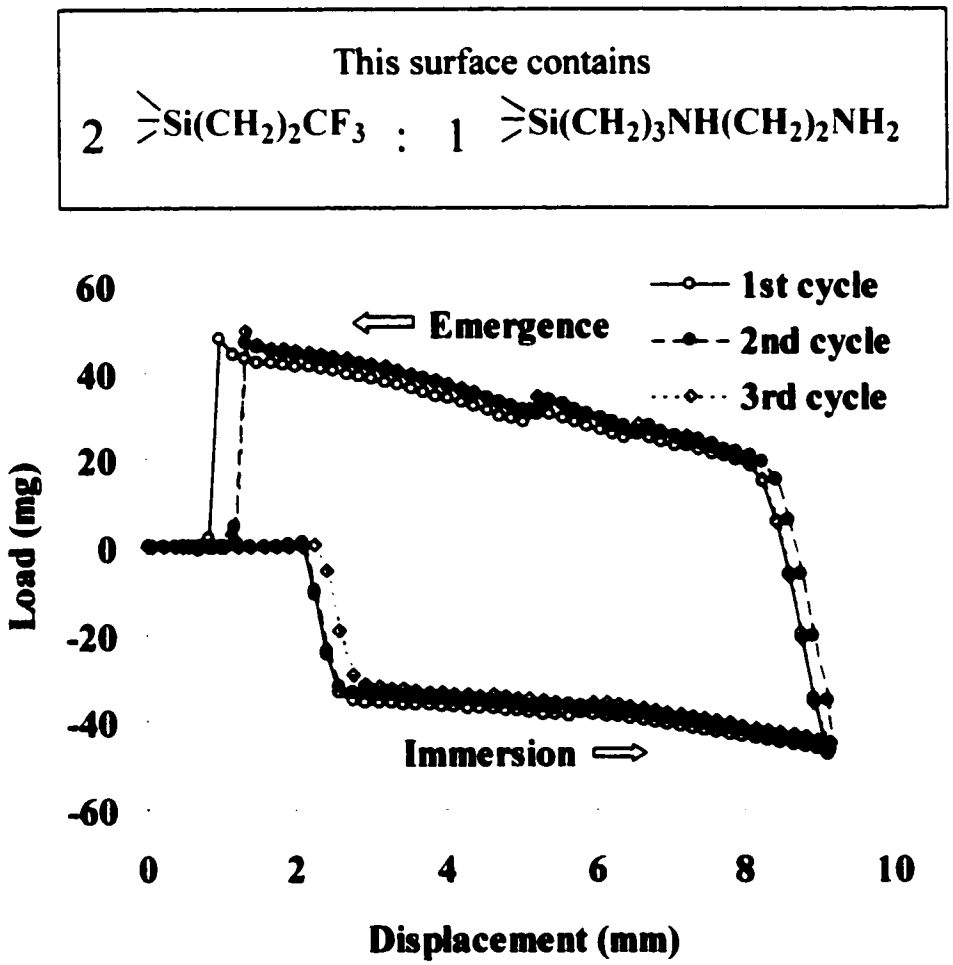

Figure 1.5. Typical raw data from the Wilhelmy-plate experiment [166], which is performed to glean data on advancing (θ_A) and receding (θ_R) contact angles. For this specimen with a mole fraction of 2/3 F3, θ_{A1} = 100.5 °, and θ_{R1} = 74.8 °; θ_{A3} = 99.3 °, and θ_{R3} = 73.7 °. These data demonstrate a slight swelling of the sample with repeated wetting, manifest as an increase in load.

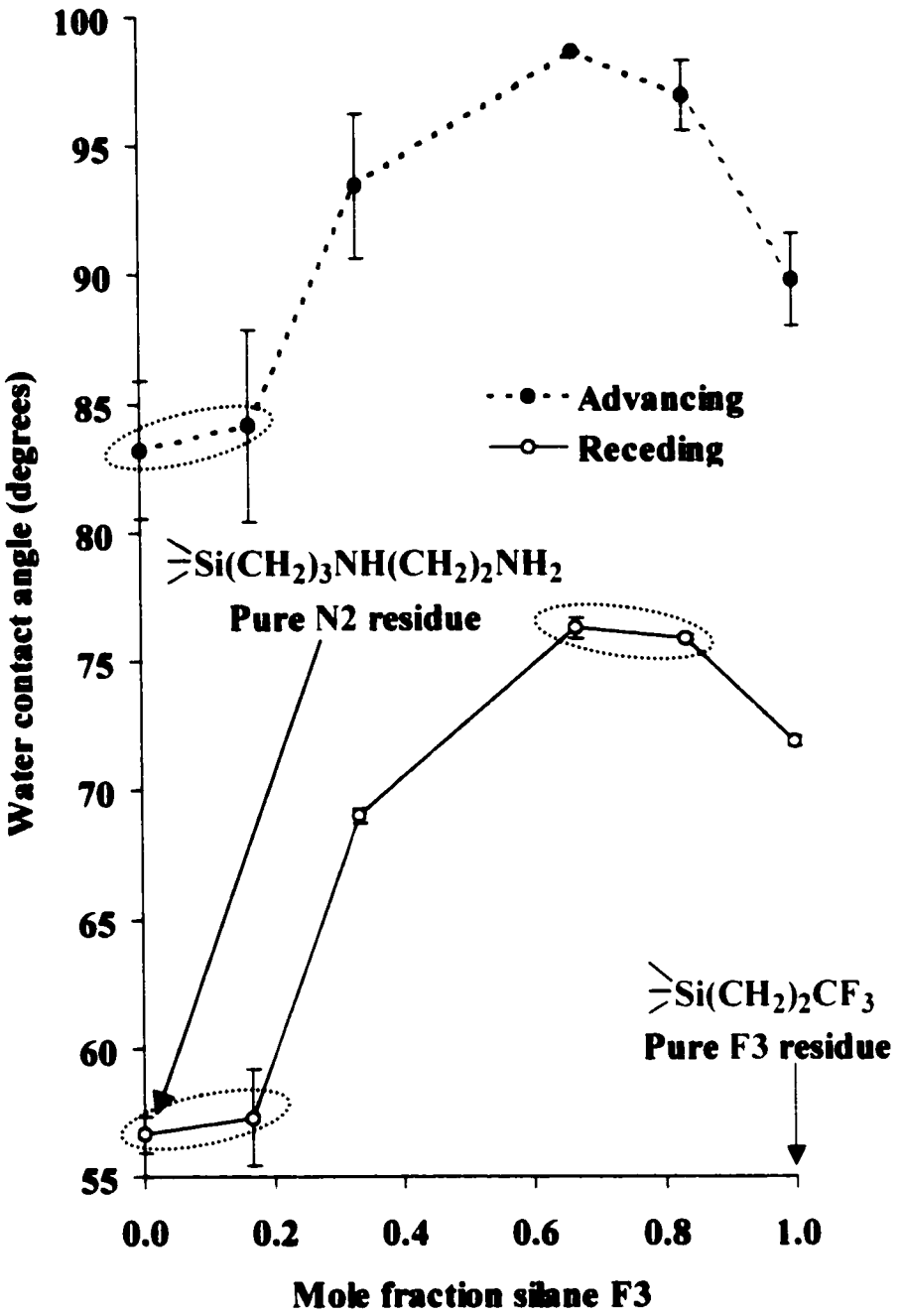

Figure 1.6. Advancing and receding water-contact angles (θ_A and θ_R, respectively) for silanized surfaces. Data enclosed in dashed ellipses do not differ from one another (Tukey-Kramer HSD test, $p \geq 0.05$).

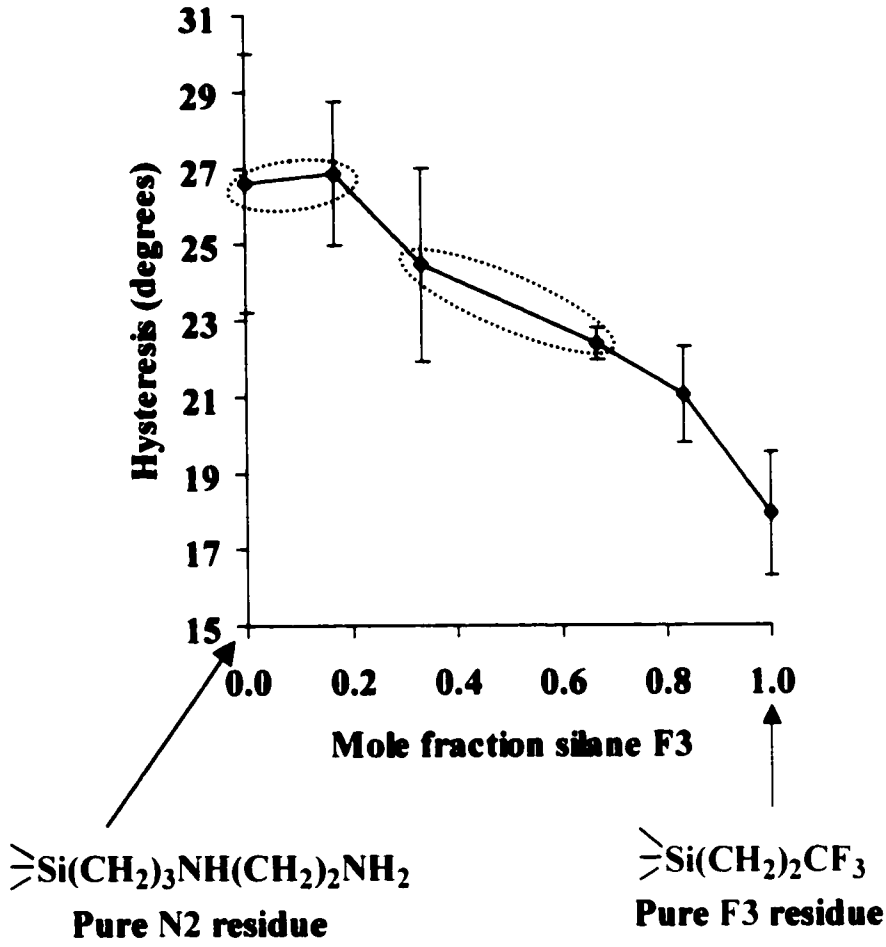

Figure 1.7. Contact-angle hysteresis (θ_H) for silanized surfaces. Data enclosed in dashed ellipses do not differ from one another (Tukey-Kramer HSD test, $p \geq 0.05$).

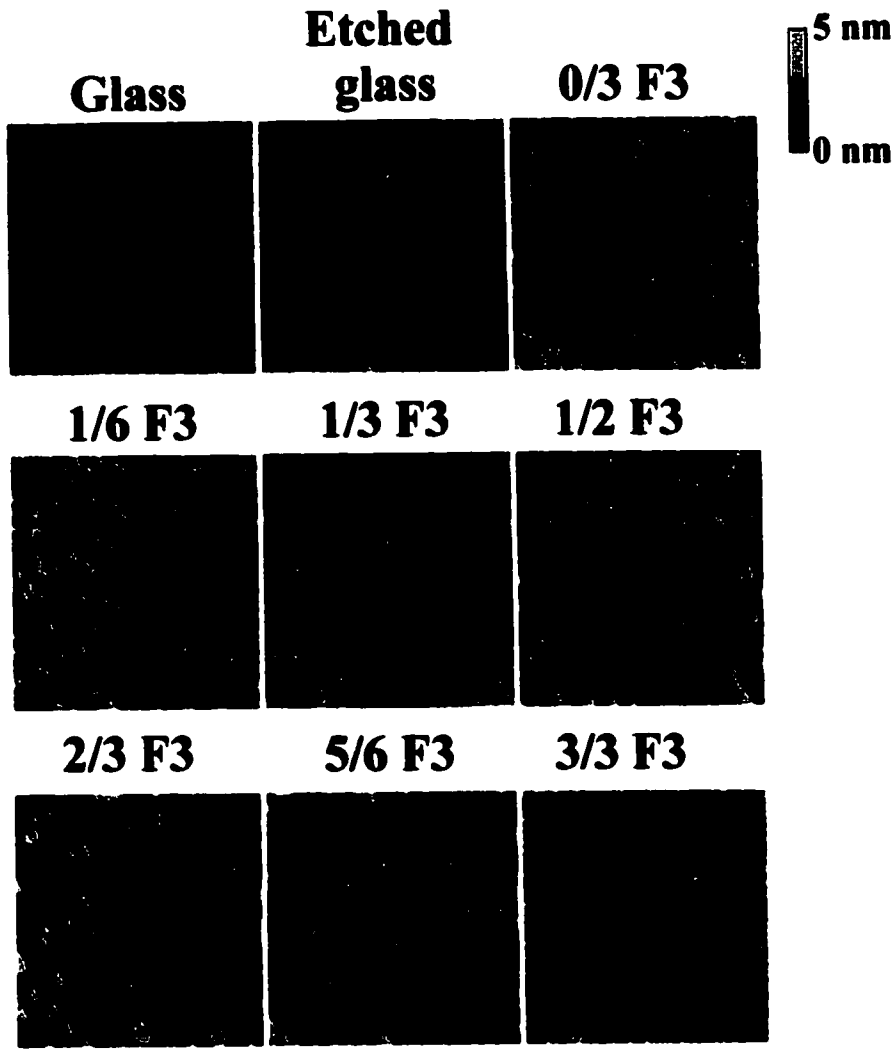

Figure 1.8. False-color portraits of glass, etched-glass, and silanized-glass surfaces under atomic-force microscopy. Each image represents a square sample area 3 microns on a side.

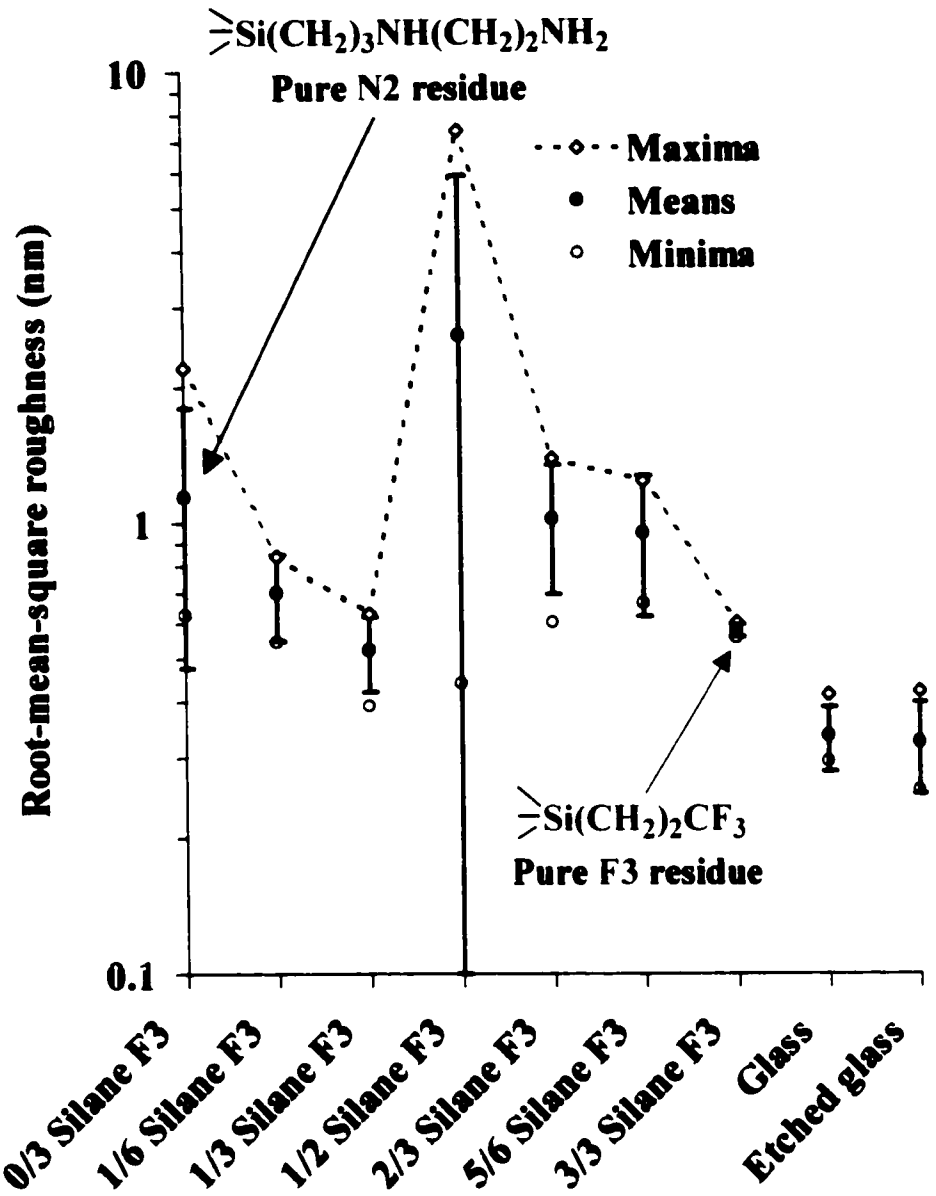

Figure 1.9. Root-mean-square (RMS) roughness of silanized and glass surfaces. Note the logarithmic scaling. Average RMS roughness values for all materials are statistically indistinguishable ($p \geq 0.05$, Tukey-Kramer HSD test).

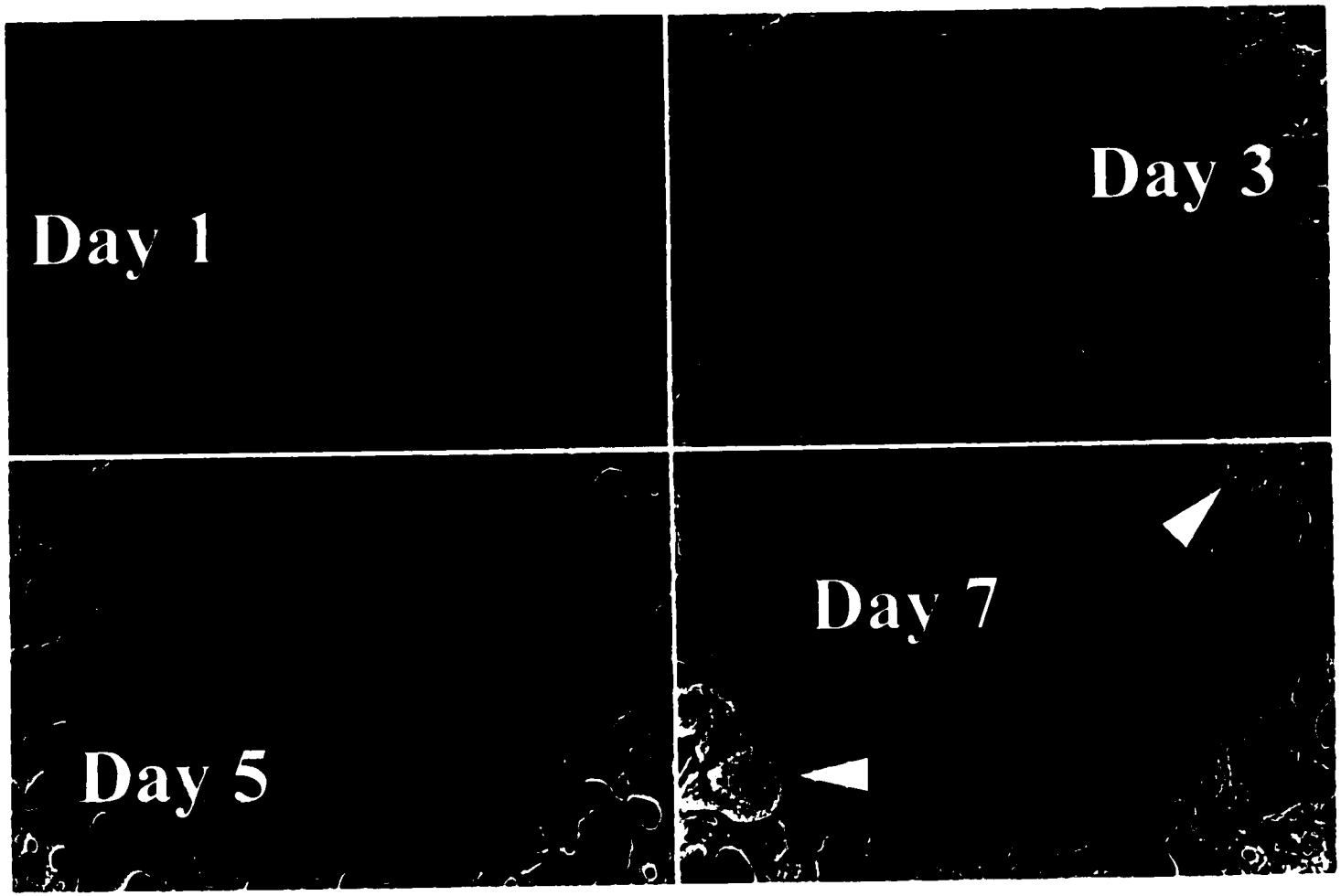

Figure 1.10. βG I/17 cells growing on alkaline-etched borosilicate glass, a permissive surface. Arrows show emergent colonies. Phase-contrast microscopy. Each image represents a sample area measuring 1.36 × 0.9 mm.

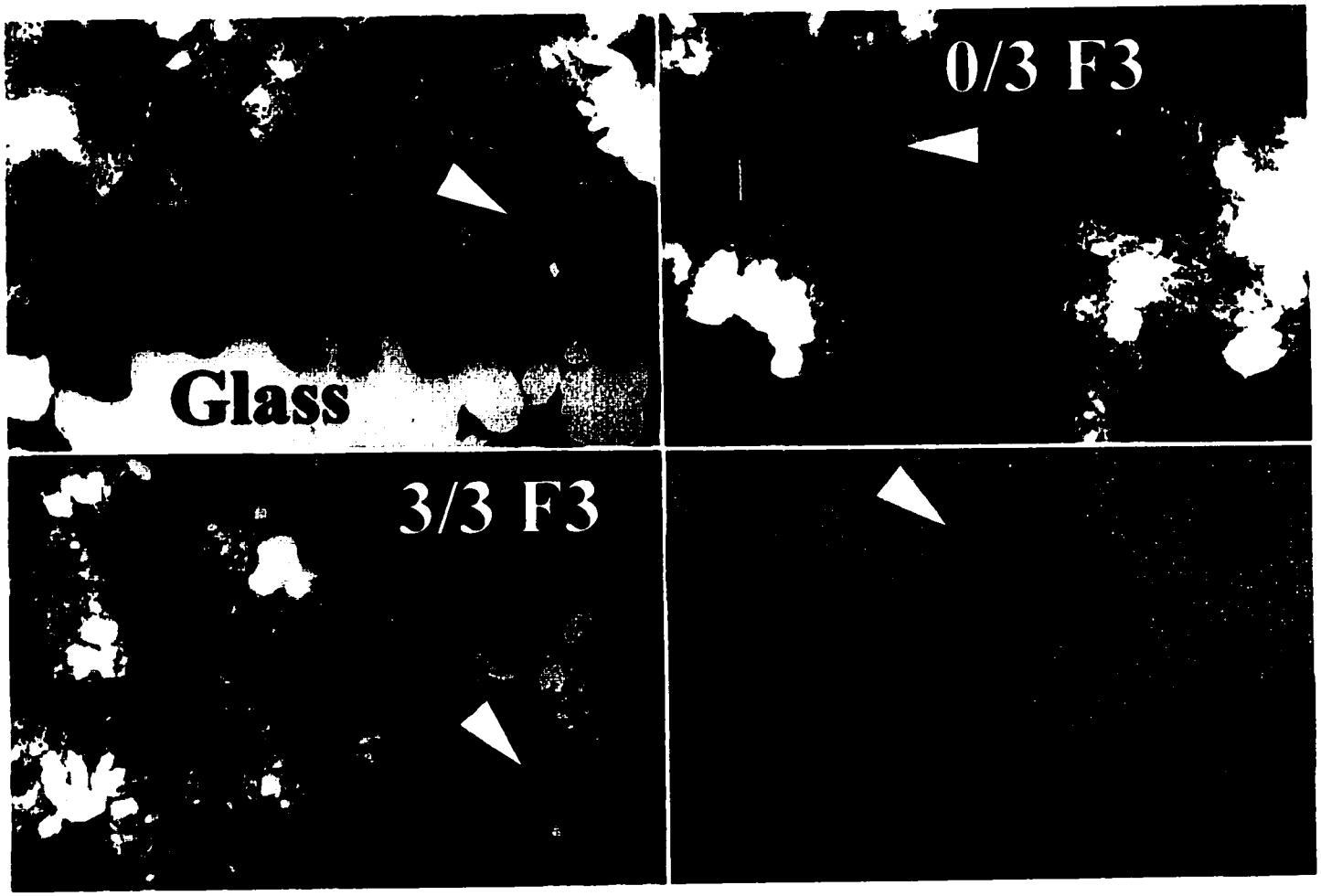

Figure 1.11. Appearance of fixed, stained cultures of βG I/17 cells after stimulation with the "Swiss cocktail" of secretagogues. Arrows show emergent colonies. Hematoxylin and eosin stain. Bright-field microscopy, with Köhler illumination. Each image represents an area of 1.36 × 0.9 mm.

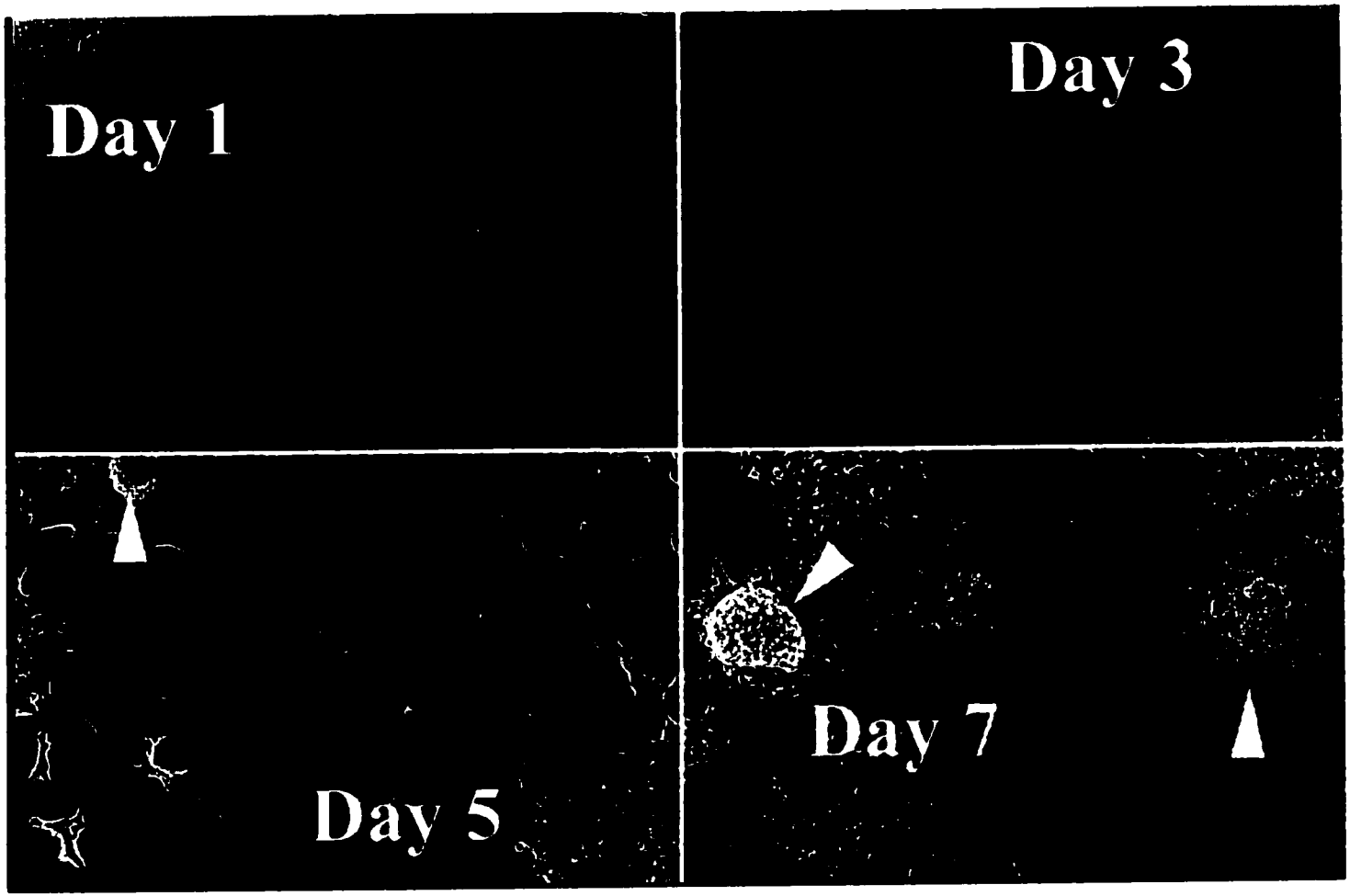

Figure 1.12. βG I/17 cells growing on the pure diaminosiloxane surface (viz., 0/3 F3 or 100 % N2), a permissive surface. Arrows show emergent colonies. Phase-contrast microscopy. Each image represents an area of 1.36 × 0.9 mm.

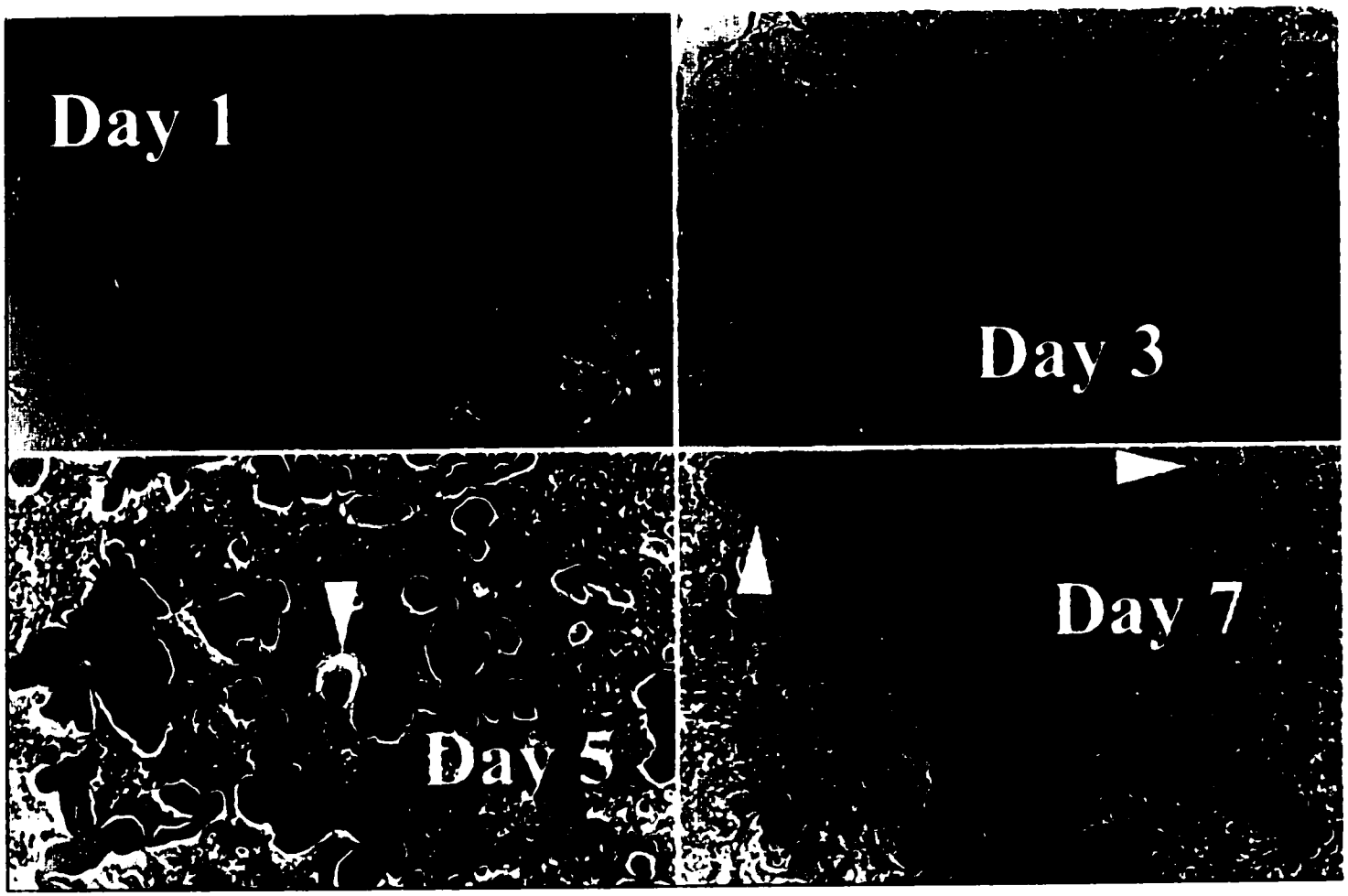

Figure 1.13. βG I/17 cells growing on the pure trifluoropropyl surface (viz., 3/3 F3), a permissive surface. Arrows show emergent colonies. Phase-contrast microscopy. Each image represents an area of 1.36 × 0.9 mm.

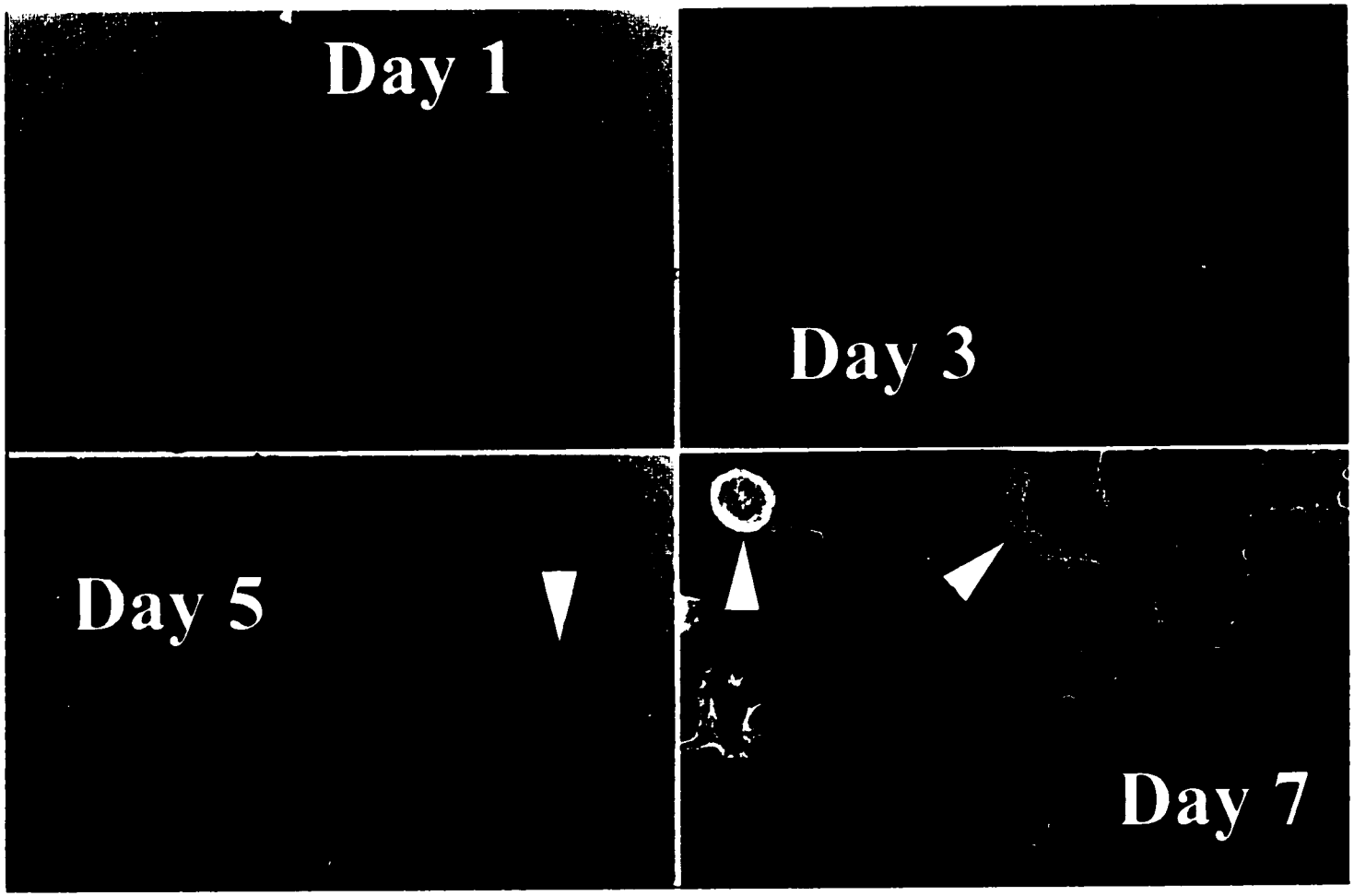

Figure 1.14. βG I/17 cells growing on untreated polystyrene or UPS, the negative control. Arrows show emergent colonies. Phase-contrast microscopy. The five-day image was taken at low magnification to show formation of a macroscopic, emergent colony, and represents an area 3.35 × 2.23 mm. Other images represent areas of 1.36 × 0.9 mm.

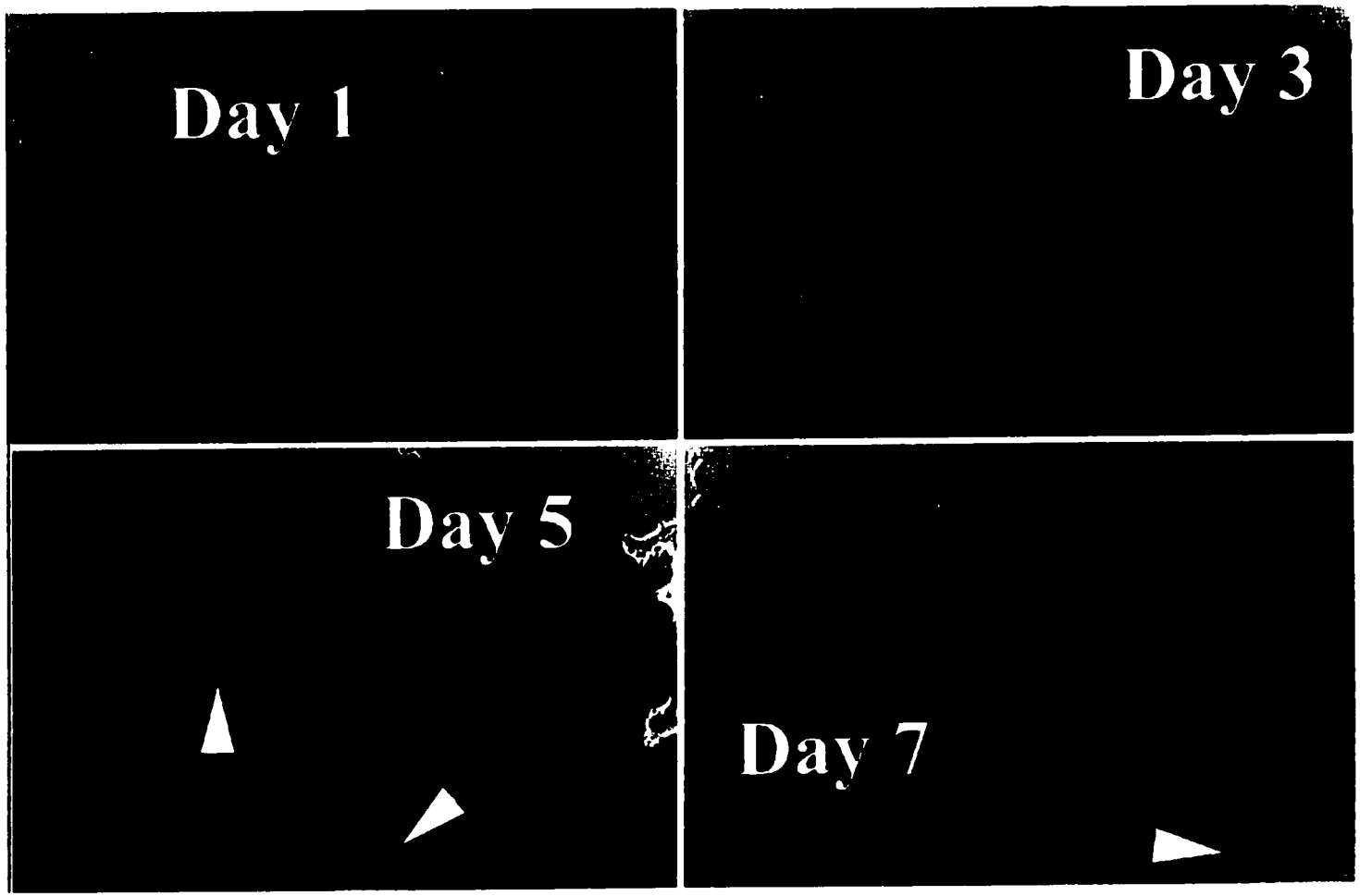

Figure 1.15. βG I/17 cells growing on the 2/3 F3 surface. Arrows show emergent colonies. Phase-contrast microscopy. Each image represents an area of 1.36 × 0.9 mm.

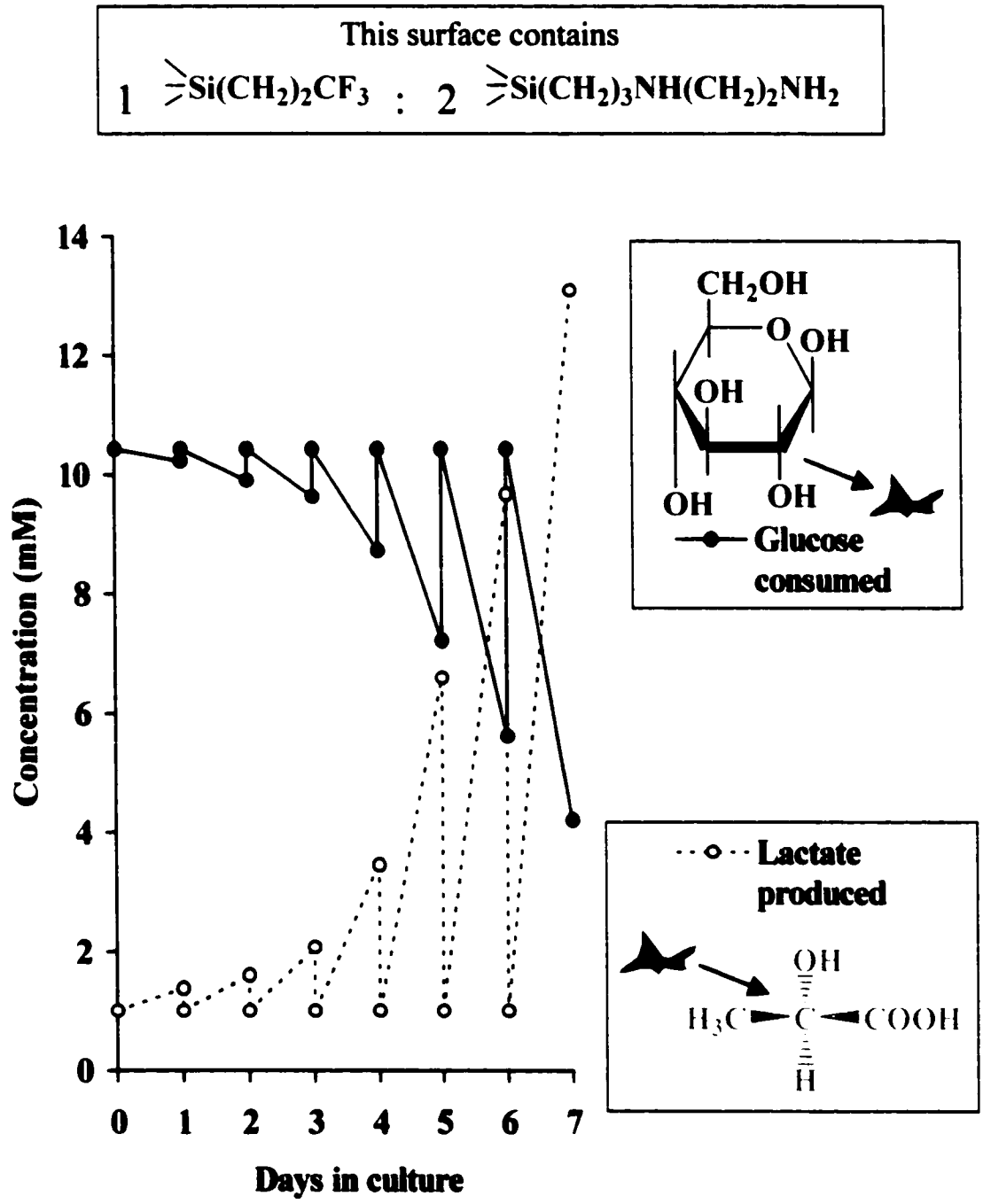

Figure 1.16. Characteristic "saw tooth" profile of raw data on glucose consumption and lactate production by a single culture grown a mixed aminofluorosiloxane surface with a mole fraction 1/3 silane F3. This is a permissive surface, allowing growth as rapid as alkaline-etched borosilicate glass, the positive control. Culture volume = 1 mL.

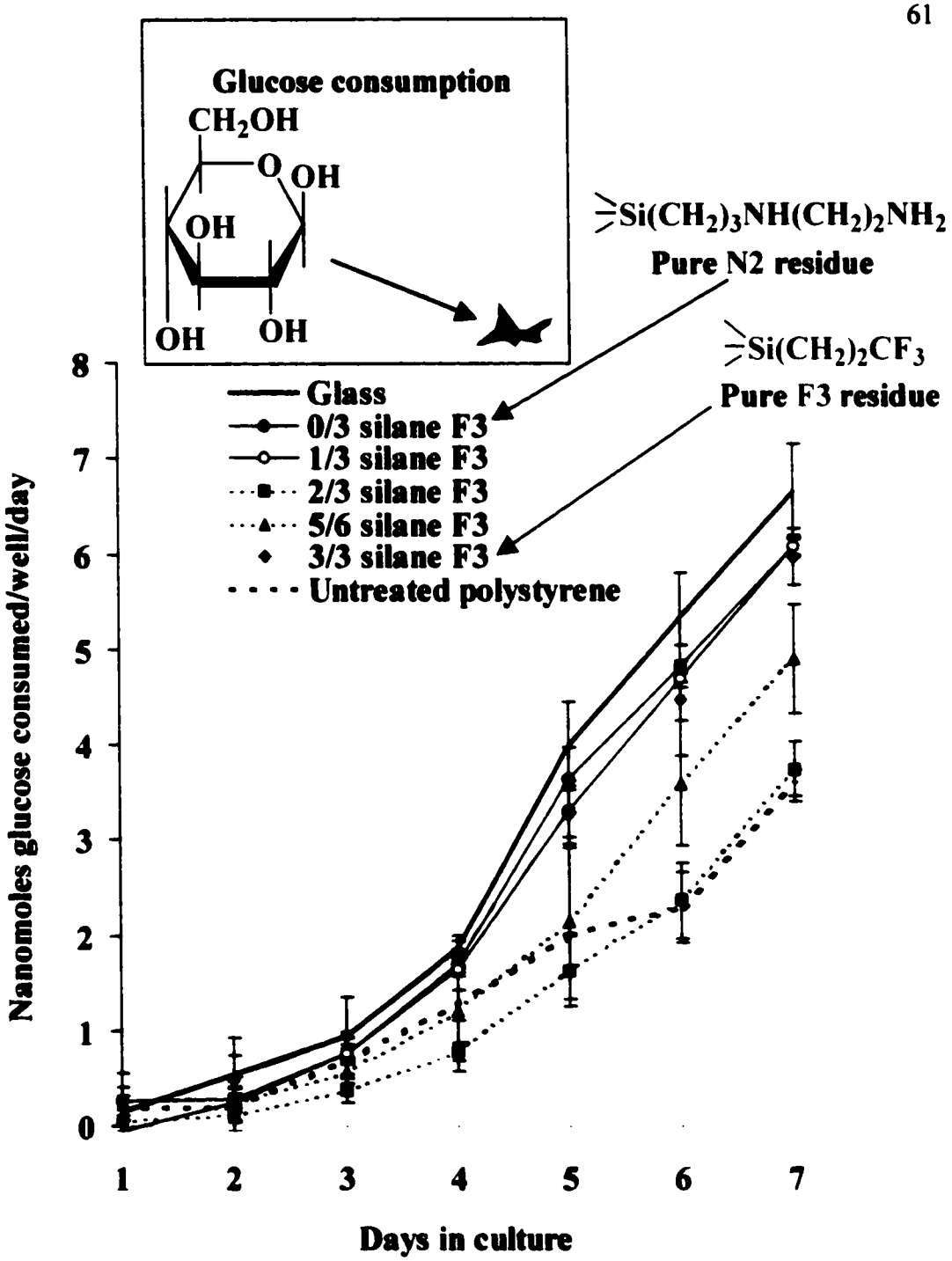

Figure 1.17. Glucose consumption by βG I/17 cells cultured on aminofluorosiloxanes and two reference materials.

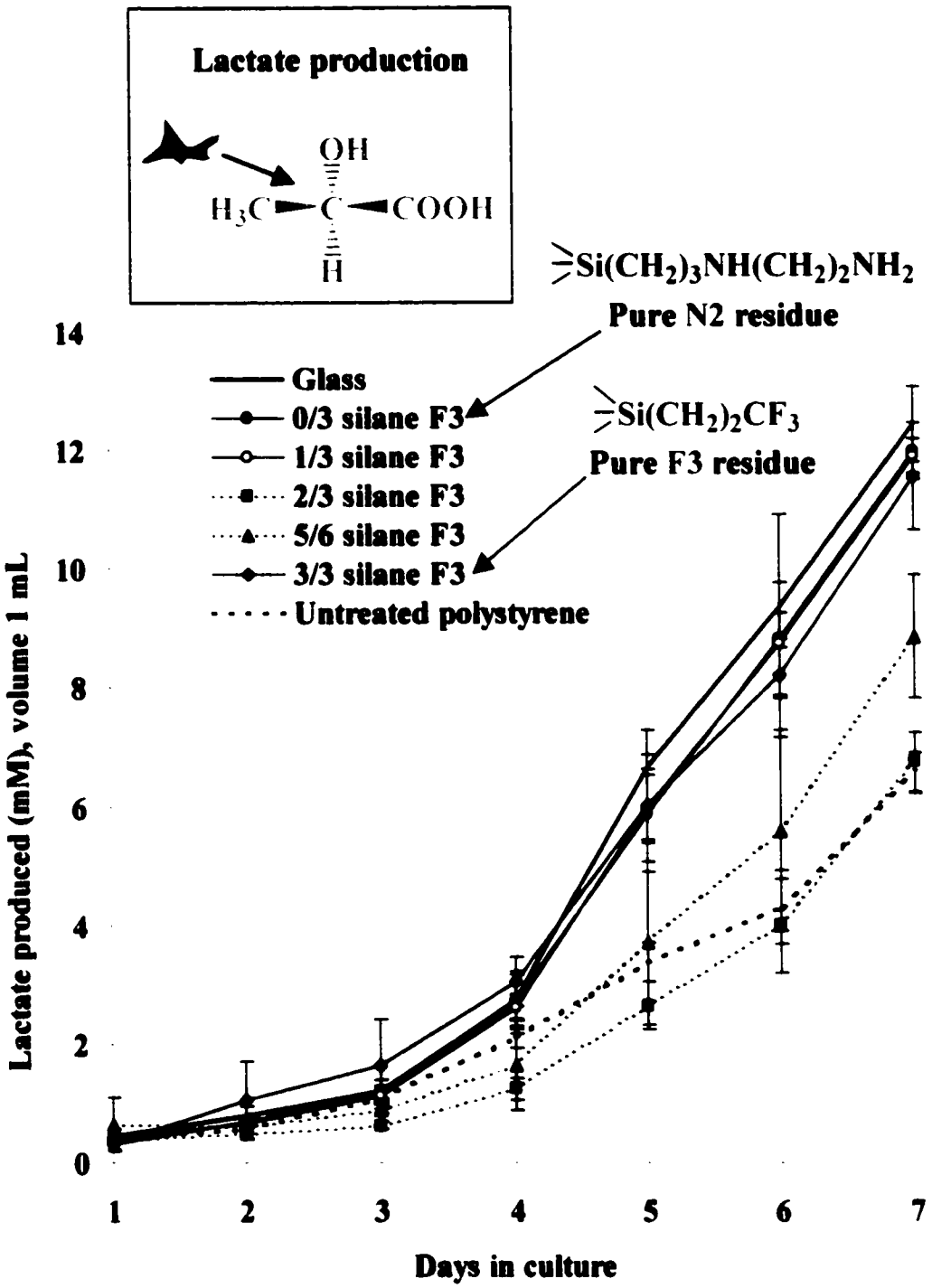

Figure 1.18. Lactate production by βG I/17 cells cultured on aminofluorosiloxanes and two reference materials.

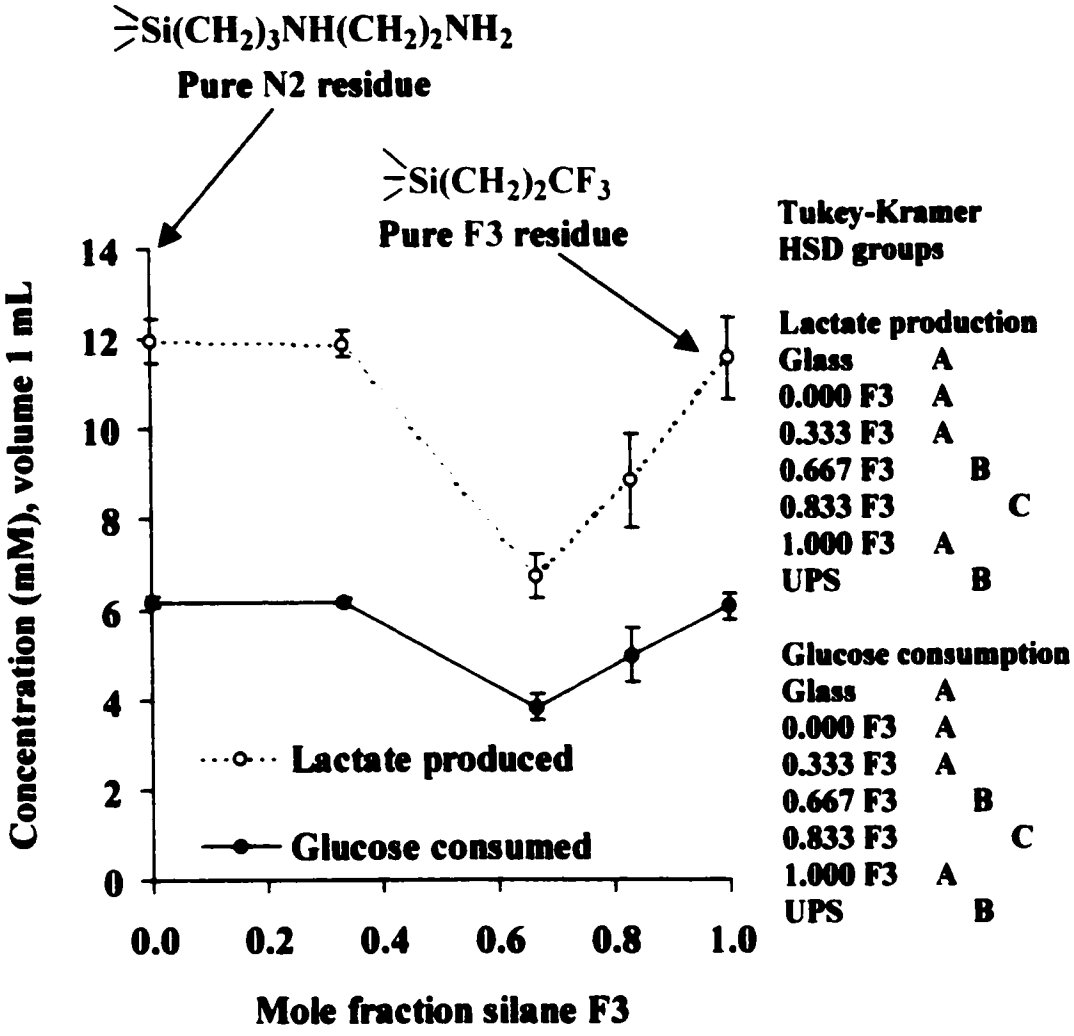

Figure 1.19. Glucose consumption and lactate production for the final 24-hour culture period, plotted as a function of the mole fraction of silane F3 residues in the culture surface. UPS = untreated polystyrene.

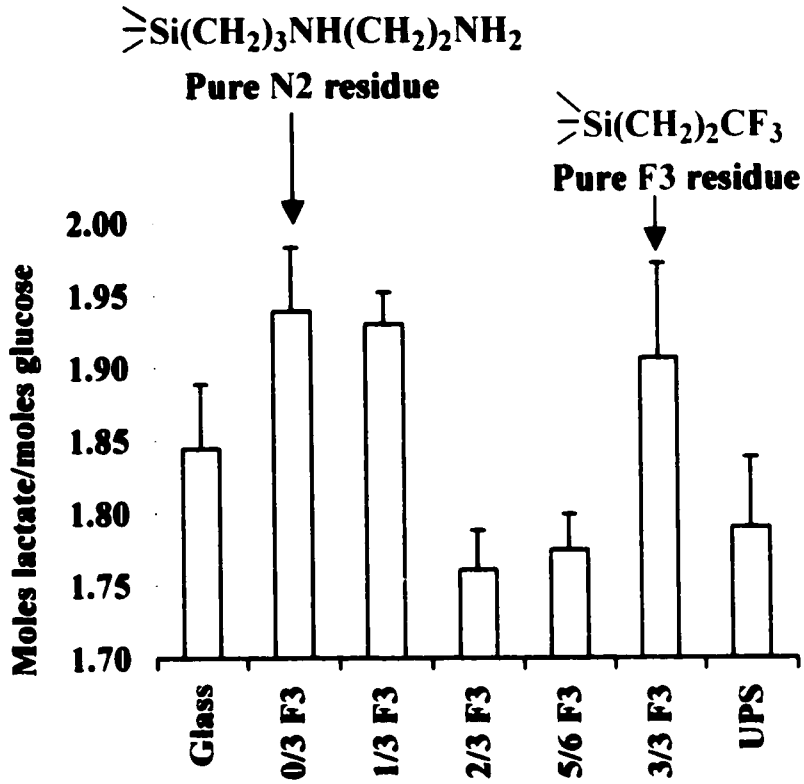

	UPS	0.000 F3	0.333 F3	0.667 F3	0.833 F3	1.000 F3
0.000 F3	*					
0.333 F3	*	-				
0.667 F3	-	*	*			
0.833 F3	-	*	*	-		
1.000 F3	-	-	-	*	*	
Glass	-	-	-	-	-	-

*p<0.05, Tukey-Kramer HSD test

Figure 1.20. Molar ratio of lactate produced to glucose consumed. Complete conversion of glucose to lactate via pyruvate would give a ratio of 2.0. See text. UPS = untreated polystyrene.

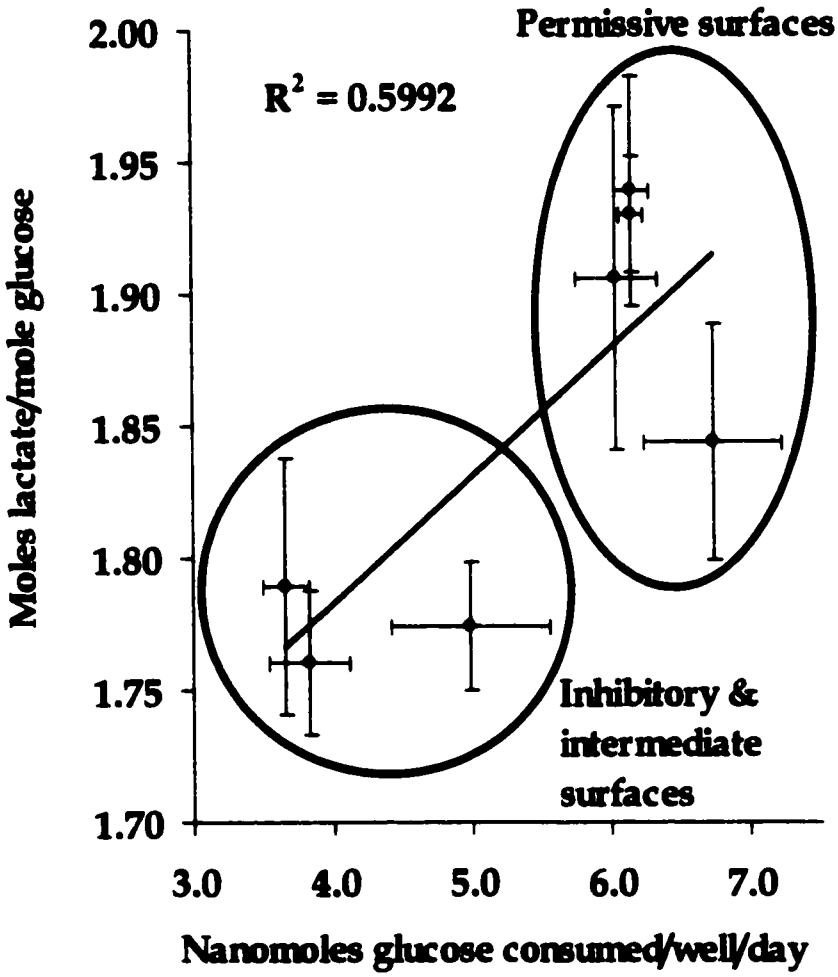

Figure 1.21. Cross plot of the lactate/glucose ratio as a function of glucose consumption. Rapidly growing cultures on permissive surfaces are apparently more anaerobic than slower, more rounded colonies growing on inhibitory surfaces.

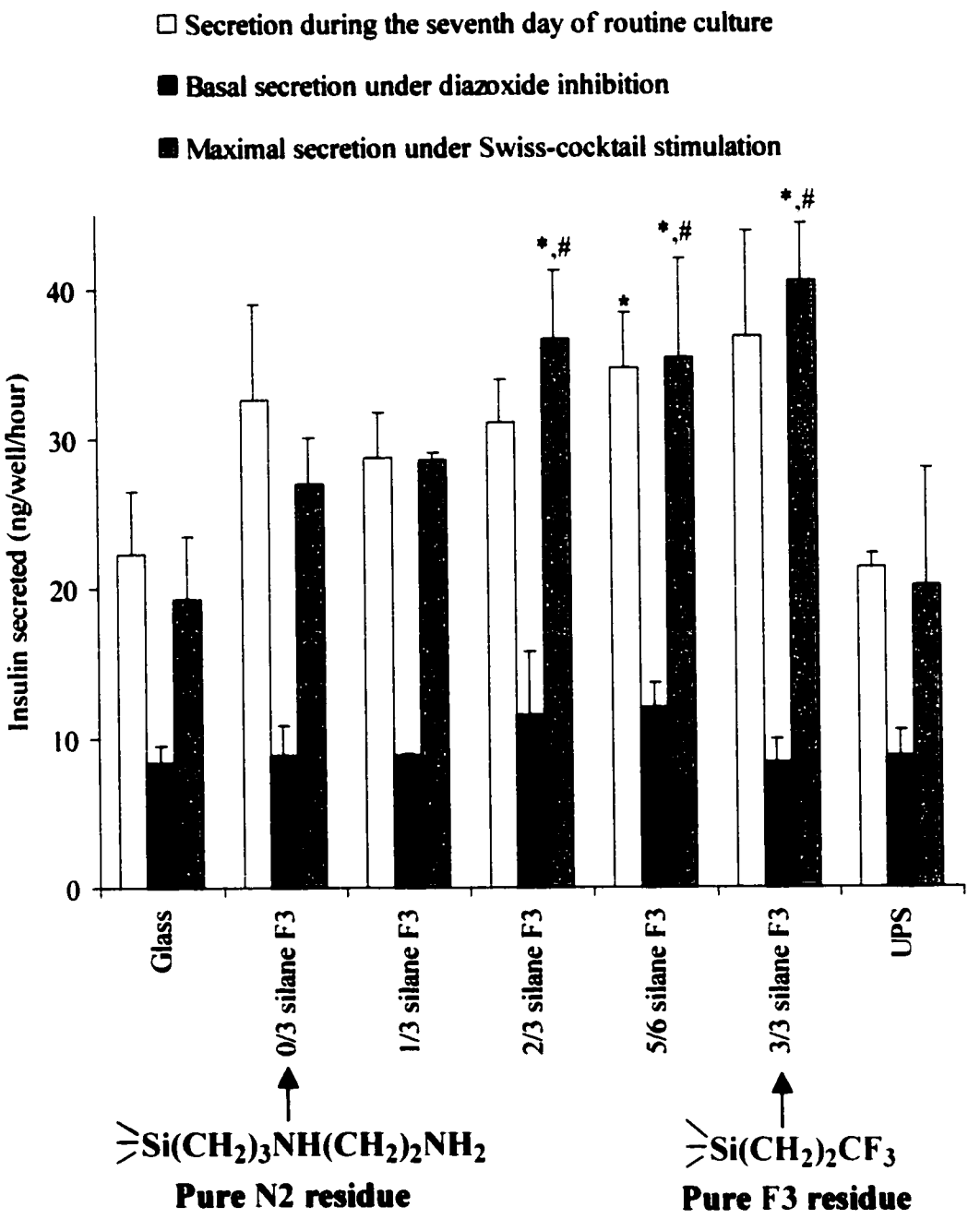

Figure 1.22. Insulin secretion by βG I/17 cells cultured on aminofluorosiloxanes N2-F3 and two reference materials. UPS = untreated polystyrene.

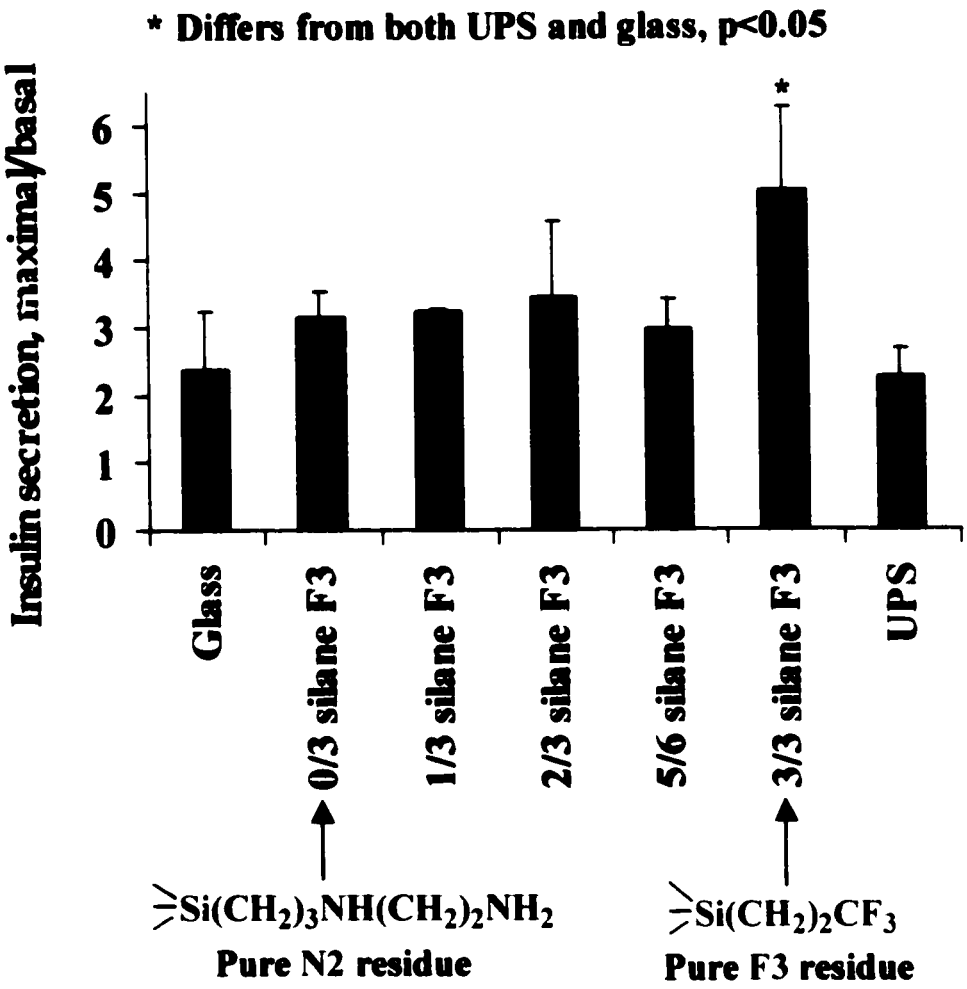

Figure 1.23. Ratio of stimulated to basal insulin secretion. UPS = untreated polystyrene.

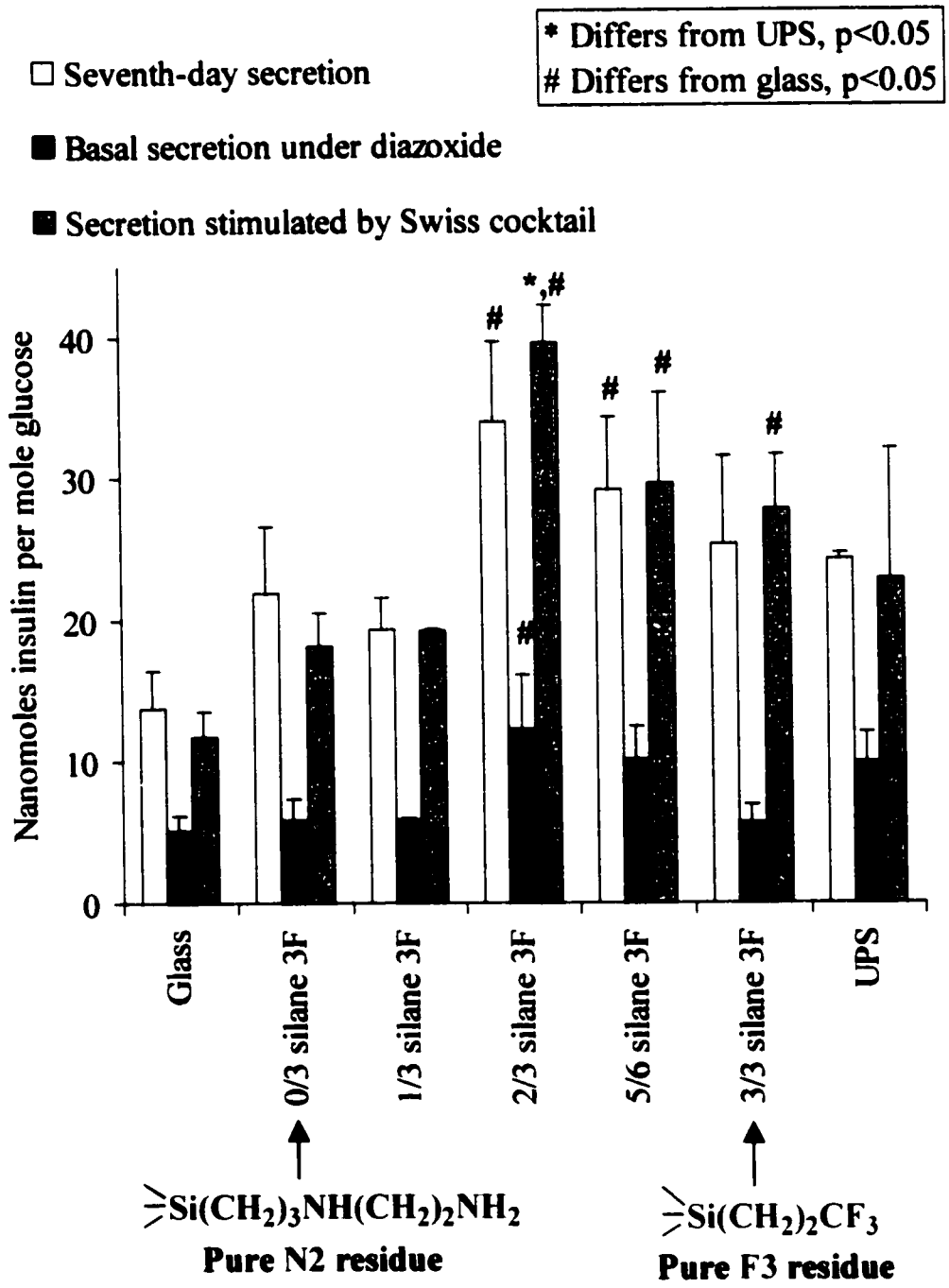

Figure 1.24. Hourly insulin secretion by βG I/17 cells normalized to daily glucose consumption during the final day of culture.

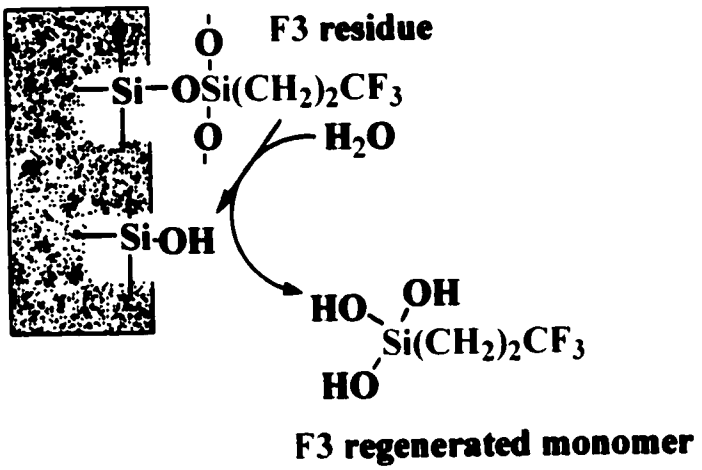

Figure 1.25. Hypothetical in-vitro hydrolysis of F3 residues.

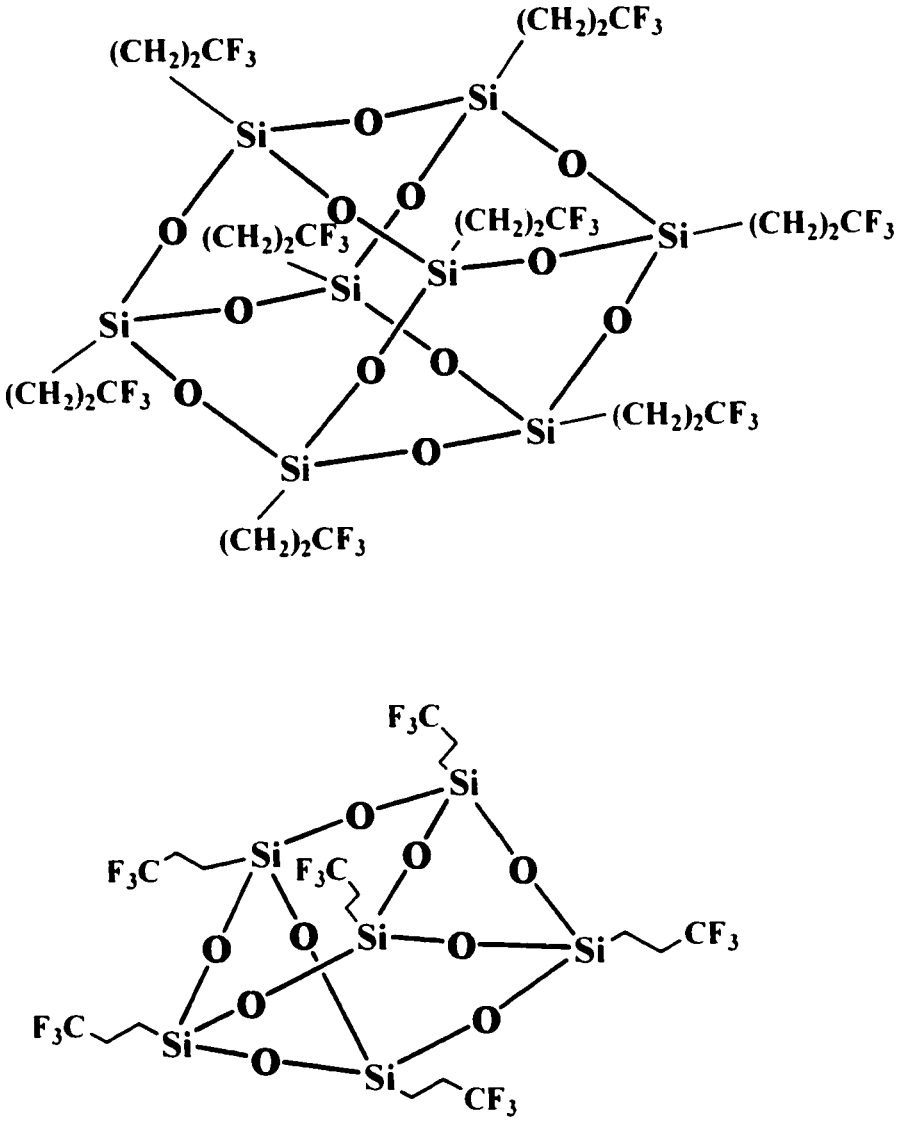

Figure 1.26. Clathrate fluorosiloxane oligomers that might have been generated in vitro from hydrolyzed F3 residues (Fig. 1.25). Trifunctional silanes are known condense into such silsesquioxanes. The quasi-cubic octamer (above) is octa [(3,3,3-trifluoropropyl)-silsesquioxane]. The quasi-triangular-prismatic hexamer (below) is hexa [(3,3,3-trifluoropropyl)-silsesquioxane]. Other common forms include the decamer and the dodecamer. Certain silsequioxanes of these shapes are known to have biologic activity [246].

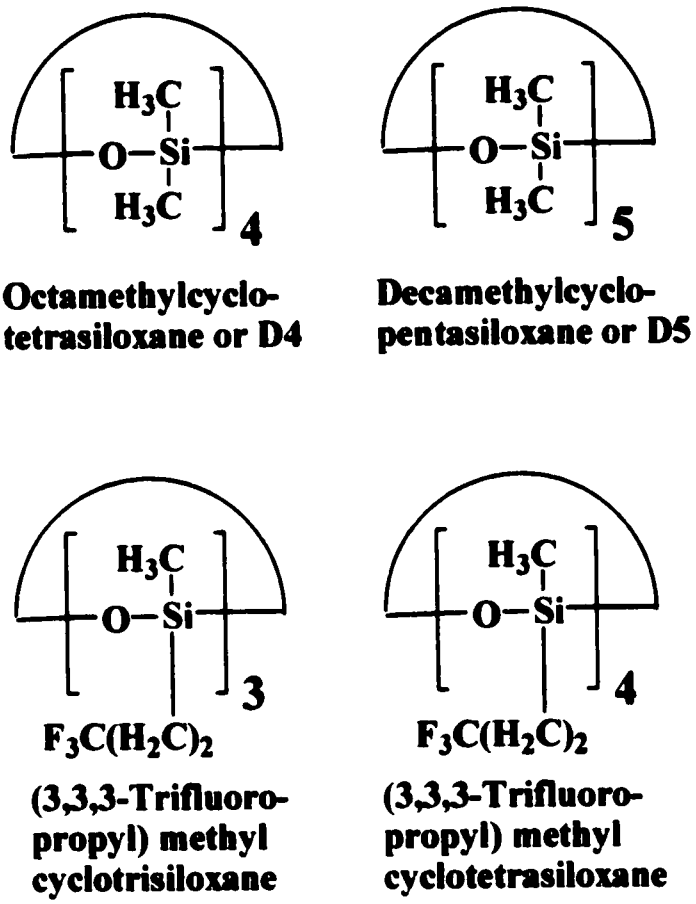

Figure 1.27. Exemplars of cyclic siloxane oligomers used in human implants. All four are known to have biologic activity [130, 242-245]. Cyclomethicones D4 and D5, above, and linear oligomers are eluted in vivo from gel-filled breast and testicle implants [242-243, 245, 247]. The fluorinated oligomers (below) are components of fluorosilicone oils that are injected into the eye for tamponade in severe cases of retinal detachment [244-248].

Chapter 2. Laminin-containing extracellular matrix secreted by βG I/17 insulinoma cells onto trifluoropropyl surfaces promotes insulin secretion by subsequent cultures of the same cells

2.0. Summary

In culture systems, growth and function of secretory cells can be affected by the physical environment. In particular, coatings of extracellular matrix proteins are known to help some specialized cells maintain and express differentiated phenotypes in vitro. This short study evaluated growth and insulin secretion by βG I/17 transgenic insulinoma cells on trifluoropropyl-silanized (F3) surfaces that had been previously conditioned by βG I/17 cells. Growth rates were the same on conditioned and unconditioned surfaces. Hormone secretion, when normalized to nanograms human insulin secreted per hour per million cells, was roughly 50 % greater on the conditioned surface during the seventh day of culture. Incubation of conditioned surfaces with high concentrations of a polyclonal anti-laminin serum prior to re-plating partially abolished this improvement in secretory function. Laminin-coated F3 surfaces might be useful in bioreactors and artificial organs.

2.1. Introduction

When designing artificial endocrine organs containing transgenic insulinoma cells, or when culturing such cells in bioreactors for the mass production of polypeptide hormones, it might be advantageous to provide the cells with an appropriate extracellular matrix (ECM) in the form of fibers, gels, or surface coatings (Chapter 1, supra).

This study evaluated growth and function of transgenic βG I/17 insulinoma cells when cultured on trifluoropropyl or F3 surfaces previously conditioned by βG I/17 cultures.

2.2. Materials and methods

2.2.1. Surface synthesis and conditioning by insulinoma cells

Surfaces were silanized with the monomer, (3,3,3-trifluoropropyl) trimethoxysilane or F3, then annealed, as described in sections 1.2.1.2 to 1.2.3 (supra). The transgenic insulinoma cell line, βG I/17, was cultured on the F3 surface for seven days, exactly as described above in sections 1.2.7 to 1.2.8, with three exceptions. First, a lower passage of cell stock was employed in this investigation (passage 14 for surface conditioning, passage 15 for re-plating). Second, different lots of serum and medium were used. Third, at the end of 7 days of growth, rather than treating the cells with drugs that inhibit and stimulate insulin secretion (Chapter 1), the maturing cells were stripped from the surface without the use of enzymes. This was accomplished by rinsing the cultures twice with Hanks' balanced-salt solution without $CaCl_2$, $MgCl_2$, $MgSO_4$, or Phenol Red (HBSS; GIBCO-BRL Products, Grand Island, NY), then incubating them under a proprietary, isotonic, enzyme-free, chelating solution (GIBCO-BRL catalog number 13151-014). Two sequential chelation treatments were performed, each followed by a firm smack of the plate onto the lab bench. This caused most cells to break free into the overlying chelation bath. Cells removed in this manner were removed with a pipette and discarded.

The very few cells remaining on the surface were then lysed with 20 mM, sterile-filtered ammonium hydroxide for 5 minutes at room temperature, a procedure that previous workers developed to remove cells while at the same time preserving ECM

molecules in a functional state [291-292]. Finally, plates were rinsed extensively with HBSS, given fresh, dry lids, and stored briefly under HBSS at 37 °C in preparation for re-plating. Some plates were incubated with antibodies prior to re-plating (vide infra).

2.2.2. Rationale for the selection of anti-laminin reagents to challenge re-plating

To gain insight into the mechanisms of any differences observed between cultures growing on fresh F3 surfaces versus βG I/17-conditioned F3 surfaces, I sought to challenge the re-plating exercise with immune reagents raised against ECM proteins that might be involved.

This led me to ask, 'which cell-adhesion ligands are known to be used by native islet β cells and the insulinomas derived from them?'

In vivo, the connective tissue supporting pancreatic islets contains collagens, laminins, and fibronectins. Interactions among pancreatic endocrine cells and their surrounding extracellular matrices, or ECMs, are thought to influence such processes as embryogenesis, proliferation, hormone secretion, inflammation, healing, neoplasia, senescence, apoptosis, and necrosis [17, 258-265].

Which cell-surface receptors mediate interactions of islets and insulinomas with their surrounding ECM? Healthy islets, adenomas (benign tumors), and carcinomas (malignant tumors) of the human pancreas express laminin and laminin receptors in vitro and in vivo (e.g., α6β4, α3β1, α6β1), including some primary insulinomas [264, 275, 280-285]. The present study employed a cell line derived from a rat insulinoma (Fig. 1.2a, supra). Fewer data on ECM receptors are available for rodent versus human pancreata, but rodent islets of Langerhans and at least some rodent insulinoma lines are

known to express laminin and laminin receptors, including various combinations of the α3, β1, and α6 integrin subunits [42, 241, 266, 285-286].

Taken together, these published observations, along with my preliminary immunofluorescence results (infra), suggest that laminin might be secreted onto F3 surfaces by βG I/17 rat insulinoma cells during the first week of culture. I therefore decided to challenge re-plating onto conditioned surfaces with anti-laminin antibodies, rather than with antibodies to other pancreatic ECM proteins, such as fibronectin or collagen IV.

2.2.3. Selection of anti-laminin reagents by indirect immunofluorescence

First, I searched for antibodies against rat laminins. Eight antibody preparations were procured and screened. Monoclonals (Table 2.1) were obtained from Dr. David R. Soll, Developmental Studies Hybridoma Bank, National Institute of Child Health and Human Development, Department of Biological Sciences, University of Iowa, Iowa City, IA. All monoclonals were produced in mouse-mouse hybridomas. Two polyclonal antisera were evaluated (Table 2.1): Z0097 (Dako A/S Produktionsvej, Glostrup, Denmark) and 5620-3019 (Biogenesis, Ltd., Poole, England). Negative controls for monoclonals and polyclonals were the mouse $Ig_{1,\,KAPPA}$, MOPC-21 (catalog number 03171D, Becton-Dickinson PharMingen, San Diego, CA) and rabbit serum (catalog number R-9133, Sigma Chemical Co., Saint Louis, MO), respectively.

Phosphate-buffered saline or PBS (GIBCO-BRL catalog number 10010-023) with 1 % w/v radioimmunoassay-grade bovine-serum albumin (RIA-BSA; Sigma catalog number A-7888) served as a diluent for antibodies. The RIA-BSA was not heat-treated prior to use.

PBS-RIA-BSA solution was sterilized by filtration. All monoclonals except D5 were evaluated at dilutions of 1:100, 1:200, and 1:300. D5, received as a raw culture supernatant (Table 2.1), was used full strength, and at dilutions of 1:10 and 1:100. Dako polyclonal Z0097 was diluted 1:25, 1:50, and 1:100. Rabbit serum and Biogenesis polyclonal 5620-3019 were diluted 1:30, 1:100, and 1:300.

βG I/17 cells grown for one week on 3/3 F3 and other members of the aminofluorosilane series (Chapter 1) were rinsed thrice with 1 mL warm PBS, fixed in situ with ice-cold methanol for ten minutes, again rinsed thrice with 1 mL warm PBS, incubated for an hour at 37 °C under the primary antibodies, rinsed twice with PBS, then incubated under the appropriate, fluorescently labeled, secondary antibody, for one hour at 37 °C. Secondary antibodies were Texas-Red-X®-conjugated goat anti-mouse IgG for monoclonal preparations, and Texas-Red-X-conjugated goat-anti-rabbit IgG for polyclonals (catalog numbers T-6390 and T-6391, respectively, Molecular Probes, Inc., Eugene, OR). Cultures were rinsed yet again, then examined and photographed immediately using a Diaphot 300 inverted microscope (Nikon, Inc., Melville, NY). This microscope was equipped with an epifluorescent apparatus with a Texas Red filter set (Chiu Technical Corporation, Kings Park, NY).

2.2.4. Antibody challenge to re-plating

Results of the indirect immunofluorescence studies (infra) suggested that Biogenesis polyclonal 5620-3019 might be able to inhibit cellular responses to laminin deposited on the conditioned surfaces by the initial cultures of βG I/17. Insulinoma-conditioned surfaces were incubated for 90 minutes under antiserum diluted to 1:30 and 1:300 with

PBS-RIA-BSA. Controls included conditioned F3 surfaces incubated under rabbit serum (diluted 1:30) and F3 incubated under plain PBS-RIA-BSA.

2.2.5. Re-plating and secondary culture

Cells propagated on tissue-culture polystyrene (TCPS) T-flasks were plated into sample wells and fed daily for seven days, exactly as described in section 1.2.8 (supra). Note that these cells were exposed to trypsin immediately prior to the plating experiment. Controls included TCPS (Falcon Multiwell 3047, Becton Dickinson Labware, Franklin Lakes, NJ) and fresh, unconditioned F3 wells. TCPS was used as received. Unconditioned F3 controls were incubated under RIA-PBS prior to use.

At the completion of the week of secondary culture, media conditioned during the final 24 hours of cell growth were removed and sealed in polypropylene cryobiology vials, where they were held at –20 °C for later analysis of insulin.

2.2.6. Terminal cell counting

Plates were rinsed in HBSS, and then trypsinized (0.5 mL 0.05 % porcine trypsin, 0.53 mM tetrasodium salt of ethylene diamine tetraacetic acid, in HBSS; GibcoBRL). Cells were suspended in their individual culture wells by repeatedly pipetting up and down with a 1 mL disposable pipette tip. Because I knew it would take many hours to count all the samples (allowing for the occasional aperture jams that are perhaps inevitable with such preparations), I lightly fixed each individual culture by adding 0.5 mL of 0.05 % v/v glutaraldehyde in GIBCO-BRL cell-dissociation buffer (catalog number 13151-014), for a total volume of 1 mL per well. Aliquots of the fixed cell

suspensions were diluted in Coulter Isoton® for counting in a Coulter Counter (model Z1, Coulter Electronics, Inc., Hialeah, FL).

2.2.7. Insulin assay

Human insulin was assayed in media conditioned during the seventh day of culture using an insulin radioimmunoassay kit (Coat-A-Count® insulin kit number TKIN2) and a bench-top gamma counter, both from the Diagnostic Products Corporation (Los Angeles, CA). Statistical analysis is described above in Chapter 1.

2.3. Results

2.3.1. Surface conditioning

At no time did the initial cultures differ in appearance from cultures of the later-passage cells used in Chapter 1 (Fig. 1.11, lower left, and Fig. 1.13). No cells survived lysis in ammonium hydroxide, as evidenced by background insulin levels in three control wells, in which cells had been lysed, and then the wells had been fed daily during the week of culture (data not shown).

2.3.2. Indirect immunofluorescence

None of the monoclonal antibodies (Table 2.1) gave a response above the background fluorescence seen with the negative control (viz., the mouse $Ig_{1,KAPPA}$, MOPC-21). Dako polyclonal Z0097 showed only slightly more fluorescence than the negative control, rabbit serum (Table 2.1).

Biogenesis polyclonal anti-laminin, 5620-3019, yielded immunofluorescence that was strong and localized to specific sites on cell surfaces and inside cells that had been disrupted during processing. Fluorescence was strongest at the 1:30 dilution. Brightest

staining was seen on the undersurfaces of cell sheets at sites of local delamination. There appeared to be a polarization, with the greatest amount of presumptive laminin on the surfaces of cells in contact with the F3 surface, and on the silanized surface itself, where "footprints" of cells and their neurite-like processes fluoresced brightly. These observations were the basis for the use of 1:30 Biogenesis 5620-3019 antiserum to challenge the re-plating exercise.

2.3.3. Secondary cultures: Insulin secretion and cell numbers at the end of one week

To my surprise, morphology of the growing cultures never differed appreciably from that seen on permissive surfaces evaluated in Chapter 1 (e.g., etched borosilicate glass, pure F3, or pure N2). TCPS and fresh-F3 controls had much less amorphous debris on their surfaces at the micron scale than the cell-conditioned surfaces, but the morphologic progression of the cell cultures was the same in all cases: solitary cells and small groups with neurite-like processes grew into sheets fenestrated with lacunae, with formation of emergent dome-like structures in the final days of culture (e.g., Fig. 1.10).

Terminal cell counts (Fig. 2.1) confirmed the morphologic findings. Populations on all surfaces were statistically equivalent (Tukey-Kramer HSD test, $p > 0.05$). Conditioned F3 surfaces and unconditioned F3 were equally permissive to cell growth as TCPS, the positive control.

Bulk insulin secretion (Fig. 2.2, in ng human insulin secreted/well/hour) and insulin productivity normalized to cell number (Fig. 2.3, in ng human insulin secreted per million cells per hour) were ~ 50 % greater on conditioned versus unconditioned surfaces. Pre-

treatment of conditioned surfaces with high concentrations of the Biogenesis anti-laminin reagent partially abolished this improvement in secretory function (Figs. 2.2 and 2.3).

2.4 Discussion

In vitro, whole islets of Langerhans, purified beta cells, and insulinoma cells from mammals, as well as the homologous cells from birds, have been observed to grow and function well on surfaces or inside gels comprising collagen, fibronectin, laminin, or crude ECM. Increasingly, laminin-coated surfaces are identified as desirable culture substrata for such cells and tissue fragments [17, 39, 51, 57, 69, 86, 202, 205, 208, 213, 235, 239-241, 259, 265-279, 291, 293].

The present work confirms and extends these prior observations.

2.5. Conclusions

Conditioning of trifluoropropyl (F3)-silanized surfaces by βG I/17 cells promoted insulin secretion by subsequent cultures. A polyclonal antiserum raised against rat laminin largely negated this effect, indicating that laminin might be involved.

F3 silicones, which are already used in approved medical devices [244, 247-248, 287-290], or F3-silanized surfaces (Chapters 1 and 2), when coated with laminin, might be useful in bioreactors and in artificial organs that employ transgenic insulinoma cells.

In particular, should anyone ever develop a stable, glucose-sensitive, implantable line of human insulinoma cells, scaffoldings of F3 silicones coated with recombinant human laminin might be useful cell supports inside the artificial endocrine pancreas.

2.6. Table

Epitopic specificity	Reagent	Isotype (monoclonals) or species immunized (polyclonals)	Antigen; remarks	Indirect immuno-fluorescence of insulinoma cell ECM
Mono-clonal	Clone 2E8	IgG1, kappa	Human laminin from term placenta; thought to bind at the center of the laminin cross; known to cross-react with some rat laminins [294].	Negative
Mono-clonal	Clone 3.1C12	IgG	Embryonic rat spinal cord membranes; known to cross-react with some rat laminins [295].	Negative
Mono-clonals	Clones C4, D5, and D7	IgG1*	190 kiloDalton s-laminin from the anterior lens capsule of the bovine eye; known to cross-react with some rat laminins [296-297].	Negative
Mono-clonal	Clone D18	IgG	200 kiloDalton B2 fragment of rat laminin, from the glomelular basement membrane of the kidney [296].	Negative
Polyclonal	Z0097	Rabbit, purified immunoglobulin	Rat laminin, from a yolk-sac tumoral cell line.	Weakly positive
Polyclonal	5620-3019	Rabbit, lyophilized immunoglobulin fraction	Rat laminin, 96 % pure.	Strongly positive

Table 2.1. Monoclonal and polyclonal antibodies screened for reactivity against extracellular matrix secreted by βG I/17 cells. *D5 was received as a raw culture supernatant—all other monoclonals were partially purified gamma globulins.

2.7. Figures

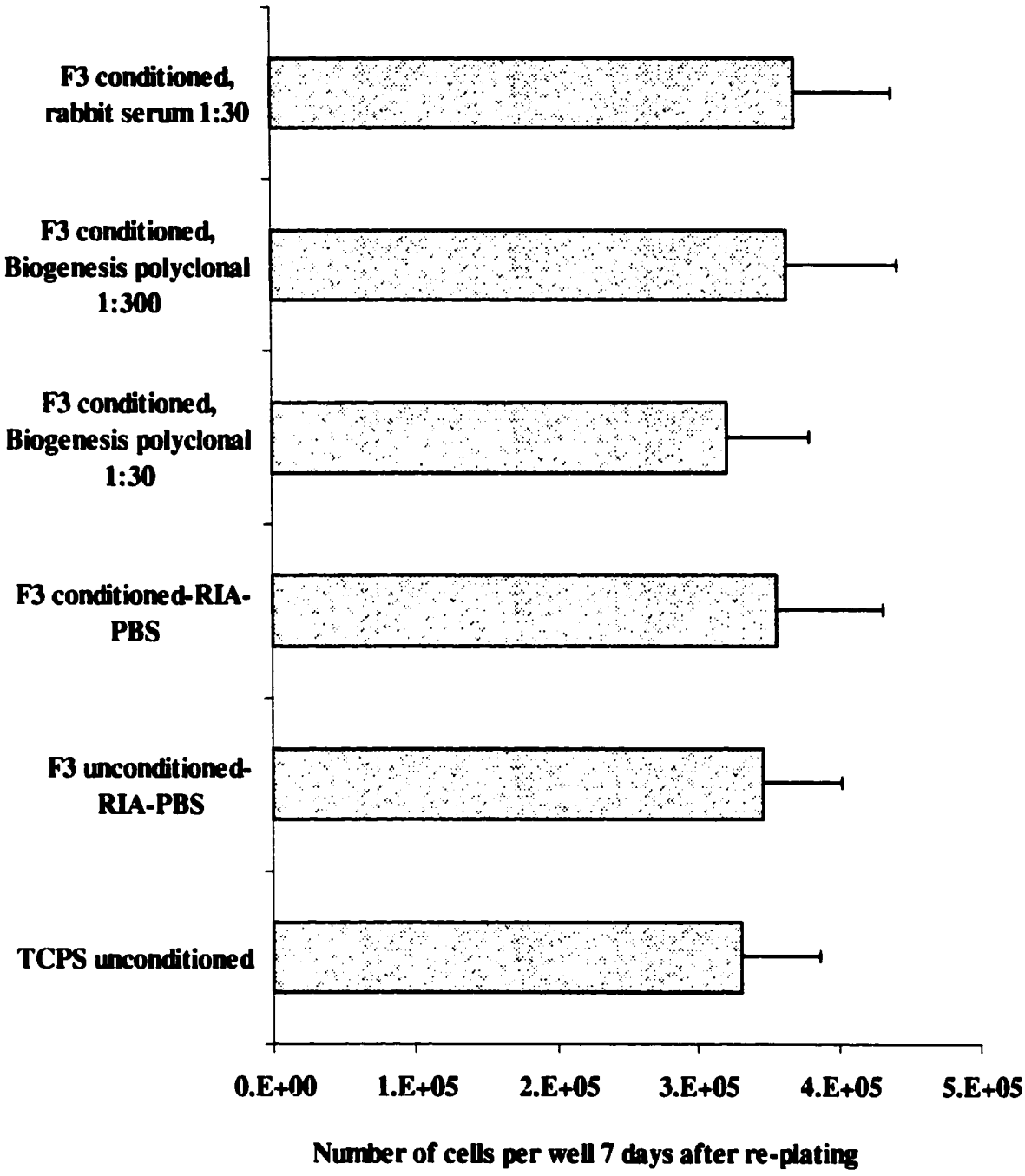

Figure 2.1. Insulinoma cell numbers one week after re-plating. All six populations are statistically equivalent (Tukey-Kramer HSD test, $p > 0.05$, $n = 6$ in each case).

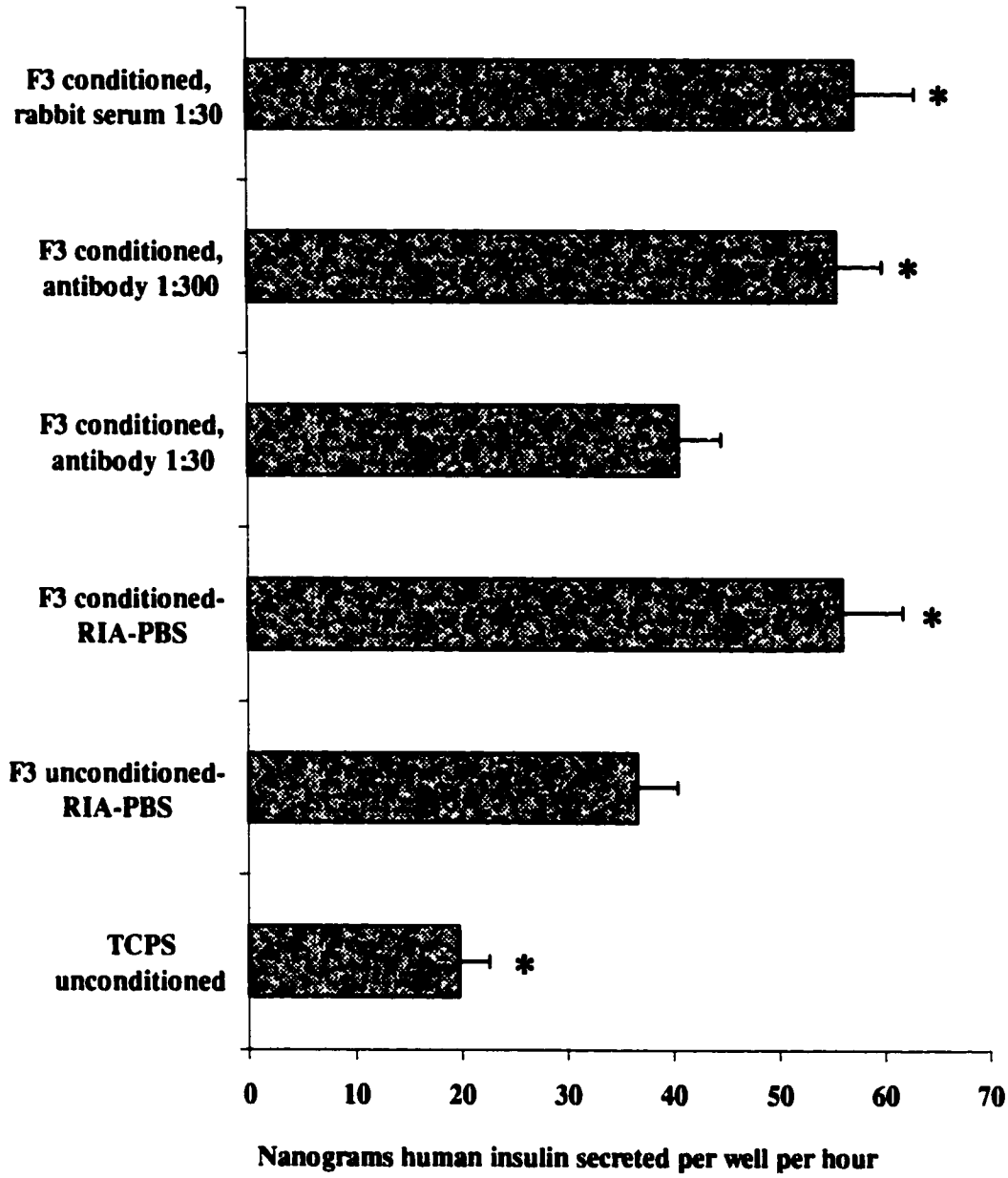

Figure 2.2. Bulk insulin secretion during the seventh day of culture after re-plating. *Differs from cultures on the unconditioned F3 surface, $p < 0.05$, Tukey-Kramer HSD test; $n = 6$ in each case.

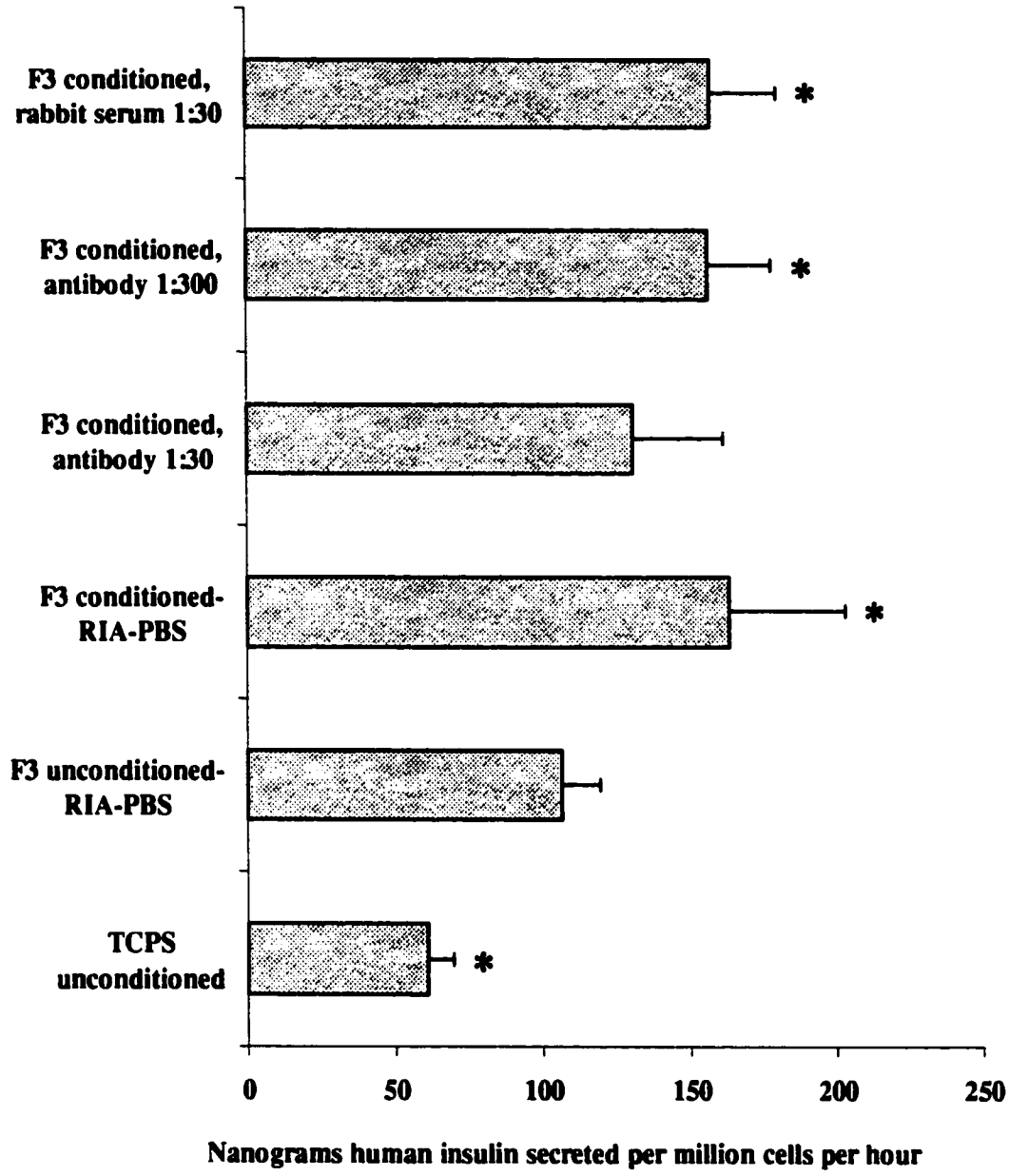

Figure 2.3. Insulin productivity on the seventh day, normalized to cell number. *Differs from cultures on the unconditioned F3 surface, $p < 0.05$, Tukey-Kramer HSD test; $n = 6$ in each case.

Chapter 3. Glycophase glass is neither protein- nor cell-repellant

3.0. Summary

Glycophase glass has been promoted as a non-fouling surface, resistant to protein adsorption and cell attachment. But I found that glycophase glass adsorbs more albumin than glass. Moreover, the growth rates, morphologies, and functions of transgenic βG I/17 insulinoma cell cultures were equivalent on the two surfaces. Glycophase glass is neither protein- nor cell repellant.

3.1. Introduction

Biomaterials scientists have long sought to create surfaces that would resist fouling by adsorption of proteins and attachment of living cells [298-299]. Such protein- and cell-repellant surfaces would be useful in numerous applications, including medical implants, immunoassays, bioreactors, pharmaceutical packaging, and surfaces exposed to seawater.

In a much-cited series of papers, Hubbell and coworkers promoted "glycophase glass" as a non-fouling surface on which one could create cell-type-specific culture surfaces via covalent immobilization of oligopeptide cell-adhesion ligands (quotes and citations below in section 3.7, Endnotes). Glycophase glass, prepared by hydrolysis of an oxirane silane residue (Figures 3.1 and 3.2), bears pendant diol groups on its surface. While my data confirm observations that this surface is a useful support for ligand immobilization [300-316], I cannot support Hubbell's contention that glycophase glass resists protein adsorption and cell attachment.

Glycophase glass is therefore not suitable for use as a non-fouling surface.

Portions of this Chapter are reproduced from my preliminary reports [317-318].

3.2. Materials and methods

3.2.1. Selection, cleaning, and silanization of borosilicate glass

Borosilicate glass coverslips (12 mm circles) were purchased from Carolina Biological Supply (Burlington, NC). Briefly, the coverslips were manufactured as follows: sheets of borosilicate glass D263 were poured by Schott-Deutsche Spezialglas (Mainz, Germany), and cut into the final shape and sold under the trade name "Assistent®" by Glaswarenfabrik Karl Hecht GmbH and Company (Sondheim/Rhön, Germany). Procedures for cleaning glass samples, along with the glassmaker's formulation and my own data on chemical analysis and wettability of this glass, are given in detail in Chapter 1.

Unless otherwise noted, all reagents employed in this study were from Sigma-Aldrich-Fluka (Saint Louis, MO).

Clean borosilicate glass coverslips were etched with sodium hydroxide (pH 13.7) for 30 minutes at 20° C to expose free silanol anions, then silanized with a 1 % v/v solution of (γ-glycidoxypropyl) trimethoxysilane (Hüls America, Inc., Piscataway, NJ) in water, pH 5.3, for 2 hours at 90° C (Fig. 3.1). Epoxy groups were then hydrolyzed to the diol by immersion in 1 mM hydrochloric acid for 1 hour at 90° C (Fig. 3.2), creating glycophase glass.

A brief note on nomenclature is in order. The term "glycophase glass," alone and with several suffixes, has been used to denote a variety of different surfaces, including several ion-exchange resins. To complicate matters further, the word "Glycophase" and

some of its variants were formerly registered trademarks of the Pierce Chemical Company (Rockford, IL) and Corning, Inc. (Corning, NY). As used here, "glycophase glass" refers to glycerylpropylsilyl glass, as shown schematically in Fig. 3.2.

3.2.2. Ligand design, iodination, and covalent immobilization

I sought to create culture surfaces attractive to cells bearing the integrin, α4β1. Useful cells that express α4β1 include certain hæmatopoietic progenitors [317, 319], among many others. The heptapeptide ligand, Gly-Ile-Asp-Ala-Pro-Ser-Tyr or GIDAPSY, was selected for solid-phase immobilization. I designed the GIDAPSY molecule around the fibronectin sequence, IDAPS, a ligand of the integrin, α4β1. An amino-acid sequence bound by the α4β1 cell-surface receptor is variously given as IDAPS or IDAP [320-324]. All immobilizations were carried out via the amino (or N) terminus. N-terminal glycine was added as a steric swivel, and C-terminal tyrosine was added to enable radio-iodination [325]. The Howard Hughes Medical Institute, University of Washington, synthesized and purified GIDAPSY, and provided it to me in lyophilized form.

All investigators handling radionuclides during the present study passed the required University of Washington course on Principles of Radiation Protection prior to performing lab work, and were subject to thyroid monitoring in the days following radio-iodinations. In preparation for radio-iodination reactions, three Iodo-Beads® (Pierce, Rockford, IL; Fig. 3.5) were rinsed in phosphate-buffered saline (PBS; catalog number P3813, Sigma, Saint Louis, MO; 0.138 M NaCl and 0.0027 KCl, pH ~7.4) to remove any oxidant that was dislodged from the surface during shipping and handling

(Fig. 3.5). The three nonporous beads were then incubated for 5 minutes at ~20 °C with a mixture of 10 μL $Na^{125}I$ in water (~100 milliCuries/mL; Amersham Life Science, Inc., Arlington Heights, IL) and 490 μL PBS. Oligopeptide solution was then added to the reaction mixture (50 μL at 1.0 mg GIDAPSY/mL PBS). Iodination proceeded 20 minutes at ~20 °C, and was terminated by removal of the beads with forceps.

For separation of peptide from free iodine species, the reaction mixture was immediately loaded onto a disposable C_{18} column (Waters SepPakPlus®, catalog number 20515, Waters Chromatography Division, Milford, ME). Just prior to loading, the C_{18} columns were rinsed with 0.8 mL of a mixture comprising: 80 % v/v methanol; 19.8 % v/v deionized, distilled water (ddH_2O); and 0.2 % v/v trifluoroacetic acid (TFA); they were then equilibrated with PBS. Once loaded, columns were eluted by sequential reversal of the mobile phase, beginning with 99 % water: 1 % TFA (99W1TFA), and followed by stepwise ten-percent increases in methanol, to a maximum of 30 % 99W1TFA: 80 % methanol. Most free iodine eluted in the zero-percent-methanol loading solution, while approximately 90 % of the peptide eluted in the 40-to-60-percent-methanol fractions. These three fractions were pooled, lyophilized, and stored frozen at –20 °C for later use.

Glycophase glass discs were loaded into fluoropolymer racks (described in detail in Chapter 1). For peptide immobilization, glycophase glass was activated for 15 minutes with 2.5 % w/v 1,1'-carbonyldiimidazole (CDIZ) in acetone (Fig. 3.3). The activated glass was rinsed twice in fresh acetone to remove free CDIZ. Many coupling experiments were performed. In a typical experiment, coupling proceeded unstirred for

20 hours at 20 °C, with the oligopeptide dissolved in 0.2 M $NaHCO_3$ buffer, pH adjusted to 9.0. The covalent linkage that forms between the peptide and the surface is an N-alkyl-carbamate or urethane (Fig. 3.4). After ligand immobilization, racked glass discs were rinsed five times in large volumes of fresh ddH_2O, with blotting on Kimwipes® (Kimberly-Clark Corporation, Roswell, GA) after the first three rinses. Gamma counting (Gamma Trac 1185, TM Analytic, Elk Grove Village, IL) consistently showed that radiation levels in the rinse baths fell to background after the third rinse. In some experiments, the effects of a subsequent blocking reaction were evaluated. The blocking solution, 0.8 M ethanolamine, pH 9.0, in 0.2 M $NaHCO_3$, was applied for 2 hours, followed by three aqueous rinses.

3.2.3. Why study protein adsorption and cell growth on glycophase glass?

My suspicions that glycophase might not be a useful non-fouling surface were first aroused when I observed that the $\alpha 4\beta 1$-positive human melanoma cell line, A-375 (American Type Culture Collection, Manassas, VA), attached, spread, and grew equally well on tissue-culture polystyrene, glycophase glass, etched glass, and GIDAPSY-liganded glycophase glass. I performed the A-375 cultures under serum-containing medium [317-318]. This observation caused me to question claims that the short glyceryl groups on the surface of glycophase glass are able to repel protein adsorption and cell attachment (section 3.7, Endnotes, infra). I therefore endeavored to study protein adsorption and cell growth on glycophase glass.

3.2.4. Protein selection, iodination, adsorption, and desorption

Bovine serum albumin (BSA; Sigma catalog number A7638) was chosen as a model

protein, since it is the most abundant protein in most cell-culture systems, and the only extracellular protein in many cell-attachment assays and cell-sorting procedures [317-318]. A sub-sample of BSA was radiolabeled with iodine-125 using Iodo-Beads (supra), and then separated from free iodine species by two passes on disposable gel-filtration columns (Sephadex® G-25M, Amersham Pharmacia Biotech AB, Uppsala, Sweden). Non-labeled albumin was spiked with radiolabeled albumin to a specific activity of two million cpm/mg [318].

Adsorption studies were conducted at 0.1 mg BSA/mL in CPBSzI buffer (0.01 M sodium citrate, 0.01 M Na_2HPO_4, 0.11 M NaCl, 0.01 M NaI, 0.02 % w/v NaN_3, pH adjusted to 7.4). This phosphate-saline buffer included citrate for consistency with concomitant studies of fibrinogen adsorption in which citrate served as an anticoagulant (data not shown). Iodide was added to competitively reduce binding by any free iodine-125 species, and sodium azide (NaN_3) was employed as an antimicrobial agent. Samples subjected to protein adsorption-desorption studies included low-density polyethylene (LDPE, Penn Fibre and Specialty Company, Inc., Fort Washington, PA), etched borosilicate glass, glycophase glass, CDIZ-activated-then-ethanolamine-blocked glycophase glass, and glycophase glass liganded with 10 picomoles/cm^2 GIDAPSY (Fig. 3.4) [318]. Prior to adsorption experiments, samples were hydrated overnight in CPBSzI at 4 °C. Adsorption proceeded 2 hours at 37 °C, and was terminated by dilution-displacement rinsing with 25 volumes (100 mL) CPBSzI delivered hydraulically at a flow rate of 100 mL/minute [318]. During and after gamma counting of the protein adsorbate (supra), desorption in citrate-phosphate buffer, along a pH series 2.2 - 7.4, proceeded for 48 hours at ~20 °C, followed by dip rinsing and

recounting [318].

3.2.5. Culture of βG I/17 transgenic insulinoma cells on glycophase glass

Unconvinced that glycophase glass was cell-repellant, as had been claimed by Hubbell and his coworkers (section 3.7, Endnotes, infra), I cultured the transgenic insulinoma cell line, βG I/17, on glycophase glass and on two controls, etched borosilicate glass and untreated polystyrene, exactly as described in Chapter 1. Assays of outcome included glucose consumption, lactate production, and insulin secretion (supra, sections 1.2.7 to 1.2.13).

Statistical methods are described in Chapter 1.

3.3. Results

3.3.1. Solid-phase immobilization of the heptapeptide, GIDAPSY

Empirical experimentation with reaction conditions led to a coupling procedure that yielded defined surface concentrations of the fibronectin-inspired ligand spanning three logarithmic decades (Fig. 3.6). In the example shown in Fig. 3.6, the coupling reaction was allowed to continue for 20 hours at 20 °C, in stagnant 0.2 M $NaHCO_3$ buffer, pH adjusted to 9.0. In this case, variability in the outcome was most pronounced at low peptide concentrations, due to radiation levels near background, and at high concentrations, where the peptide approached the limit of its solubility in the linkage buffer (Figure 3.6). Under similar conditions, when peptide concentration was raised above 2.0 mg/mL in an attempt to create even higher surface densities of the ligand, the solution became cloudy, and the oligopeptide began to precipitate during the 20-hour incubation.

For protein-adsorption studies, I selected glycophase glass liganded with 10 picomoles GIDAPSY/cm^2, because Massia and Hubbell reported that at this surface density, another fibronectin-inspired oligopeptide, GRGDY, provided a useful cell-culture surface [326].

3.3.2. Adsorption and desorption of the model protein, bovine serum albumin

Contrary to Hubbell's claims (vide infra, section 3.7), plain glycophase glass adsorbed more protein than the glass control (Fig. 3.7) [317-318].

GIDAPSY-linked glycophase glass adsorbed half the BSA of glass, and a third as much as glycophase glass (Fig. 3.7). The positive control, low-density polyethylene, adsorbed more than six times the BSA of all glass-based surfaces (216.3 $\pm$ 11.1 ng BSA/cm^2 adsorbed on LDPE, n = 27).

Desorption in the pH series (Fig. 3.8, n = 3 at each point) revealed that albumin was most tightly bound to all surfaces near its isoelectric point (pI ~4.9). Above BSA's pI, all glass-based surfaces showed decreasing protein retention with increasing pH. This included surfaces bearing the immobilized oligopeptide, with its two carboxylate groups (Asp, pKa ~3.9, C-terminal Tyr, pKa ~2.2). Borosilicate glass, which I had etched at pH 13.7 to expose silanol anions prior to use (Chapter 1, supra), showed the strongest effect of pH on albumin desorption (Fig. 3.8). Tight binding of albumin to LDPE was relatively insensitive to pH (Fig. 3.8). Not unexpectedly, in all cases, at pH 7.4, 1 % w/v sodium dodecyl sulfate in buffer was more effective at stripping albumin from surfaces than buffer alone (data not shown).

3.3.3. Cell culture on glass and glycophase glass

Growth of the transgenic insulinoma line, βG I/17, was equivalent on glass and glycophase glass in the week of culture, as evidenced by data on glucose consumption and lactate production (Figs. 3.9 and 3.10). Insulin secretions under diazoxide inhibition and secretagogue stimulation were equivalent (Fig. 3.11).

When comparing cultures on glass and glycophase glass, neither I nor any of my co-workers in the lab could distinguish the morphology of the living cultures under phase-contrast microscopy. Nor could we detect any morphologic differences when examining the fixed, stained cultures by conventional bright-field microscopy. Photomicrographs documenting morphology of cultures grown on glycophase glass are qualitatively indistinguishable from those of cultures grown on glass (e.g., Figs. 1.10 and 1.11, supra).

3.4. Discussion

3.4.1. Carbonyldiimidazole-activated glycophase glass is a useful support for immobilization of oligopeptide ligands

My data confirm that glycophase glass is useful support for solid-phase immobilization of organic molecules [300-316].

By chance, in the present study, I was able to achieve much higher surface densities of fibronectin-inspired oligopeptides than Hubbell's group was able to create on glycophase glass, probably because the reactive intermediates formed by their sulfonyl-chloride methods are less stable in water than the imidazolyl-carbamate intermediate that I employed (Fig. 3.3). By working near the limits of solubility of the GIDAPSY

oligopeptide ligand in the linkage buffer, I achieved ligand densities that were more than a hundredfold greater than the highest densities of sundry ligands achieved by Massia and Hubbell (compare my Fig. 3.6 to their Fig. 1 [327]). However, this result came at a cost. Their sulfonyl-chloride method creates a given surface concentration of peptide at much lower input concentrations of peptide. Thus, in choosing between the two methods for immobilizing ligands on glycophase glass, one might select the sulfonyl-chloride chemistry for economy of peptide, or the carbonyldiimidazole chemistry to achieve high ligand densities.

3.4.2. Glycophase glass is not protein-repellant

Under the conditions of this study, glycophase glass adsorbed more protein than glass itself (Fig. 3.7). Moreover, at physiologic pH, albumin bound more tightly to glycophase glass than to glass (Fig. 3.8). Clearly, glycophase glass cannot be considered a non-fouling surface.

As early as 1989, Bruin et al. [303] reported that chromatographic surfaces with immobilized poly (ethylene glycol) or PEG provided better non-fouling surfaces than glycophase glass. In their study, glycophase glass exhibited strong interactions with lysozyme, trypsin, and chymotrypsinogen at pH > 5 (their Fig. 5b). Similarly, Xiao and Truskey [316] observed more fibronectin adsorption to glycophase glass than to glass under two of the three adsorption conditions they evaluated (their Table 1).

In the current study, relatively low binding of albumin to GIDAPSY-liganded glycophase glass at pH 7.4 (Fig. 3.7, note logarithmic scaling) might have been due in part to charge-charge repulsion between the net negative charges on albumin (pI ~4.9) and the N-terminal-immobilized GIDAPSY groups (pKa Asp ~3.9, pKa carboxy

terminus ~2.2).

Binding of bovine serum albumin to glass was strongest near BSA's isoelectric point (pI ~4.9; Fig. 3.8), a phenomenon observed by others since at least the 1950s [328]. Glycophase glass and GIDAPSY-liganded glycophase glass also showed decreasing BSA retention with increasing pH above pH ~5 (Fig. 3.8). Many proteins exhibit adsorption maxima near their isoelectric points, particularly when adsorbed from unitary solutions onto uncharged or weakly charged surfaces [329-330].

The positive control, low-density polyethylene, adsorbed much more albumin than any glass-based surface (Fig. 3.7). Binding of BSA to LDPE was relatively tight and pH-insensitive (Fig. 3.8), presumably due to hydrophobic interactions between the protein adsorbate and the surface of this polyolefin [318].

3.4.3. Glycophase glass is not cell-repellant

Neither morphologic appearance nor metabolic data revealed any substantive differences between cell growth and function on glycophase glass and glass (Figs. 3.9 to 3.11). For most anchorage-dependent vertebrate cells that can be propagated in vitro, glass is a permissive culture surface. This observation dates from the earliest days of vertebrate cell culture [331-333]. In serum-containing media, βG I/17 insulinoma cells, which can be exquisitely sensitive to surface chemistry (Chapter 1, supra), grow and function equally well on glass and surface-oxidized, tissue-culture polystyrene (TCPS, data not shown). In recent decades, TCPS has come to supplant glass as a routine, inexpensive, and permissive culture surface in laboratories worldwide.

In view of all this, glycophase glass should be considered a permissive culture surface, perhaps on par with glass and TCPS, and not a cell-repellant surface, as proposed by Massia, Hubbell, and their coworkers (section 3.7, Endnotes, infra).

In the present study, one datum did suggest a subtle difference in cell function on glass versus glycophase glass. Hourly insulin secretion during the seventh and final day of routine culture (Fig. 3.11) was significantly higher on glycophase glass. This apparent difference was not confirmed under the more rigorous metabolic conditions of diazoxide inhibition and secretagogue stimulation (Fig. 3.11). Such drug-influenced secretory changes serve as standards by which the performance of many endocrine cells is evaluated [10, 12, 27-28, 31, 51, 61-62, 84, 172, 235]. Therefore, I attach no great biologic importance to the apparent differences in insulin secretion during the seventh day of routine culture.

Independent studies support the notion that cells can attach, spread, and grow on glycophase glass. After publication of my results in abstract form [317-318], Clémence et al. [305] suggested, "unmodified glycophase glass is an adhesive substrate for NG 108-15 [neuroblastoma × glioblastoma] cells, both in serum-containing medium and in serum-free medium," and Xiao and Truskey [316] found that bovine aortic endothelial cells adhered well to fibronectin adsorbed onto either glass or glycophase glass.

Moreover, concomitant with and subsequent to my initial reports [317-318], one member of the Hubbell lab reported data that conflicted with the group's earlier claims that glycophase glass repelled adhesion by cells. Drumheller [334-335] found that 100 % of the human foreskin fibroblasts (HFF) he plated onto glycophase glass had adhered

to the surface within the first day of culture. This finding is in stark contrast to earlier studies from the same lab, in which it was claimed that HFF and other cell types did not adhere well to glycophase glass (reviewed in section 3.7, Endnotes, infra).

3.5. Conclusions

I do not doubt that Hubbell's group observed differences in the attachment and spreading of cells in the initial minutes and hours after plating cells onto glycophase glass and sundry surfaces derived from it. In serum-containing media, I suspect that most such differences would disappear in a day or two. In view of the data presented here, and considering the very short-term nature of their studies, Massia and Hubbell's claims that glycophase glass resists protein adsorption and cell attachment (section 3.7, infra) must be interpreted narrowly.

While it might indeed be possible to create cell-type-specific culture surfaces by immobilizing ligands on non-fouling surfaces, I consider Massia and Hubbell's claims of success to have been premature.

At the time this manuscript was written (June 2001), glycophase glass products were no longer commercially available. A search of trademark records at the United States Patent and Trademark Office (Washington, DC) uncovered no active trademarks based on the term "glycophase." Few chromatographers reported the use of homemade glycophase glass after about 1990.

Those in search of non-fouling surfaces might find more productive hunting in the great diversity of poly (ethylene glycols) and polysaccharides.

3.6. Figures

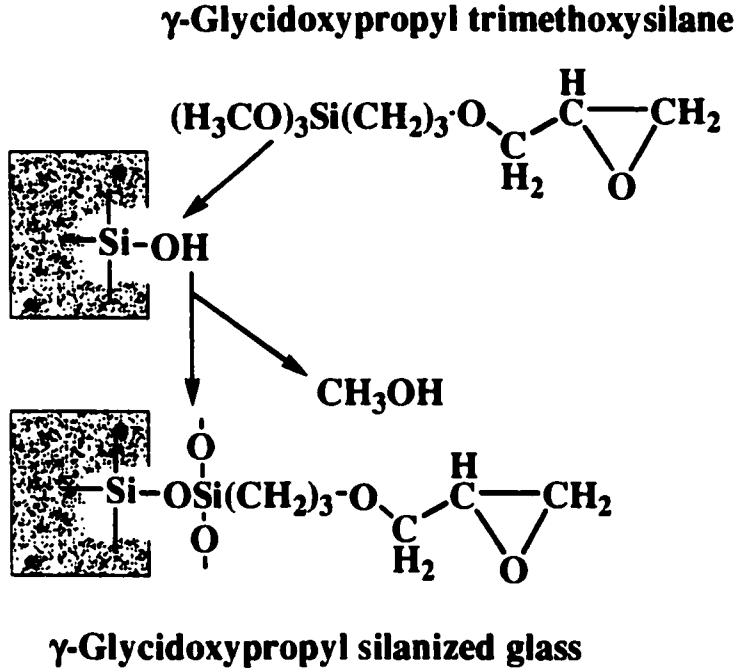

Figure 3.1. Organosilanization of etched borosilicate glass with an epoxy silane. A monolayer is shown for simplicity. Surfaces silanized with short silane monomers are typically patchy (Chapter 1).

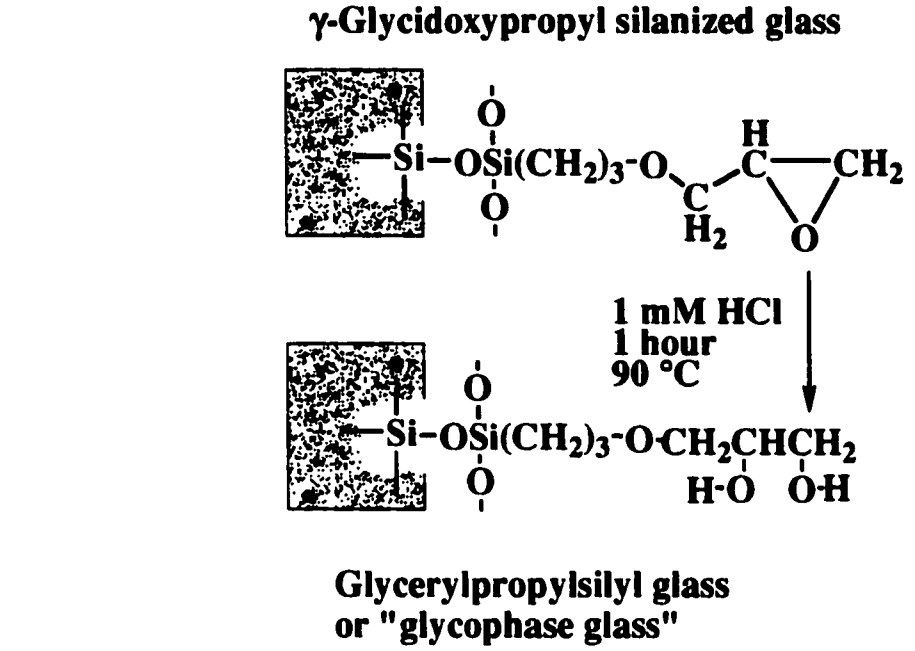

Figure 3.2. Acidic hydrolysis of the epoxy group to a diol.

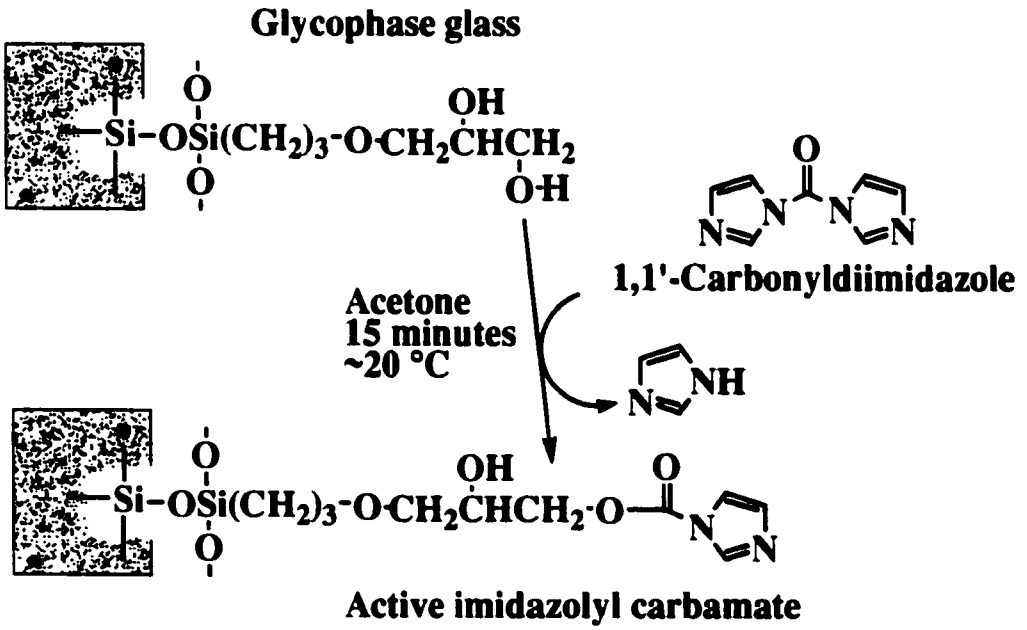

Figure 3.3. Activation of glycophase glass with 1,1'-carbonyldiimidazole.

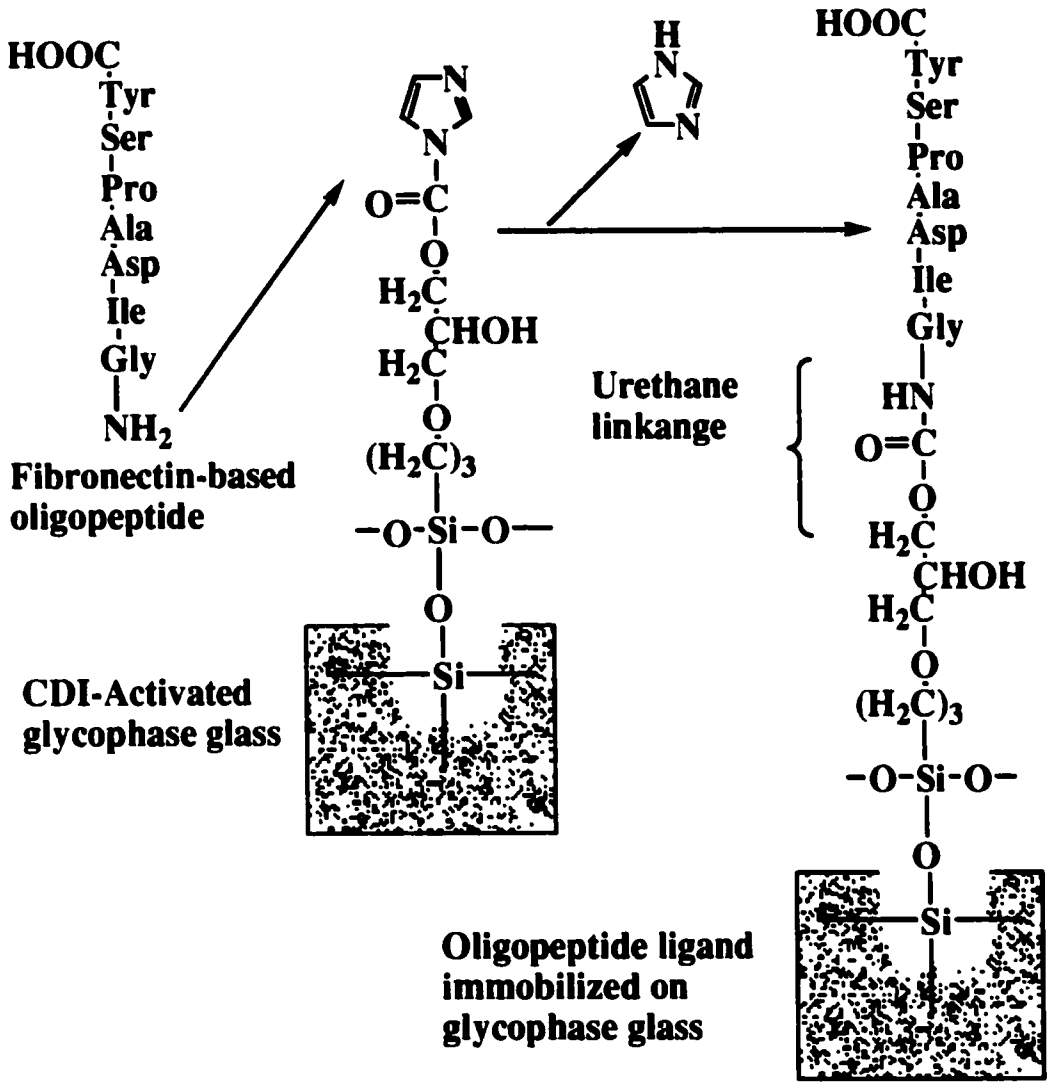

Figure 3.4. Solid-phase immobilization of the oligopeptide ligand, Gly-Ile-Asp-Ala-Pro-Ser-Tyr or GIDAPSY.

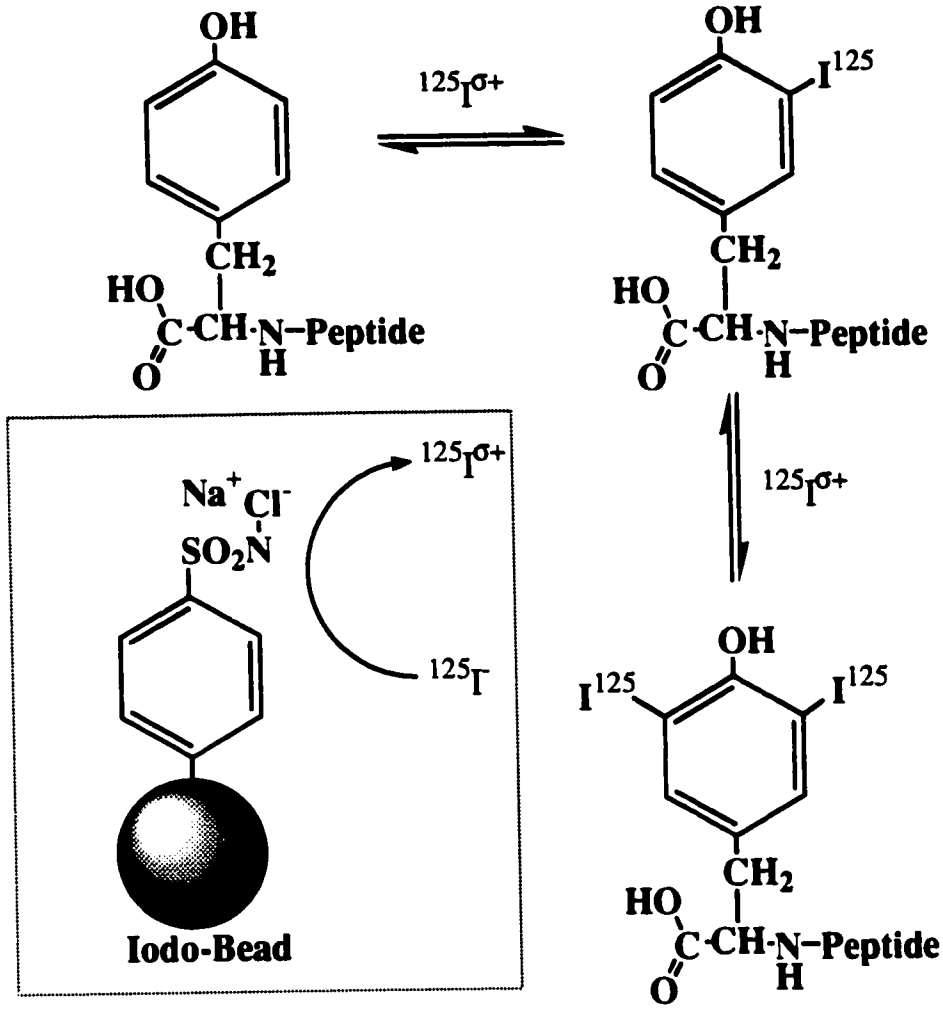

Figure 3.5. Radio-iodination of the tyrosine residue on the synthetic oligopeptide ligand, Gly-Ile-Asp-Ala-Pro-Ser-Tyr or GIDAPSY. N-chlorobenzenesulfonamide reagent or chloramine-T immobilized on polystyrene (Iodo-Beads®, Pierce Chemical Company, Rockford, IL) oxidizes the iodide anion (I^-) to a reactive, weakly electropositive state ($I^{\sigma+}$), which is capable of inserting itself onto the tyrosine ring ortho to the phenolate oxygen [336-337]. Under the reaction conditions used here and in most biologic studies, the mono-iodotyrosinyl form (upper right) probably dominates the population of iodinated peptides [338]. Fortunately, the heptapeptide, GIDAPSY, does not contain other amino-acid residues that can be halogenated by the $I^{\sigma+}$ electrophile (viz., histidine, phenylalanine, cysteine, methionine, and perhaps tryptophan), some of which form unstable adducts with iodine [337, 339, 340]. Most or all of the bound ^{125}I was therefore probably on tyrosyl residues, as shown.

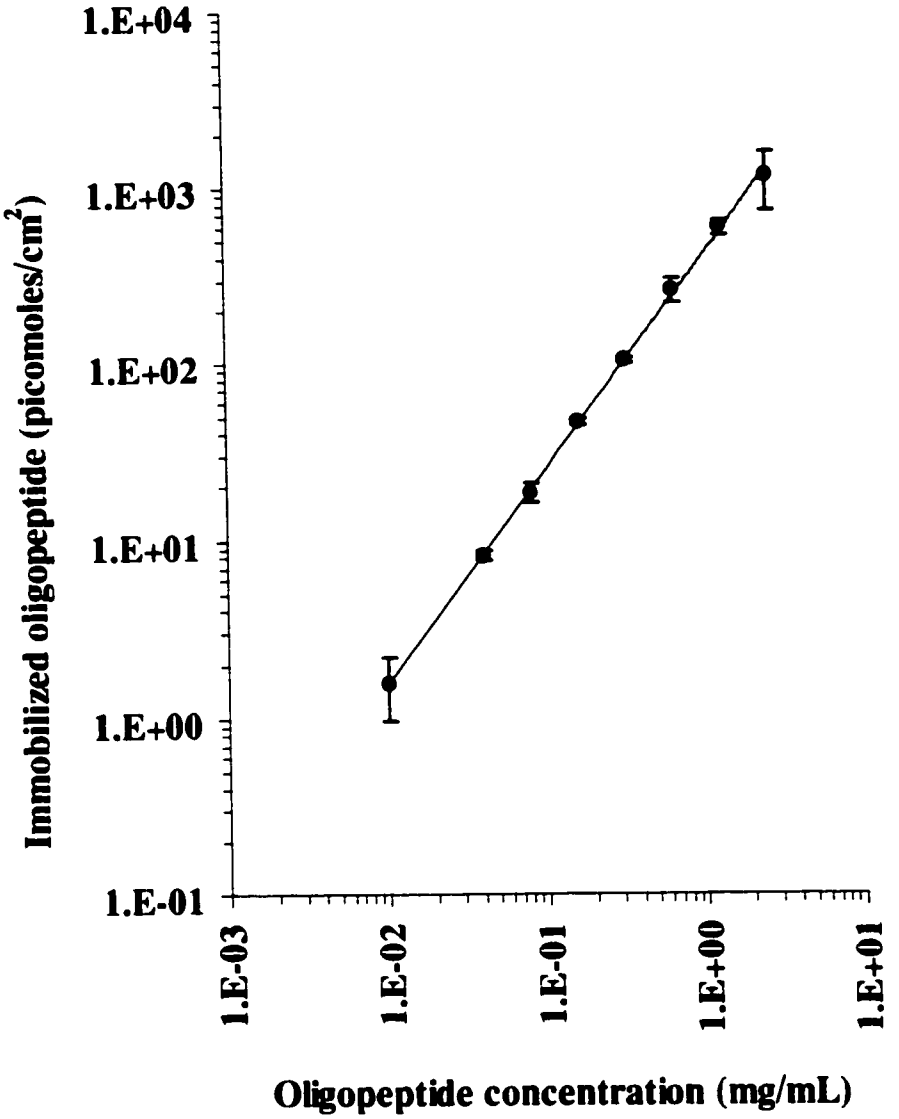

Figure 3.6. N-terminal immobilization of the heptapeptide ligand, GIDAPSY, on carbonyldiimidazole-activated glycophase glass ($r^2 = 0.993$).

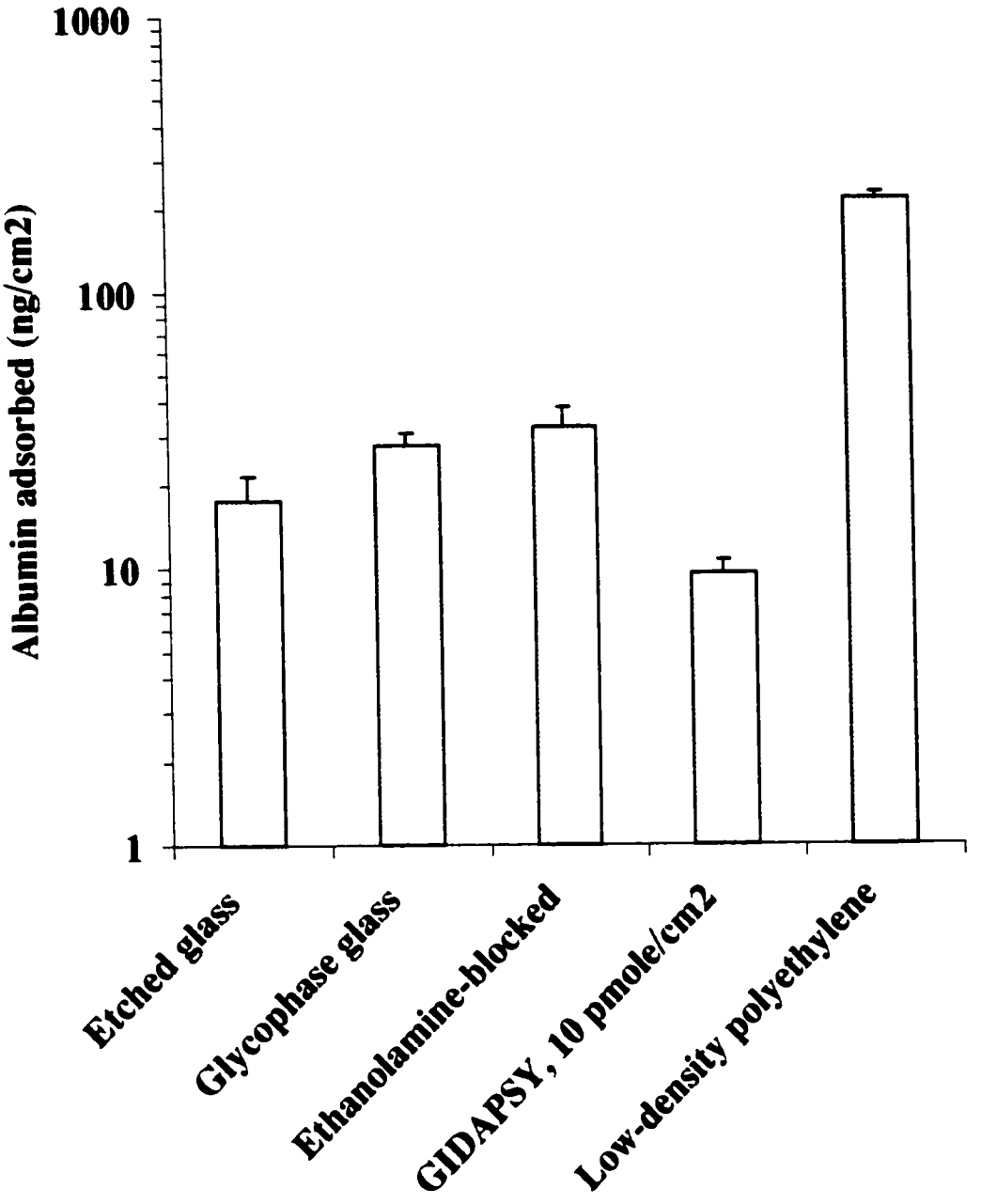

Figure 3.7. Albumin adsorption on model surfaces. n = 27 in all cases, except CDIZ-activated, ethanolamine-blocked glycophase glass, where n = 3. Adsorption on etched glass, GIDAPSY-liganded glycophase glass, and LDPE differed significantly from adsorption on glycophase glass (Tukey-Kramer HSD test, $p < 0.01$).

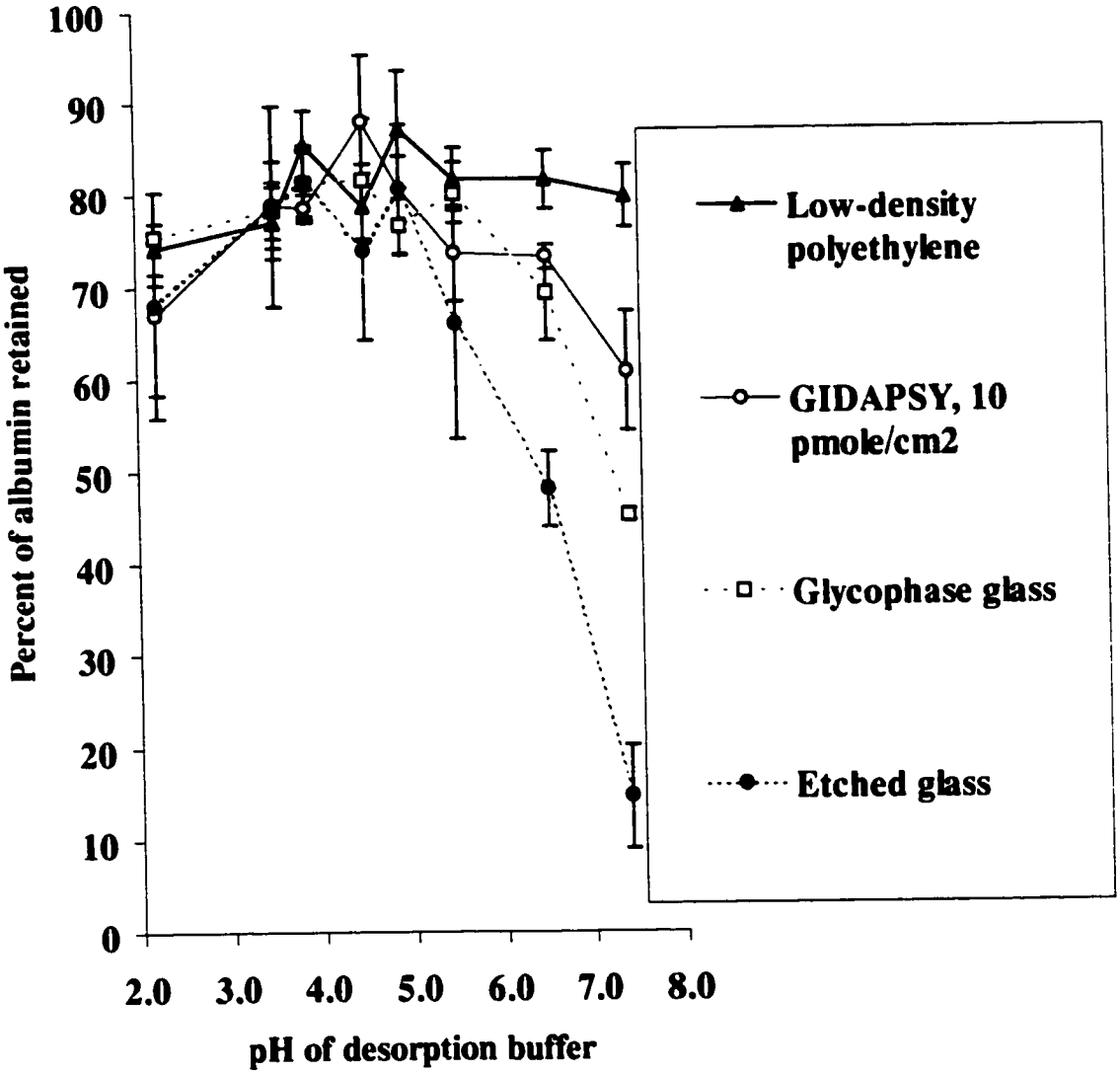

Figure 3.8. Desorption of albumin from four surfaces.

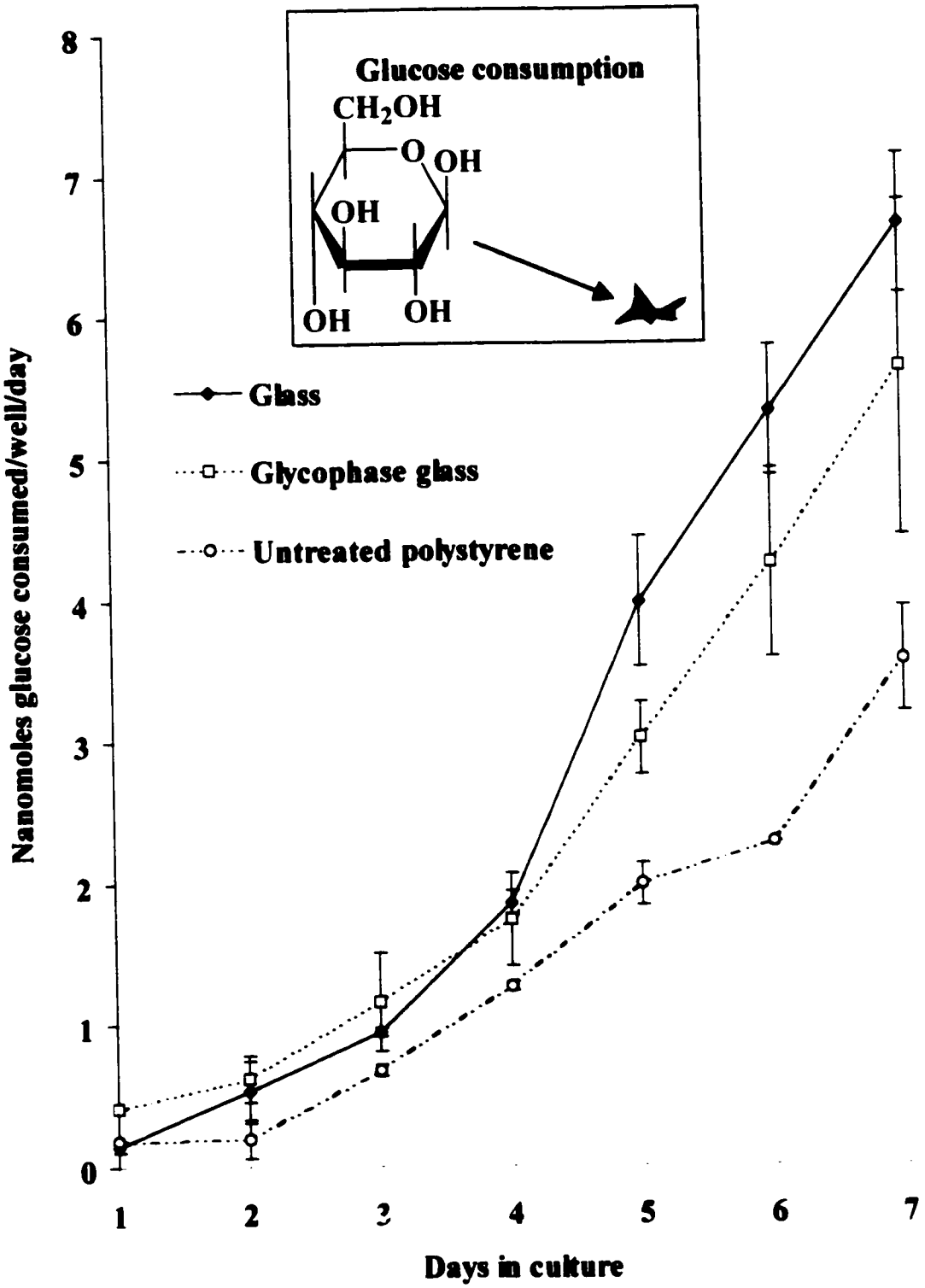

Figure 3.9. Glucose consumption by transgenic βG I/17 insulinoma cells cultured on glycophase glass and two control materials. At no time point did cultures on glass differ from those on glycophase glass ($p > 0.05$).

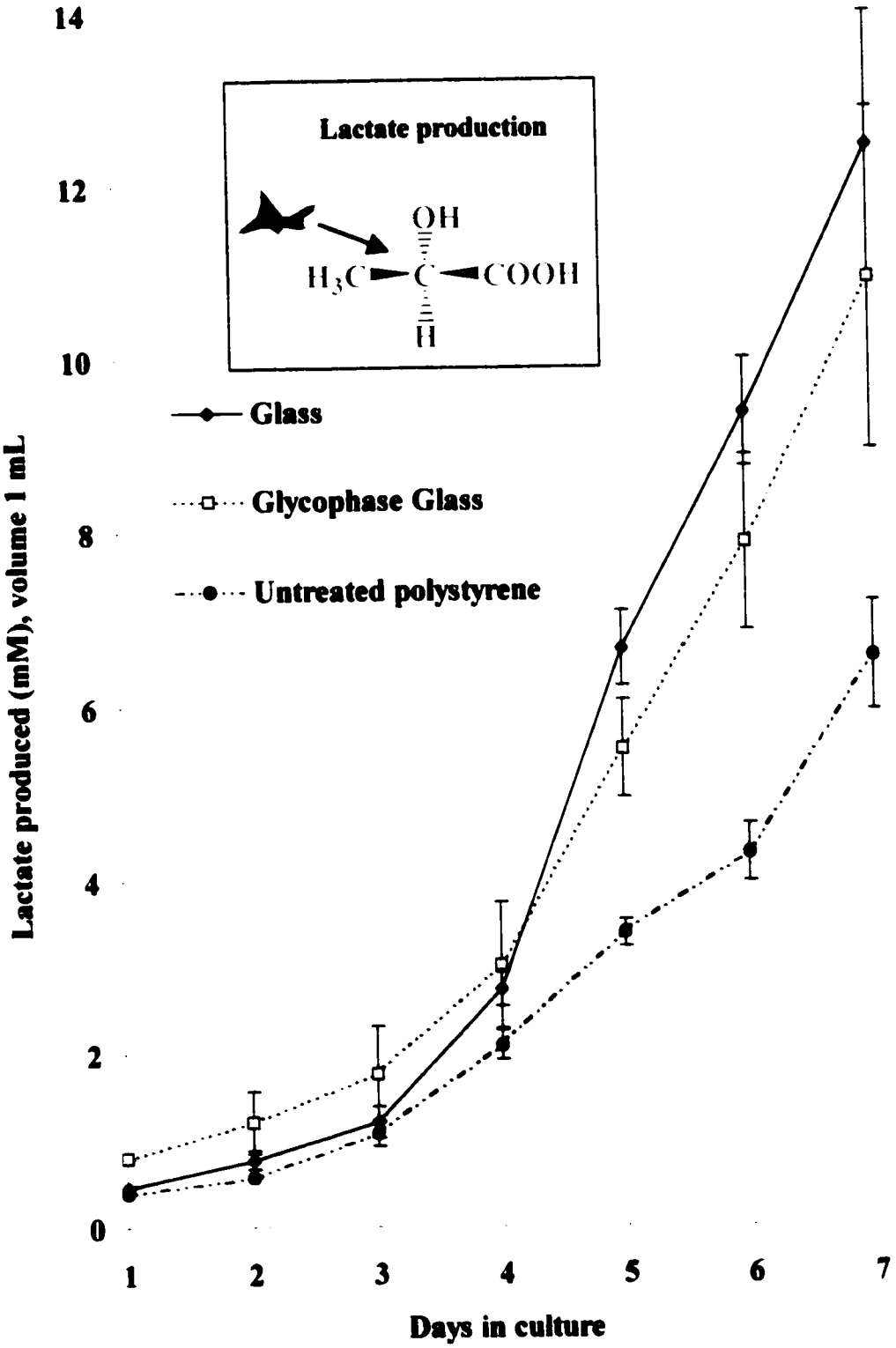

Figure 3.10. Lactate production by transgenic βG I/17 insulinoma cells cultured on glycophase glass and two control materials. At no time point did cultures on glass differ from those on glycophase glass ($p > 0.05$).

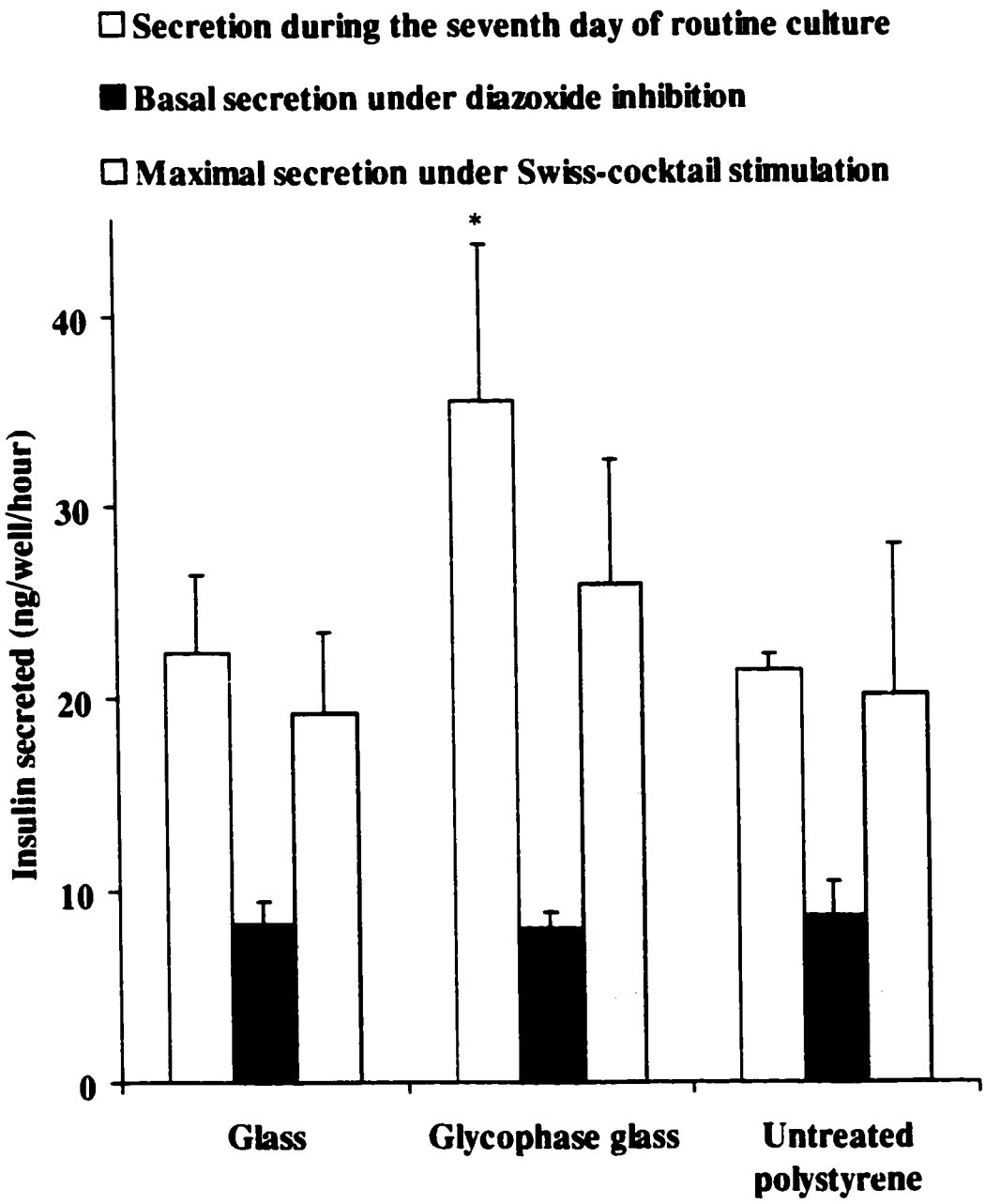

Figure 3.11. Insulin secretion by transgenic βG I/17 insulinoma cells cultured on glycophase glass and two control materials. *Differs significantly from glass ($0.05 > p > 0.01$).

3.7. Endnotes. Characterizations of glycophase glass as a non-fouling surface

"cell nonadhesive" [325].

"cell nonadhesive or poorly adhesive" [341].

"effects of potentially adsorbing proteins from cellular or culture medium sources were minimal" [342].

"Glycophase glass—a model cell nonadhesive substrate to which peptides can be coupled" [341].

"Glycophase glass was examined as a cell-nonadhesive substrate prior to modification [...] glycophase glass did not support adhesion or spreading even in the presence of serum" [343].

"Glycophase glass, the nonadhesive substrate, supported spreading and adhesion of cells only when adhesion peptides were immobilized on this surface" [343].

"no spreading or adhesion occurred on the unmodified glycophase glass" [344].

"nonadhesive" [327, 345].

"nonadhesive modified glass surface" [327].

"no spreading occurred on these substrates, and most of the cells were observed to be nonadherent. This can be interpreted to mean that adsorption of cell adhesion proteins on the glycophase glass is minimal." [327].

"poor substrate for cell adhesion without further modifications" [344, 345].

"poorly adhesive" [326, 342].

"poorly adhesive silane-modified glass" [346].

"poorly cell adhesive" [347].

"poor protein-adsorbing properties of the base glass substrate" [326].

"relatively poorly cell adhesive" [348].

"Untreated glycophase glass supported no cell adhesion, even when cells were incubated on this substrate in serum-supplemented medium" [327].

"Untreated glycophase glass was found to support no cell adhesion, even when cells were incubated on this substrate in serum-supplemented medium, which is indicative of a low protein-binding substrate" [341].

Bibliography

[1] P. Onkamo, S. Väänänen, M. Karvonen, J. Tuomilehto. Diabetologia 42 (1999) 1395.

[2] M.E. Craig, N.J. Howard, M. Silink, A. Chan. J. Pediat. Endocrinol. Metabol. 13 (2000) 363.

[3] A.T. Cheung, B. Dayanandan, J.T. Lewis, G.S. Korbutt, R.V. Rajotte, M. Bryer-Ash, M.O. Boylan, M.M. Wolfe, T.J. Kieffer. Science 290 (2000) 1959.

[4] D. Klein, C. Ricordi, A. Pugliese, R.L. Pastori. Hum. Gene Ther. 11 (2000) 1033.

[5] H.A. Clayton, N.J.M. London. Cell Transplant. 5 (1996) 1.

[6] R.G. Gill, in B. Draznin, D. LeRoith (eds.), Molecular Biology of Diabetes, Part I, Humana, Totowa, NJ, 1994, chapter 3.

[7] A.M.J. Shapiro, J.R.T. Lakey, E.A. Ryan, G.S. Korbutt, E. Toth, G.L. Warnock, N.M. Kneteman, R.V. Rajotte. New Engl. J. Med. 343 (2000) 230.

[8] D.E. Sutherland, R.W. Gruessner, D.L. Dunn, A.J. Matas, A. Humar, R. Kandaswamy, S.M. Mauer, W.R. Kennedy, F.C. Goetz, R.P. Robertson, A.C. Gruessner, J.S. Najarian. Ann. Surg. 233 (2001) 463.

[9] C.G. Groth, A. Tibell, L. Wennberg, O. Korsgren. J. Mol. Med. 77 (1999) 153.

[10] N.H. McClenaghan, P.R. Flatt. J. Mol. Med. 77 (1999) 235.

[11] A. Sambanis. Diabetes Technol. Ther. 2 (2000) 81.

[12] S.J. Persaud. Adv. Mol. Cell Biol. 29 (1999) 21.

[13] P. Soon-Shiong. Adv. Drug Deliv. Rev. 35 (1999) 259.

[14] K.K. Papas, R.C. Long, Jr., A. Sambanis, I. Constantinidis. Biotechnol. Bioengr. 66 (1999) 219.

[15] B. Soria, E. Roche, G. Berná, T. León-Quinto, J.A. Reig, F. Martin. Diabetes 49 (2000) 157.

[16] J. Oberholzer, F. Triponez, R. Mage, E. Andereggen, L. Bühler, N. Crétin, B. Fournier, C. Goumaz, J. Lou, J. Philippe, P. Morel. Transplantation 69 (2000) 1115.

[17] G.M. Beattie, G. Leibowitz, A.D. Lopez, F. Levine, A. Hayek. Cell Transplant. 9 (2000) 431.

[18] R.B. Elliott, L. Escobar, O. Garkavenko, M.C. Croxson, B.A. Schroeder, M. McGregor, G. Ferguson, N. Beckman, S. Ferguson. Cell Transplant. 9 (2000) 895.

[19] G. Luca, M. Calvitti, L.M. Neri, E. Becchetti, S. Capitani, G. Basta, G. Angeletti, C. Fanelli, P. Brunetti, R. Calafiore. J. Invest. Med. 48 (2000) 441.

[20] S. Efrat. Ann. New York Acad. Sci. 875 (1999) 286.

[21] W.M. Macfarlane, R.E. O'Brien, P.D. Barnes, R.M. Shepherd, K.E. Cosgrove, K.J. Lindsley, A. Aynsley-Green, R.F.L. James, K. Docherty, M.J. Dunne. Diabetes 49 (2000) 953.

[22] M.A. Lipes, Q. Chen. World Intellect. Prop. Org., Munich, Germany, Intl. [Patent] Publ. No. WO 99/07868, (1999).

[23] K. Burczak, Y. Ikada, in W.M. Kühtreiber, R.P. Lanza, W.L. Chick (eds.), Cell Encapsulation: Technology and Therapies, Birkhäuser, Boston, MA, 1999, chapter 17.

[24] G. Leibowitz, F. Levine. Diabetes Rev. 7 (1999) 124.

[25] V.K. Ramiya, M. Maraist, K.E. Arfors, D.A. Schatz, A.B. Peck, J.G. Cornelius. Nat. Med. 6 (2000) 278.

[26] J. Dinsmore. U.S. Patent 5,837,236 (1998).

[27] H.E. Hohmeier, H. Mulder, G. Chen, R. Henkel-Rieger, M. Prentki, C.B. Newgard. Diabetes 49 (2000) 424.

[28] C.B. Newgard, S. Clark, H. BeltrandelRio, H.E. Hohmeier, C. Quaade, K. Normington. Diabetologia 40 (1997) S42.

[29] H.-E. Hohmeier, A. Thigpen, V.V. Tran, R. Davis, C.B. Newgard. J. Clin. Invest. 101 (1998) 1811.

[30] L. Gros, E. Riu, L. Montoliu, M. Ontiveros, L. Lebrigand, F. Bosch. Hum. Gene Ther. 10 (1999) 1207.

[31] J.C. Irminger, F.M. Vollenweider, M. Neerman-Arbez, P.A. Halban. J. Biol. Chem. 269 (1994) 1756.

[32] M.R. Bochan, R.A. Sidner, R. Shah, O.W. Cummings, M. Goheen, R.M. Jindal. Transplant. Proc. 30 (1998) 453.

[33] B.E. Tuch, M.T. Tablin, F.M. Casamento, A.M. Simpson, G.M. Marshall. Transplant. Proc. 30 (1998) 473.

[34] V. Poitout, L.K. Olson, R.P. Robertson. Diabet. Metabol. 22 (1996) 7.

[35] W. Heng, X. Xinhua, F. Fude, S. Qi. Chinese Med. J. 111 (1998) 899.

[36] O. Jordan, P. Aebischer, J.-F. Clemence. U.S. Patent 6,080,412 (2000).

[37] M. Asfari, P. Czernichow. U.S. Patent 5,902,577 (1999).

[38] A.J. Brothers. U.S. Patent 5,928,942 (1999).

[39] H.G. Coon, F.S. Ambesi-Impiombato, F. Curcio. U.S. Patent 5,888,816 (1999).

[40] D.M. Desai, G.A. Adams, X. Wang, E.J. Alfrey, R.K. Sibley, D.C. Dafoe. Transplantation 68 (1999) 491.

[41] A.M. Davalli, F. Galbiati, F. Bertuzzi, L. Polastri, A.E. Pontiroli, L. Perego, M. Freschi, G. Pozza, F. Folli, C. Meoni. Hum. Cell Transplant. 9 (2000) 841.

[42] H. Mashima, S. Yamada, T. Tajima, M. Seno, H. Yamada, J. Takeda, I. Kojima. Diabetes 48 (1999) 304.

[43] S. Motoyoshi, T. Shirotani, E. Araki, K. Sakai, K. Kaneko, H. Motoshima, K. Yoshizato, A. Shirakami, H. Kishikawa, M. Shichiri. Diabetologia 41 (1998) 1492, erratum published in Diabetologia 42 (1999) 498.

[44] A. Powers, L. Wu. World Intellect. Prop. Org., Munich, Germany, Intl. [Patent] Publ. No. WO 99/54451, (1999).

[45] D. Bu, R.A. Fisher, J.M. Coghill, J. Tawes, M. Thompson, M. Posner. Surg. Forum 50 (1999) 411.

[46] W.J. Schnedl. Wien. Klin. Wochenschr. 111 (1999) 428.

[47] L. Wagner, E. Templ, G. Reining, W. Base, M. Weissel, P. Nowotny, K. Kaserer, W. Waldhäusl. J. Endocrinol. 156 (1998) 469.

[48] F. Atouf, P. Czernichow, R. Scharfmann. J. Biol. Chem. 272 (1997) 1929.

[49] J.L. Brady, A.M. Lew. Transplantation 69 (2000) 724.

[50] L.A. Stephens, H.E. Thomas, T.W.H. Kay. J. Autoimmun. 10 (1997) 293.

[51] S. Bonner-Weir, M. Taneja, G.C. Weir, K. Tatarkiewicz, K.-H. Song, A. Sharma, J. O'Neil. Proc. Natl. Acad. Sci. USA 97 (2000) 7999.

[52] H.-P.H. Moore, M.D. Walker, F. Lee, R.B. Kelly. Cell 35 (1983) 531.

[53] R.F. Selden, M.J. Skoskiewicz, P.S. Russell, H.M. Goodman. New Eng. J. Med. 317 (1987) 1067.

[54] H. Wu, E.S. Avgoustiniatos, L. Swette, S. Bonner-Weir, G.C. Weir, C.K. Colton. Ann. New York Acad. Sci. 875 (1999) 105.

[55] A.W.K. Tso, K.S.L. Lam. Curr. Opin. Endocrinol. Diabetes 7 (2000) 83.

[56] W.R. Osborne, N. Ramesh. World Intellect. Prop. Org., Munich, Germany, Intl. [Patent] Publ. No. WO 99/63101, (1999).

[57] T.W. Yoon, K. Seodaemoon. Europ. Patent Applic., Europ. Patent Off., Munich, Germany, Publ. No. EP0994185A2, (2000).

[58] V.M. Rivera, X. Wang, S. Wardwell, N.L. Courage, A. Volchuk, T. Keenan, D.A. Holt, M. Gilman, L. Orci, F. Cerasoli, Jr., J.E. Rothman, T. Clackson. Science 287 (2000) 826.

[59] P. Dupraz, C. Rinsch, W.F. Pralong, E. Rolland, R. Zufferey, D. Trono, B. Thorens. Gene Ther. 6 (1999) 1160.

[60] H. Taniguchi, K. Fukao, H. Nakauchi. J. Surg. Res. 70 (1997) 41.

[61] M. Tiedge, M. Elsner, N.H. McClenaghan, H.-J. Hedrich, D. Grube, J. Klempnauer, S. Lenzen. Hum. Gene Ther. 11 (2000) 403.

[62] P.M. Thulé, J. Liu, L.S. Phillips. Gene Ther. 7 (2000) 205.

[63] M. Borkenhagen. World Intellect. Prop. Org., Munich, Germany, Intl. [Patent] Publ. No. WO 99/60105, (1999).

[64] B.H. Kram, S.L. Mish, M.J. Muehlbauer, J.R. Bain. World Intellect. Prop. Org., Munich, Germany, Intl. [Patent] Publ. No. WO 00/58437, (2000).

[65] C.B. Newgard, P. Halban, K.D. Normington, S.A. Clark, A.E. Thigpen, C. Quaade, F. Kruse. U.S. Patent 6,194,176 (2001).

[66] G. Chen, H.E. Hohmeier, C.B. Newgard. J. Biol. Chem. 276 (2001) 766.

[67] J. Chun, G.M. Doherty. Curr. Opin. Oncol. 13 (2001) 52.

[68] D. Zhou, E. Kintsourashvili, S. Mamujee, I. Vacek, A.M. Sun. Ann. New York Acad. Sci. 875 (1999) 208.

[69] M.E. Laurence, D. Knaack, D.M. Fiore, O.D. Hegre. U.S. Patent 5,773,255 (1998).

[70] C.P. Pathak, A.S. Sawhney, J.A. Hubbell. J. Am. Chem. Soc. 114 (1992) 8311.

[71] A.Y. Wang, R.S. Ward, K.A. White, R.W. Kuhn, J.E. Taylor, J.K. John. Mater. Res. Soc. Symp. Proc. 331 (1994) 165.

[72] M. Butler, S. Mish. U.S. Patent 5,980,889 (1999).

[73] P. Aebischer, B. Zielinski. World Intellect. Prop. Org., Munich, Germany, Intl. [Patent] Publ. No. WO 94/07999, (1994).

[74] T. Loudovaris, S. Jacobs, S. Young, D. Maryanov, J. Brauker, R.C. Johnson. J. Mol. Med. 77 (1999) 219.

[75] J. Honiger, S. Darquy, G. Reach, E. Muscat, M. Thomas, C. Collier. Int. J. Artif. Org. 17 (1994) 46.

[76] H. Iwata, N. Ogawa, J. Mizoguchi. Polym. Prepr. (Am. Chem. Soc., Div. Polym. Chem.) 33 (1992) 474.

[77] S. Hirotani, R. Eda, T. Kawabata, S. Fuchinoue, S. Teraoka, T. Agishi, H. Ohgawara. Cell Transplant. 8 (1999) 399.

[78] G.H. Algire, M.L. Borders, V.J. Evans. J. Natl. Cancer Inst. 20 (1958) 1187.

[79] M. Fakir, A. Penfornis, N. Elian, P.-H. Cugnenc, J.J. Altman. Int. J. Art. Org. 20 (1997) 637.

[80] P. Aebischer, P.A. Tresco. U.S. Patent 5,871,472 (1999).

[81] P.M. Galletti, J.J. Altman. Trans. Am. Soc. Artif. Intern. Org. 30 (1984) 675.

[82] J.R. Brooks, G.J. Hill, II. Am. J. Surg. 99 (1960) 588.

[83] S.N. Mamujee, D. Zhou, M.B. Wheeler, I. Vacek, A.M. Sun. Ann. Transplant. 2 (1997) 27.

[84] T.A. Desai, Microfabricated Biocapsules for the Immunoisolation of Pancreatic Islets of Langerhans, Ph.D. dissertation, University of California, San Francisco and Berkeley, 1998, xii + 256 pages.

[85] K.E. Dionne, D.W. Scharp. U.S. Patent 5,916,554 (1999).

[86] S. Kumamoto, Y. Tanaka, J. Ono, R. Takaki. In Vitro Cell. Dev. Biol. 28A (1992) 80.

[87] J.V. Gardiner, M. Mahoodi, S.R. Bloom. Transplant. Proc. 29 (1997) 2019.

[88] N. Oturan, H. Serne, G. Reach, M. Jozefowicz. J. Biomed. Mater. Res. 27 (1993) 705.

[89] N. Aubert, G. Reach, H. Serne, M. Jozefowicz. J. Biomed. Mater. Res. 21 (1987) 585.

[90] C. Stabler, K. Wilks, A. Sambanis, I. Constantinidis. Biomaterials 22 (2001) 1301.

[91] K. Park, M. Goto, R. Takei, A. Maruyama, K. Kobayashi, J. Miyazaki, C. Cho, T. Akaike. J. Biomater. Sci. Polym. Ed. 11 (2000) 903.

[92] B. Arkles, J.R. Steinmetz, J. Zazyczny, P. Mehta, in R. Anderson, G.L. Larson, C. Smith (eds.), Silicon Compounds: Register and Review, 5th ed., Hüls America, Inc., Piscataway, NJ, 1991, pp. 65-73.

[93] P.G. Pape, E.P. Plueddemann. J. Adhes. Sci. Technol. 5 (1991) 831.

[94] T. Groth, G. Altankov, A. Kostadinova, N. Krasteva, W. Albrecht, D. Paul. J. Biomed. Mater. Res. 44 (1999) 341.

[95] S. Kouvroukoglou, K.C. Dee, R. Bizios, L.V. McIntire, K. Zygourakis. Biomaterials 21 (2000) 1725.

[96] G.A. Truskey, T.L. Proulx. Biomaterials 14 (1993) 243.

[97] A.S. Köhler, P.J. Parks, D.L. Mooradian, G.H.R. Rao, L.T. Furcht. J. Biomed. Mater. Res. 32 (1996) 237.

[98] S. Saneinejad, M.S. Shoichet. J. Biomed. Mater. Res. 42 (1998) 13.

[99] N. Yayapour, H. Nygren. Colloids Surf. B: Biointerf. 15 (1999) 127.

[100] T.O. Collier, C.H. Thomas, J.M. Anderson, K.E. Healy. J. Biomed. Mater. Res. 49 (2000) 141.

[101] S.N. Bhatia, U.J. Balis, M.L. Yarmush, M. Toner. J. Biomater. Sci. Polym. Ed. 9 (1998) 1137.

[102] K.E. Healy, B. Lom, P.E. Hockberger. Biotechnol. Bioengr. 43 (1994) 792.

[103] C.D. McFarland, C.H. Thomas, C. DeFilippis, J.G. Steele, K.E. Healy. J. Biomed. Mater. Res. 49 (2000) 200.

[104] W. Shain, H. Ancin, H.C. Craighead, M. Isaacson, L.C. Kam, B. Roysam, D. Szarowski, J.N. Turner, S.W. Turner. Proc. Fifth World Cong. Biomater., Toronto, Canada, p. 310, (1996).

[105] H.B. Lee, J.H. Lee in D.L. Wise, D.J. Trantolo, D.E. Altobelli, M.J. Yaszemski, J.D. Gresser, E.R. Schwartz (eds.), Encyclopedic Handbook of Biomaterials and

Bioengineering. Part A. Materials.Vol. 1., Dekker, NY, NY, 1995, chapter 11.

[106] L.A. Culp, C.N. Sukenik. J. Biomater. Sci. Polym. Ed. 9 (1998) 1161.

[107] S. Margel, E.A. Vogler, L. Firment, T. Watt, S. Haynie, D.Y. Sogah. J. Biomed. Mater. Res. 27 (1993) 1463.

[108] M. Matsuzawa, R.S. Potember, D.A. Stenger, V. Krauthamer. J. Neurosci. Meth. 50 (1993) 253.

[109] M. Matsuzawa, S. Tokumitsu, W. Knoll, H. Sasabe. Langmuir 14 (1998) 5133.

[110] T.G. Ruardy, H.E. Moorlag, J.M. Schakenraad, H.C. van der Mei, H.J. Busscher. J. Colloid Interf. Sci. 188 (1997) 209.

[111] J.H. Silver, R.W. Hergenrother, J.-C. Lin, F. Lim, H.-B. Lin, T. Okada, M.K. Chaudhury, S.L. Cooper. J. Biomed. Mater. Res. 29 (1995) 535.

[112] D.A. Stenger, J.H. Georger, C.S. Dulcey, J.J. Hickman, A.S. Rudolph, T.B. Nielsen, S.M. McCort, J.M. Calvert. J. Am. Chem. Soc. 114 (1992) 8435.

[113] J.J. Swalec, Jr., The Vapor Phase Deposition, Polymerization, and Surface Characterization of Methyltrimethoxysilane and 3-Chloropropyl Trimethoxysilane on a Glass Substrate, Master's thesis, University of Washington, Seattle, Washington, 1981, xii + 225 pages.

[114] R.L. Williams, J.A. Hunt, P. Tengvall. J. Biomed. Mater. Res. 29 (1995) 1545.

[115] K. Webb, V. Hlady, P.A.Tresco. J. Biomed. Mater. Res. 41 (1998) 422.

[116] P.M. St. John, L. Kam, S.W. Turner, H.G. Craighead, M. Isaacson, J.N. Turner, W. Shain. J. Neurosci. Meth. 75 (1997) 171.

[117] B.M. Cooke, S. Usami, I. Perry, G.B. Nash. Microvasc. Res. 45 (1993) 33.

[118] J.A. Hubbell, C.P. Pathak, A.S. Sawhney, N.P. Desai, J.L. Hill, S.F.A. Hossainy. U.S. Patent 5,858,746 (1999).

[119] J.P. Ranieri, R. Bellamkonda, J. Jacob, T.G. Vargo, J.A. Gardella, P. Aebischer. J. Biomed. Mater. Res. 27 (1993) 917.

[120] A. Rezania, C.H. Thomas, K.E. Healy. Ann. Biomed. Engr. 25 (1997) 190.

[121] P. Clark, D. Coles, M. Peckham. Exp. Cell Res. 230 (1997) 275.

[122] S. Britland, P. Clark, P. Connolly, G. Moores. Exp. Cell Res. 198 (1992) 124.

[123] B.C. Wheeler, J.M. Corey, G.J. Brewer, D.W. Branch. J. Biomech. Engr. 121

(1999) 73.

[124] D. Kleinfeld, K.H. Kahler, P.E. Hockberger. J. Neurosci. 8 (1988) 4098.

[125] R. Kapur, A.S. Rudolph. Exp. Cell Res. 244 (1999) 275.

[126] T.O. Acarturk, M.M. Peel, P. Petrosko, W. LaFramboise, P.C. Johnson, P.A. DiMilla. J. Biomed. Mater. Res. 44 (1999) 355.

[127] K. Webb, V. Hlady, P.A. Tresco. J. Biomed. Mater. Res. 49 (2000) 362.

[128] B.K. Mann, A.T. Tsai, T. Scott-Burden, J.L. West. Biomaterials 20 (1999) 2281.

[129] J. Wetterö, T. Bengtsson, P. Tengvall. J. Biomed. Mater. Res. 51 (2000) 742.

[130] R.R. LeVier, M.L. Chandler, S.R. Wendel, in G. Bendz, I. Lindqvist (eds.), Biochemistry of Silicon and Related Problems, Plenum, NY, NY, 1978, pp. 473-514.

[131] M. Franco, P.F. Nealey, S. Campbell, A.I. Teixeira, C.J. Murphy. J. Biomed. Mater. Res. 52 (2000) 261.

[132] P. Filippini, G. Rainaldi, A. Ferrante, B. Mecheri, G. Gabrielli, M. Bombace, P.L. Indovina, M.T. Santini. J. Biomed. Mater. Res. 55 (2001) 338.

[133] D.A. Offord, J.H. Griffin. Langmuir 9 (1993) 3015.

[134] P.W. Wojciechowski, J.L. Brash. Colloids Surf. B: Biointerf. 1 (1993) 107.

[135] R.G. Dillingham, F.J. Boerio. J. Adhes. Sci. Technol. 6 (1992) 207.

[136] M.L. Hunnicutt, J.M. Harris. Anal. Chem. 58 (1986) 748.

[137] E.P. Plueddemann, P.G. Pape. Mod. Plast. July (1985) 78.

[138] M.J. Wirth, H.O. Fatunmbi. Anal. Chem. 65 (1993) 822.

[139] K. Kojio, S. Ge, A. Takahara, T. Kajiyama. Langmuir 14 (1998) 971.

[140] J.R. Bain, A.S. Hoffman, T.A. Horbett. 37th International Symposium on Macromolecules, July 12-17, 1998, Gold Coast, Queensland, Australia, World Polymer Congress, Int. Union Pure Appl. Chem., preprints, p. 789.

[141] W.L. McKeehan, R.G. Ham. J. Cell Biol. 71 (1976) 727.

[142] H.J. Griesser, R.C. Chatelier, T.R. Gengenbach, G. Johnson, J.G. Steele. J. Biomater. Sci. Polym. Ed. 5 (1994) 531.

[143] B. Ziegler, M. Schlosser, B. Fürll, S. Witt, M. Ziegler. Diabet. Res. 16 (1991) 41.

[144] M. Kriat, J. Fantini, J. Vion-Dury, S. Confort-Gouny, J.P. Galons, P.J. Cozzone.

Biochemie 74 (1992) 949.

[145] G.E. Grampp, A. Sambanis, G.N. Stephanopoulos. Adv. Biochem. Engr. Biotechnol. 46 (1992) 35.

[146] J.G. Aunins, D.I.C. Wang. Biotechnol. Bioengr. 34 (1989) 629.

[147] P.C. Letourneau. Devel. Biol. 44 (1975) 77.

[148] A. Bruil, J.I. Sheppard, J. Feijen, I.A. Feuerstein. J. Biomater. Sci. Polym. Ed. 5 (1994) 263.

[149] U.T. Rüegg, F. Hefti. Neurosci. Lett. 49 (1984) 319.

[150] J.G. Steele, B.A. Dalton, G. Johnson, P.A. Underwood. Biomaterials 16 (1995) 1057.

[151] T.G. van Kooten, J.M. Schakenraad, H.C. van der Mei, H.J. Busscher. Biomaterials 13 (1992) 897.

[152] J.D. Andrade, L.M. Smith, D.E. Gregonis, in J.D. Andrade (ed.), Surface and Interfacial Aspects of Biomedical Polymers. Volume 1. Surface Chemistry and Physics, Plenum Press, NY, NY, 1985, pp. 249-293.

[153] R.J. Good. Adv. Chem. Ser. 43 (1964) 74.

[154] R.E. Johnson, Jr., R.H. Dettre. Surfact. Sci. Ser. 49 (1993) 1.

[155] J.M. Schakenraad, H.J. Busscher, C.R.H. Wildevuur, J. Arends. J. Biomed. Mater. Res. 20 (1986) 773.

[156] P.B. van Wachem, T. Beugeling, J. Feijen, A. Bantjes, J.P. Detmers, W.G. van Aken. Biomaterials 6 (1985) 403.

[157] W.A. Zisman. Adv. Chem. Ser. 43 (1964) 1.

[158] D.K. Pettit, T.A. Horbett, A.S. Hoffman. J. Biomed. Mater. Res. 26 (1992) 1259.

[159] B. Kanner, in R. Anderson, B. Arkles, G.L. Larson (eds.), Silicon Compounds: Register and Review, Petrarch Systems, Bristol, PA, 1987, pp. 40-46.

[160] J.W. Bovenkamp, B.V. Lacroix. Indust. Eng. Chem. Prod. Res. Develop. 20 (1981) 130.

[161] M.J. Owen, D.E. Williams. J. Adhesion Sci. Technol. 5 (1991) 307.

[162] D.E. Williams, T.J. Tangney, in D.E. Leyden (ed.), Silanes, Surfaces, and Interfaces, Gordon and Breach, NY, NY, 1986, pp. 471-480.

[163] J.M. Harris, J.M. Dust, R.A. McGill, P.A. Harris, M.J. Edgell, R.M. Sedaghat-Herati, L.J. Karr, D.L. Donnelly. Am. Chem. Soc. Symp. Ser. 467 (1991) 420.

[164] S.M. Wojcik, D.A. Puleo. Trans. Soc. Biomater. 21 (1998) 487.

[165] D. Leach-Scampavia, University of Washington, provided the paragraph describing ESCA analysis. The paragraph that comprises section 1.2.4. is a modified version of her written communication to J. Bain, dated 31 May 1995.

[166] E.A. Vogler. Surfact. Sci. Ser. 49 (1993) 183.

[167] W.L. Chick, S. Warren, R.N. Chute, A.A. Like, V. Lauris, K.C. Kitchen. Proc. Natl. Acad. Sci. USA 74 (1977) 628.

[168] A.F. Gazdar, W.L. Chick, H.K. Oie, H.L. Sims, D.L. King, G.C. Weir, V. Lauris. Proc. Natl. Acad. Sci. USA 77 (1980) 3519.

[169] J. Philippe, W.L. Chick, J.F. Habener. J. Clin. Invest. 79 (1987) 351.

[170] S.A. Clark, B.L. Burnham, W.L. Chick. Endocrinology 127 (1990) 2779.

[171] S. Ferber, H. BertrandelRio, J.H. Johnson, R.J. Noel, L.E. Cassidy, S. Clark, T.C. Becker, S.D. Hughes, C.B. Newgard. J. Biol. Chem. 269 (1994) 11523.

[172] H.E. Hohmeier, H. BeltrandelRio, S.A. Clark, R. Henkel-Rieger, K. Normington, C.B. Newgard. Diabetes 46 (1997) 968.

[173] S.A. Clark, C. Quaade, H. Constandy, P. Hansen, P. Halban, S. Ferber, C.B. Newgard, K. Normington. Diabetes 46 (1997) 958.

[174] P. Petit, M.M. Loubatières-Mariani. Fund. Clin. Pharmacol. 6 (1992) 123.

[175] R.R. Sokal, F.J. Rolf. Biometry, 2nd ed., W.H. Freeman and Co., San Francisco, CA, 1981, chapter 9.

[176] B.D. Ratner, J.J. Rosen, A.S. Hoffman, L.H. Scharpen, in K.L. Mittal (ed.), Surface Contamination, Vol. 2, Plenum Press, NY, NY, 1979, pp. 669-686.

[177] T.H. Elmer, in D.E. Leyden, W.T. Collins, (eds.), Silylated Surfaces, Gordon and Breach, NY, NY, 1980, pp. 1-30.

[178] A. Menawat, J. Henry, Jr., R. Siriwardae. J. Colloid Interf. Sci. 101 (1984) 110.

[179] K.P. Battjes, A.M. Barolo, P. Dreyfuss. J. Adhesion Sci. Technol. 5 (1991) 785.

[180] E.P. Plueddemann, in D.E. Leyden, W.T. Collins (eds.), Silylated Surfaces, Gordon and Breach, NY, NY, 1980, pp. 31-53.

[181] D.J. Dunaway, R.L. McCarley. Langmuir 10 (1994) 3598.

[182] R.L. Alley, K. Komvopoulos, R.T. Howe. J. Appl. Phys. 76 (1994) 5731.

[183] A. Barrat, P. Silberzan, L. Bourdieu, D. Chatenay. Europhys. Lett. 20 (1992) 633.

[184] D.H. Flinn, D.A. Guzonas, R.-H. Yoon. Colloids Surf. A. Physicochem. Engr. Asp. 87 (1994) 163.

[185] S. Gauthier, J.P. Aimé, T. Bouhacina, A.J. Attias, B. Desbat. Langmuir 12 (1996) 5126.

[186] N.B. Sheller, S. Petrash, M.D. Foster, V.V. Tsukruk. Langmuir 14 (1998) 4535.

[187] C.A. Siedlecki, R.E. Marchant. Biomaterials 19 (1998) 441.

[188] R. Banga, J. Yarwood, A.M. Morgan, B. Evans, J. Kells. Langmuir 11 (1995) 4393.

[189] N. Ishida, N. Kinoshita, M. Miyahara, K. Higashitani. J. Colloid Interf. Sci. 216 (1999) 387.

[190] H. Brunner, T. Vallant, U. Mayer, H. Hoffmann, B. Basnar, M. Vallant, G. Friedbacher. Langmuir 15 (1999) 1899.

[191] P. Tengvall, L. Olsson, B. Wälivaara, A. Askendal, I. Lundström, H. Elwing. Adv. Biomater. 10 (1992) 511.

[192] D.W. Britt, V. Hlady. J. Colloids Interf. Sci. 178 (1996) 775.

[193] J.W. Davidovits, V. Pho, P. Silberzan, M. Goldmann. Surf. Sci. 352-354 (1996) 369.

[194] J. Fang, C.M. Knobler. J. Phys. Chem. 99 (1995) 10425.

[195] Y.L. Lyubchenko, A.A. Gall, L.S. Shlyakhtenko, R.E. Harrington, B.L. Jacobs, P.I. Oden, S.M. Lindsay. J. Biomolec. Struc. Dynam. 10 (1992) 589.

[196] H. Okusa, K. Kurihara, T. Kunitake. Langmuir 10 (1994) 3577.

[197] Y.I. Rabinovich, R.-H. Yoon. Langmuir 10 (1994) 1903.

[198] S. Ge, K. Kojio, A. Takahara, T. Kajiyama. J. Biomater. Sci. Polym. Ed. 9 (1998) 131.

[199] R. Wang, S.L. Wunder. Langmuir 16 (2000) 5008.

[200] K. Kojio, A. Takahara, T. Kajiyama. Colloids Surf. A. Physicochem. Engr. Asp. 169 (2000) 295.

[201] W.J. Tze, J. Tai. Transplantation 34 (1982) 228.

[202] H. Abrahamsson, P.-O. Berggren, B. Hellman. Am. J. Physiol. 247 (1984) E719.

[203] C.D. Roskelley, A. Srebrow, M.J. Bissell. Curr. Opin. Cell Biol. 7 (1995) 736.

[204] H.K.W. Fong, W.L. Chick, G.H. Sato. Diabetes 30 (1981) 1022.

[205] S.A. Clark, W.L. Chick. Endocrinology 126 (1990) 1895.

[206] S. Efrat, S. Linde, H. Kofod, D. Spector, M. Delannoy, S. Grant, D. Hanahan, S. Baekkesov. Proc. Natl. Acad. Sci. USA 85 (1988) 9037.

[207] J.-I. Miyazaki, K. Araki, E. Yamato, H. Ikegami, T. Asano, Y. Shibasaki, Y. Oka, K.-I. Yamamura. Endocrinology 127 (1990) 126.

[208] A.C. Hauge-Evans, P.E. Squires, S.J. Persaud, P.M. Jones. Diabetes 48 (1999) 1402.

[209] N.H. McClenaghan, C.R. Barnett, E. Ah-Sing, Y.H.A. Abdel-Wahab, F.P.M. O'Harte, T.-W. Yoon, S.K. Swanston-Flatt, P.R. Flatt. Diabetes 45 (1996) 1132.

[210] M. Noda, M. Komatsu, G.W.G. Sharp. Diabetes 45 (1996) 1766.

[211] M. Asfari, D. Janjic, P. Meda, G. Li, P.A. Halban, C.B. Wollheim. Endocrinology 130 (1992) 167.

[212] K.K. Papas, R.C. Long, Jr., I. Constantinidis, A. Sambanis. Cell Transplant. 9 (2000) 415.

[213] C.H. Thivolet, P. Chatelain, H. Nicoloso, A. Durand, J. Bertrand. Exp. Cell Res. 159 (1985) 313.

[214] H.R. Zielke, C.L. Zielke, P.T. Ozand. Fed. Proc. 43 (1984) 121.

[215] A. Sener, W. Malaisse. Experientia 40 (1984) 1026.

[216] M.W. Glacken, R.J. Fleischer, A.J. Sinskey. Biotechnol. Bioengr. 28 (1986) 1376.

[217] J. Tamarit-Rodriguez, L.-Å. Idahl, O. Alcazar, J. Sehlin. Diabetes 47 (1998) 1219.

[218] W.J. Malaisse. Diabet. Rev. 4 (1996) 145.

[219] A. Sener, W.J. Malaisse. Biochem. J. 246 (1987) 89.

[220] B. Obradovic, R.L. Carrier, G. Vunjak-Novakovic, L.E. Freed. Biotechnol. Bioengr. 63 (1999) 197.

[221] W.S. Hu, T.C. Dodge, K.K. Frame, V.B. Himes. Devel. Biol. Stand. 66 (1987) 279.

[222] G. Zubay, Biochemistry, 2nd ed., Macmillan, NY, NY, 1988, chapters 14 and 16.

[223] F. Schuit, A. de Vos, S. Farfari, K. Moens, D. Pipeleers, T. Brun, M. Prentki. J. Biol. Chem. 272 (1997) 18572.

[224] N. Sekine, V. Cirulli, R. Regazzi, L.J. Brown, E. Gine, J. Tamarit-Rodriguez, M. Girotti, S. Marie, M.J. MacDonald, C.B. Wollheim, G.A. Rutter. J. Biol. Chem. 269 (1994) 4895.

[225] E.K. Ainscow, C. Zhao, G.A. Rutter. Diabetes 49 (2000) 1149.

[226] J. Rasschaert, P.R. Flatt, C.R. Barnett, N.H. McClenaghan, W.J. Malaisse. Biochem. Molec. Med. 57 (1996) 97.

[227] G. Nowak, J.M. Griffin, R.G. Schnellmann. J. Toxicol. Environ. Health 49 (1996) 439.

[228] M.J. MacDonald. J. Biol. Chem. 270 (1995) 20051.

[229] I. Constantinidis, N.E. Mukundan, M.P. Gamcsik, A. Sambanis. Cell. Molec. Biol. 43 (1997) 721.

[230] H.K. Berman, C. Newgard. Biochemistry 37 (1998) 4543.

[231] J. Rasschaert, W.J. Malaisse. Int. J. Biochem. Cell Biol. 27 (1995) 195.

[232] K.K. Papas, R.C. Long, Jr., I. Constantinidis, A. Sambanis. Biochim. Biophys. Acta 1291 (1996) 163.

[233] R.I. Freshney, Culture of Animal Cells, 3rd ed., Wiley-Liss, NY, NY, 1994, chapter 7.

[234] G.E. Grampp, M.A. Applegate, G. Stephanopoulos. Biotechnol. Prog. 12 (1996) 837.

[235] C. Lucas-Clerc, C. Massart, J.P. Campion, B. Launois, M. Nicol. Mol. Cell. Endocrinol. 94 (1993) 9.

[236] M.J. Close, A.R. Howlett, C.D. Roskelley, P.Y. Desprez, N. Bailey, B. Rowning, C.T. Teng, M.R. Stampfer, P. Yaswen. J. Cell Sci. 110 (1997) 2861.

[237] C.S. Chen, M. Mrksich, S. Huang, G.M. Whitesides, D.E. Ingber. Biotechnol. Prog. 14 (1998) 356.

[238] H. Senoo, K. Imai, M. Sato, N. Kojima, M. Miura, R.-I. Hata. Cell Biol. Int. 20 (1996) 501.

[239] C.B. Wollheim, P. Meda, P. Halban. Meth. Enzymol. 192 (1990) 223.

[240] G.M. Beattie, J.S. Rubin, M.I. Mally, T. Otonkoski, A. Hayek. Diabetes 45 (1996) 1223.

[241] D. Bosco, P. Meda, P.A. Halban, D.G. Rouiller. Diabetes 49 (2000) 233.

[242] M.W. Lieberman, E.D. Lykissa, R. Barrios, C.N. Ou, G. Kala, S.V. Kala. Environ. Health Perspect. 107 (1999) 161.

[243] R.G. Meeks. Med. Dev. Diag. Indust. 21 (1999) 112.

[244] K. Nakamura, M.F. Refojo, D.V. Crabtree, J. Pastor, F.-L. Leong. Invest. Ophthalmol. Vis. Sci. 32 (1991) 3007.

[245] J.J. Nicholson, III, S.L. Hill, C.G. Frondoza, N.R. Rose. J. Biomed. Mater. Res. 31 (1996) 345.

[246] W.H. Siddiqui, R.G. York. Fund. Appl. Toxicol. 21 (1993) 66.

[247] S. Bondurant, V. Ernster, R. Herdman (eds.), Safety of Silicone Breast Implants, National Academy Press, Washington, DC, 2000.

[248] C. Azzolini, P.G. Gobbi, R. Brancato, L. Bosi, D. Gallo, M. Zelada, F. Patelli. Arch. Ophthalmol. 115 (1997) 899.

[249] J.F. Hayden, S.A. Barlow. Toxicol. Appl. Pharmacol. 21 (1972) 68.

[250] S. Lenzen, C.J. Bailey. Endocr. Rev. 5 (1984) 411.

[251] J.L. Bohnert, B.C. Fowler, T.A. Horbett, A.S. Hoffman. J. Biomater. Sci. Polym. Ed. 1 (1990) 279.

[252] D. Kiaei, A.S. Hoffman, T.A. Horbett, K.R. Lew. J. Biomed Mater. Res. 29 (1995) 729.

[253] D. Kiaei, A.S. Hoffman, T.A. Horbett. J. Biomater. Sci. Polym. Ed. 4 (1992) 35.

[254] A. Takahara, S. Ge, K. Kojio, T. Kajiyama. J. Biomater. Sci. Polym. Ed. 11 (2000) 111.

[255] C-G. Gölander, Y.-S. Lin, V. Hlady, J.D. Andrade. Colloids Surf. 49 (1990) 289.

[256] Y.-S. Lin, V. Hlady, J. Janatova. Biomaterials 13 (1992) 497.

[257] L. Liu, H. Elwing. J. Biomed. Mater. Res. 28 (1994) 767.

[258] T. Meyer, S. Czub, I. Chodnewska, U. Beutner, W. Hamelmann, G. Klöck, U. Zimmermann, A. Thiede, K. Ulrichs. Ann. Transplant. 2 (1997) 17.

[259] C.A. Crisera, A.S. Kadison, G.D. Breslow, T.S. Maldonado, M.T. Longaker, G.K. Gittes. Diabetes 49 (2000) 936.

[260] R.H. Kennedy, D.E. Bockman, L. Uscanga, R. Choux, J.-A. Grimaud, H. Sarles. Pancreas 2 (1987) 61.

[261] M. Hisaoka, J. Haratake, H. Hashimoto. Differentiation 53 (1993) 163.

[262] S.A. White, D.P. Hughes, H.H. Contractor, N.J.M. London. J. Mol. Med. 77 (1999) 79.

[263] A. Menke, H. Yamaguchi, T.M. Gress, G. Adler. Gastroenterology 113 (1997) 295.

[264] C. Haglund, S. Nordling, P.J. Roberts, P. Ekblom. Am. J. Surg. Path. 8 (1984) 669.

[265] D.J. Hill, in L. Rosenberg, W.P. Duguid (eds.), Cellular Inter-relationships in the Pancreas: Implications for Islet Transplantation, R.G. Landes Company, Austin, TX, 1996, chapter 4.

[266] S. Kantengwa, D. Baetens, K. Sadoul, C.A. Buck, P.A. Halban, D.G. Rouiller. Exp. Cell Res. 237 (1997) 394.

[267] R. Muschel, G. Khoury, L.M. Reid. Mol. Cell. Biol. 6 (1986) 337.

[268] I.T. Todorov, K.I. Scheyhing, J.J. Grzesiak, G. Cruz-Aranda, C.B. Stubban, Y. Mullen, C.R. Halberstadt, J.C. Jones. Transplant. Proc. 30 (1998) 455.

[269] N. Kaiser, A.P. Corcos, A. Tur-Sinai, Y. Ariav, E. Cerasi. Endocrinology 123 (1988) 834.

[270] B.B. Rawdon, A. Andrew. In Vitro Cell. Dev. Biol.-Anim. 33 (1997) 774.

[271] R. Perfetti, T.E. Henderson, Y. Wang, C. Montrose-Rafizadeh, J.M. Egan. Pancreas 13 (1996) 47.

[272] F.-X. Jiang, D.S. Cram, H.J. DeAizpurua, L.C. Harrison. Diabetes 48 (1999) 722.

[273] P. Metrakos, S. Yuan, S.J. Qi, W.P. Duguid, L. Rosenberg. Transplant. Proc. 26 (1994) 3349.

[274] P. Montesano, P. Mouron, M. Amherdt, L. Orci. J. Cell Biol. 97 (1983) 935.

[275] P.O.G. Arkhammar, B.R. Terry, H. Kofod, O. Thastrup. Meth. Cell Sci. 19 (1998) 255.

[276] S.-H. Chao, M.V. Peshwa, D.E.R. Sutherland, W.-S. Hu. Cell Transplant. 1 (1992) 51.

[277] A. Ilieva, S. Yuan, R. Wang, W.P. Duguid, L. Rosenberg. Pancreas 19 (1999) 297.

[278] C. Jesser, L. Kessler, A. Lambert, A. Belcourt, M. Pinget. Artif. Org. 20 (1996) 997.

[279] S.F. Badylak, S. Voytik, G. Boder. U.S. Patent 5,866,414 (1999).

[280] G. Pelosi, F. Pasini, E. Bresaola, G. Bogina, P. Pederzoli, S. Biolo, S. Menard, G. Zamboni. J. Pathol. 183 (1997) 62.

[281] T. Tani, A. Lumme, A. Linnala, E. Kivilaakso, T. Kiviluoto, R.E. Burgeson, L. Kangas, I. Leivo, I. Virtanen. Am. J. Pathol. 151 (1997) 1289.

[282] S.E. Baker, O. Skalli, R.D. Goldman, J.C.R. Jones. Cell Motil. Cytoskel. 37 (1997) 271.

[283] R. Paddenberg, K. Flocke, H.-P. Elsässer, G. Lesch, H.-H. Heidtmann, H.G. Mannherz. Eur. J. Cell Biol. 76 (1998) 251.

[284] M.-E. Halatsch, K.I. Hirsch-Ernst, G.F. Kahl, R.J. Weinel. Cancer Lett. 118 (1997) 7.

[285] R.N. Wang, S. Paraskevas, L. Rosenberg. J. Histochem. Cytochem. 47 (1999) 499.

[286] B. Schmeid, G. Liu, M.P. Moyer, L.S.B. Hernberg, W. Sanger, S. Batra, P.M. Pour. Carcinogenesis 20 (1999) 317.

[287] G. Friends, J. Künzler, R. Ozark, M. Trokanski. Am. Chem. Soc. Symp. Ser. 540 (1994) 76.

[288] Y. Lakshmanan, S.G. Docimo. J. Long-Term Eff. Med. Impl. 7 (1997) 65.

[289] E.P.J.M. Everaert, H.F. Mahieu, B. van de Belt-Gritter, A.J.G.E. Peeters, G.J. Verkerke, H.C. van der Mei, H.J. Busscher. Arch. Otolaryngol. Head Neck Surg. 125 (1999) 1329.

[290] W.D. Larson. Europ. Patent Spec., Europ. Patent Off., Munich, Germany, Publ. No. 0030838, (1984).

[291] C. Halberstadt, J.J. Grzesiak. U.S. Patent 5,672,361 (1997).

[292] J.C.R. Jones. U.S. Patent 5,541,106 (1996).

[293] L.G. Tillotson, C. Lodestro, M. Hocker, B. Wiedenmann, C.E. Newcomer, L.M. Reid. Pancreas 22 (2001) 91.

[294] E. Engvall, G.E. Davis, K. Kickerson, E. Ruoslahti, S. Varon, M. Manthorpe. J. Cell Biol. 103 (1986) 2457.

[295] J. Dodd, S.B. Morton, D. Karagogeos, M. Yamamoto, T.M. Jessell. Neuron 1 (1988) 105.

[296] J.R. Sanes, E. Engvall, R. Butkowski, D.D. Hunter. J. Cell Biol. 111 (1990) 1685.

[297] M. Durbeej, L. Fecker, T. Hjalt, H.-Y. Zhang, K. Salmivirta, G. Klein, R. Timpl, L. Sorokin, T. Ebendal, P. Ekblom, M. Ekblom. Matrix Biol. 15 (1996) 397.

[298] A.S. Hoffman. J. Biomater. Sci. Polym. Ed. 10 (1999) 1011.

[299] S.K. Hendricks, C. Kwok, M. Shen, T.A. Horbett, B.D. Ratner, J.D. Bryers. J. Biomed. Mater. Res. 50 (2000) 160.

[300] R. Oliver, G.P. Royer. U.S. Patent 4,0651,591 (1977).

[301] Z.L. Bandi, M.T. Moslen, E.S. Reynolds. J. Chromatog. 249 (1982) 93.

[302] F. Borrego, M. Tari, A. Manjon, J.L. Iborra. Appl. Biochem. Biotech. 22 (1989) 129.

[303] G.J.M. Bruin, R. Huisden, J.C. Kraak, H. Poppe. J. Chromatog. 480 (1989) 339.

[304] B.A. Burdick, T.W. Esders, J.R. Schaeffer, S. Lynn. Appl. Biochem. Biotech. 16 (1987) 145.

[305] J.-F. Clémence, J.P. Ranieri, P. Aebischer, H. Sigrist. Bioconjugate Chem. 6 (1995) 4111.

[306] K. Ernst-Cabrera, M. Wilchek. Analyt. Chem. 159 (1986) 267.

[307] K. Ernst-Cabrera, M. Wilchek. J. Chromatog. 397 (1987) 187.

[308] M. Glad, S. Ohlson, L. Hansson, M.-O. Månsson, K. Mosbach. J. Chromatog. 200 (1980) 254.

[309] A. Jimeno, A. Manjon, M. Canovas, J.L. Iborra. Process Biochem. 22 (1987) 13.

[310] K. Nilsson, K. Mosbach. Meth. Enzymol. 104 (1984) 56.

[311] F.E. Regnier, S.-H. Chang. U.S. Patent 4,108,603 (1978).

[312] J.R. Schaeffer, R.E. Snoke, H.W. Harris. U.S. Patent 4,111,838 (1978).

[313] J. Schacht. J. Lipid Res. 19 (1978) 1063.

[314] M.-B. Stark, K. Holmberg. Biotechnol. Bioengr. 34 (1989) 942.

[315] J.K. Stuart, V. Hlady. Colloids Surf. B: Biointerf. 15 (1999) 37.

[316] Y. Xiao, G.A. Truskey. Biophys. J. 71 (1996) 2869.

[317] J.R. Bain, A.S. Hoffman, T.A. Horbett. J. Cellular Biochem., Suppl. 18C (1994) 282.

[318] J.R. Bain, A.S. Hoffman, T.A. Horbett. Trans. Soc. Biomater. 17 (1994) 336. [Nota bene: Data in Fig. 2 of this abstract contain a minor calculation error. Corrected data appear in Fig. 3.8 of the present study.]

[319] J.R. Bain, A.S. Hoffman, T.A. Horbett. Future Perspectives of Biomedical Polymers, meeting held December 4-6, 1992, Lahaina, Maui, Hawaii, abstracts, pp. 95-96.

[320] A.P. Mould, M.J. Humphries. Europ. Molec. Biol. Org. J. 10 (1991) 4089.

[321] P. Sanchez-Aparicio, C. Dominguez-Jimenez, A. Garcia-Pardo. J. Cell Biol. 126 (1994) 271.

[322] J.M. Clements, P. Newham, M. Shepherd, R. Gilbert, T.J. Dudgeon, L.A. Needham, R.M. Edwards, L. Berry, A. Brass, M.J. Humphries. J. Cell Sci. 107 (1994) 2127.

[323] M.J. Humphries, J. Sheridan, A.P. Mould, P. Newham. Ciba Found. Symp. 189 (1995) 177.

[324] A. Sharma, J.A. Askari, M.J. Humphries, E.Y. Jones, D.I. Stuart. Europ. Molec. Biol. Org. J. 15 (1999) 1465.

[325] J.A. Hubbell, S.P. Massia, N.P. Desai, P.D. Drumheller. Bio/Technology 9 (1991) 568.

[326] S.P. Massia, J.A. Hubbell. J. Cell Biol. 114 (1991) 1089.

[327] S.P. Massia, J.A. Hubbell. Analyt. Biochem. 187 (1990) 292.

[328] H.B. Bull. Biochim. Biophys. Acta 19 (1956) 464.

[329] J.L. Brash in C.P. Sharma, M. Szycher (eds.), Blood Compatible Materials and Devices: Perspectives Towards the 21st Century, Technomic Publishing Co.,

Inc., Basel, Switzerland, 1991, chapter 2.

[330] T.A. Horbett in T.J. Ahern, M.C. Manning (eds.), Stability of Protein Pharmaceuticals, Part A: Chemical and Physical Pathways of Protein Degradation, Plenum Press, NY, NY, 1992, chapter 7.

[331] A. Carrel, M.T. Burrows. J. Exp. Med. 14 (1911) 244.

[332] R.G. Harrison. Science 34 (1911) 279.

[333] P. Weiss. J. Exp. Zool. 100 (1935) 353.

[334] P.D. Drumheller. Polymer Networks of Poly(ethylene glycol) as Biospecific Cell Adhesive Substrates, Ph.D. dissertation, University of Texas at Austin, 1994, xiii + 146 pages.

[335] P.D. Drumheller, D.L. Elbert, J.A. Hubbell. Biotechnol. Bioengr. 43 (1994) 772.

[336] H. Cheng, M.J. Rudick. Analyt. Biochem. 198 (1991) 191.

[337] D.S. Wilbur. Bioconjugate Chem. 3 (1992) 3.

[338] K.A. Krohn, L.C. Knight, J.F. Harwig, M.J. Welch. Biochim. Biophys. Acta 490 (1977) 497.

[339] J.F. Eary, K.A. Krohn, R. Kishore, W.B. Nelp, in M.R. Zalutsky (ed.), Antibodies in Radiodiagnosis and Therapy, CRC Press, Boca Raton, FL, 1989, chapter 5.

[340] X.J. Yu, J.L. Brash, in S. Dawids (ed.), Test Procedures for the Blood Compatibility of Biomaterials, Kluwer Academic Publishers, Dordrecht, the Netherlands, 1993, pp. 287-330.

[341] J.A. Hubbell, S.P. Massia, N.P. Desai. U.S. Patent 5,330,911 (1994).

[342] S.P. Massia, J.A. Hubbell. J. Biol. Chem. 268 (1993) 8053.

[343] S.P. Massia, J.A. Hubbell. J. Biomed. Mater. Res. 25 (1991) 223.

[344] S.P. Massia, J.A. Hubbell. Trans. Soc. Biomater. 13 (1990) 240.

[345] S.P. Massia, J.A. Hubbell. Trans. Soc. Biomater. 14 (1991) 238.

[346] S.F.A. Hossiany, N.P. Desai, J.A. Hubbell. J. Biomed. Mater. Res. 26 (1992) 1535.

[347] P.D. Drumheller, S.P. Massia, J.A. Hubbell. Proc. Fourth World Cong. Biomater., Berlin, Germany, p. 216, (1992).

[348] S.P. Massia, J.A. Hubbell. J. Biol. Chem. 267 (1992) 14019.

Vita

James Raymond Bain

Born March 1st, 1956, in Grants Pass, Oregon.

Bachelor of Science, Northern Arizona University, 1976
(dual majors: chemistry and zoology).

Master of Science, University of Florida, 1981
(major: zoology).